

**Dissertation zur Erlangung des Doktorgrades
der Fakultät für Chemie und Pharmazie
der Ludwig-Maximilians-Universität München**

**Impact of glycosyltransferase UGT76B1 in
Arabidopsis thaliana and its substrate isoleucic acid
on plant defense**

Wei Zhang

aus

Fuzhou, Jiangxi, P.R. China

2013

Erklärung

Diese Dissertation wurde im Sinne von § 7 der Promotionsordnung vom

28. November 2011 von Herrn PD Dr. Anton R. Schäffner betreut.

Eidesstattliche Versicherung

Diese Dissertation wurde eigenständig und ohne unerlaubte Hilfe erarbeitet.

München,

.....

(WEI ZHANG)

Dissertation eingereicht am

1. Gutachterin / 1. Gutachter: PD Dr. Anton Rudolf Schäffner

2. Gutachterin / 2. Gutachter: Prof. Dr. Jörg Durner

Mündliche Prüfung am : 18.10.2013

ABSTRACT

Plants coordinately and tightly regulate pathogen defense by the mostly antagonistic salicylate (SA)- and jasmonate (JA)-mediated signaling pathways. The *Arabidopsis thaliana* secondary metabolite glycosyltransferase UGT76B1 has been previously reported to negatively regulate the SA pathway, however to activate the JA pathway. 2-hydroxy-3-methyl pentanoic acid (isoleucic acid, ILA) has been identified as an *in vivo* substrate in *Arabidopsis*.

In accordance with these findings, loss-of-function of *UGT76B1* and constitutive overexpression of *UGT76B1* led to the enhanced and repressed susceptibility towards the necrotrophic fungal pathogen *Alternaria brassicicola*, respectively. To study the interaction of UGT76B1 with the SA- and JA-dependent pathways, mutants affecting these pathways at various positions were introgressed into *ugt76b1* knockout and *UGT76B1* overexpression lines. These genetic studies suggest that UGT76B1 primarily regulated the SA pathway. The loss-of-function of *UGT76B1* caused the suppression of JA pathway dependent on SA. The impact of UGT76B1 on both SA and JA responses was independent from *SID2*, which encodes a stress-related SA-biosynthetic gene, and NPR1, which is a key positive regulator of the SA pathway.

Exogenous application of ILA broadly activated defense responses including the activation of JA and SA marker genes and the induction of defense genes (*PAD3* and *AIG1*) independent from SA and JA pathways. This suggested a potential capability of ILA to provide protection against different pathogens. ILA can enhance the resistance against infection of biotrophic pathogen *Pseudomonas* as a novel protective agent.

Exogenous ILA application activated defense response in a way similar to the loss-of-function of *UGT76B1* including the enhancement of resistance against *Pseudomonas* and the activation of defense genes such as *FMOI* and *AIG1*. The expression of *FMOI* and *AIG1*, which was known to be uncoupled from SA abundance, was activated by ILA independent from SA. This suggested that an additional signal other than SA is involved in the regulation of defense by ILA, probably also by *UGT76B1*. Regarding the genes activated by exogenous ILA application, at least some were also responsive to acetic acid. It indicated that a subset of the transcriptional response to ILA treatment might be driven by acidification.

Using mass spectrometry a peak with the same m/z as ILA glucoside was found in other plants, *e.g.* poplar, tomato, barley and maize. First results showed that ILA can activate defense genes in barley. This provided evidence that ILA and corresponding glucosyltransferases could be associated with plant defense in other plants as well.

CONTENTS

ABSTRACT	I
-----------------------	----------

ABBREVIATIONS	VI
----------------------------	-----------

1. INTRODUCTION	1
------------------------------	----------

1.1. Different layers of pathogen recognition in plants	1
1.2. The SA pathway in plant defense	2
1.2.1. The regulation of the SA pathway	2
1.2.2. Defense response regulated by the SA pathway	5
1.3. JA pathway in plant defense	5
1.4. Ethylene pathway in plant defense	7
1.5. SA-JA/ET cross-talk	10
1.5.1. Antagonistic interactions of SA-JA pathways	10
1.5.2. Synergistic interaction of SA and JA pathways	12
1.6. Non SA, JA, ET-mediated responses	13
1.7. Plant UDP-glycosyltransferase modulates plant defense <i>via</i> interacting with SA and JA pathways	13
1.7.1. UDP-glycosyltransferase	13
1.7.2. UGTs and plant defense	15
1.8. Aim of this work	17

2. RESULTS	18
-------------------------	-----------

2.1. <i>UGT76B1</i> expression positively correlates with resistance against necrotrophic pathogen infection	18
2.2. Integration of <i>UGT76B1</i> into SA and JA pathways	19
2.2.1. Dependence of <i>UGT76B1</i> -mediated response on SA and JA pathway	19
2.2.2. <i>UGT76B1</i> impact on JA pathway is independent from JA synthesis	23
2.3. Non-targeted microarray analysis	25
2.3.1. <i>UGT76B1</i> expression negatively regulates SA-mediated response	29
2.3.2. Microarray analysis indicates a negative correlation of <i>UGT76B1</i> expression and ILA action	35
2.3.3. Genes induced by both ILA and loss-of-function of <i>UGT76B1</i> can be separated into two classes depending on their responsiveness to SA	38
2.3.4. Specific ILA effect on the JA response	45
2.3.5. Validation of the negative correlation of ILA application and the <i>UGT76B1</i> expression level in regulating defense-responsive genes	49
2.4. ILA activity	52
2.4.1. ILA enhances resistance against <i>Pseudomonas</i> infection	52
2.4.2. Involvement of <i>UGT76B1</i> in ILA action on regulation of defense genes	53
2.4.3. The requirement of SA and JA/ET pathways in ILA action on regulation of defense genes	55
2.4.4 The kinetic activation of SA- and JA-mediated defense genes by exogenous ILA application	59

2.4.5 SA- and JA-related metabolites measurement after ILA treatment	62
2.4.6 The activity of ILA in inhibiting root growth	64
2.4.6.1 The activity of ILA in inhibiting root growth regulated by <i>UGT76B1</i> expression.....	64
2.4.6.2. Response to ILA in roots does not require SA, JA and ET pathways.....	65
2.4.6.3. The activity of ILA in inhibiting root growth regulated by <i>GOX3</i> expression	66
2.5. Exogenous application of ILA leads to specific transformation to isoleucine.....	67
2.6. A potential role of ILA in regulating defense response in crop plants	68
2.6.1. Mass peaks corresponding to ILA-glycoside and valic acid-glycoside accumulation in other crop species	68
2.6.2. ILA directly impacts plant defense in barley	70
2.7. <i>UGT76B1</i> shows activity towards leucic acid and valic acid	71
2.7.1. The root inhibition by leucic acid and valic acid was dependent on <i>UGT76B1</i> expression.....	71
2.7.2. Recombinant protein <i>UGT76B1</i> glycosylates leucic acid and valic acid <i>in vitro</i>	72
2.8. Analogues of ILA can induce plant defense similar as ILA	75
2.9. Induction of defense genes by acids.....	77

3. DISCUSSION 80

3.1. The integration of <i>UGT76B1</i> in SA-JA cross-talk	80
3.2. Integration of dynamic aspects of ILA on defense including SA and JA pathways	84
3.3. ILA activated defense responses which can be observed in systemic leaves upon local pathogen infection	88
3.4. Does acidification contribute to ILA action?	89
3.5. The association of ILA activity with <i>UGT76B1</i>	91

4. MATERIALS AND METHODS..... 94

4.1. MATERIALS	94
4.1.1. Chemicals	94
4.1.2. Media.....	94
4.1.3. Bacterial strains	94
4.1.4. Vectors	95
4.1.5. Antibiotics	95
4.1.6. Primers	95
4.1.6.1. Primers used for screening homozygous lines	95
4.1.6.2. Primers used for RT-qPCR	96
4.1.7. Plant materials	97
4.2. METHODS.....	98
4.2.1. Plant growth conditions.....	98
4.2.2. Seedling grown on solid medium.....	98
4.2.3. BASTA selection.....	99
4.2.4. Wounding of <i>Arabidopsis</i> leaves	99
4.2.5. Crossing.....	99
4.2.5.1. Generation of homozygous lines combining the lines with different <i>UGT76B1</i> expression and lines deficient in the SA pathway or the JA / ET pathway.....	99
4.2.5.2. Genotyping for double mutants.....	100
4.2.5.3. Production of the <i>ugt76b1-1 sid2</i> and <i>UGT76B1-OE-7 sid2</i> double mutants.....	100
4.2.5.4. Production of the <i>ugt76b1-1 NahG</i> and <i>UGT76B1-OE-7 NahG</i> double mutants.....	101

4.2.5.5. Production of the <i>ugt76b1-1 npr1</i> and <i>UGT76B1-OE-7 npr1</i> double mutants	101
4.2.5.6. Production of the <i>ugt76b1-1 jar1</i> and <i>UGT76B1-OE-7 jar1</i> double mutant	102
4.2.6. Observation of root growth of <i>Arabidopsis</i> on plates containing chemicals	102
4.2.7. ILA treatment	102
4.2.8. Pathogen infections	102
4.2.8.1. Biotrophic pathogen infection of <i>Arabidopsis</i>	102
4.2.8.2. Necrotrophic pathogen infection of <i>Arabidopsis</i>	103
4.2.9. Preparation of plant genomic DNA	103
4.2.10. RNA isolation	103
4.2.11. Real-time PCR	104
4.2.11.1. Primer design	104
4.2.11.2. Synthesis of the first-strand cDNA without contamination of genomic DNA	106
4.2.11.3. Quantitative real time polymerase chain reaction (RT-qPCR)	106
4.2.11.4. Selection of reference genes and normalization of RT-qPCR	107
4.2.12. Separation and analysis of the DNA fragments based on DNA gel electrophoresis ..	107
4.2.12. SA determination	107
4.2.13. Non-targeted Metabolome Analysis by FT-ICR MS	109
4.2.14. Fragmentation Studies using FT-ICR MS	110
4.2.15. Measurement of JA-related metabolites by GC-MS	110
4.2.16. Production of the recombinant protein UGT76B1	110
4.2.17. <i>In vitro</i> analysis of the recombinant UGT76B1	111
4.2.18. Microarray Analyses	111
4.2.19. Microarray data analysis	112
4.2.20. Bioinformatic analyses	113

REFERENCES **115**

CURRICULUM VITAE **130**

ACKNOWLEDGEMENTS **132**

ABBREVIATIONS

AGI	<i>Arabidopsis</i> Genome Initiative
cDNA	complementary DNA
CTAB	Cetyltrimethylammonium bromide
MS	Murashige and Skoog
NDP	nucleoside diphosphate
PCR	Polymerase chain reaction
RNA	Ribonucleic Acid
rpm	revolutions per minute
RT-PCR	Reverse Transcription-PCR
RT-qPCR	Real-time quantitative PCR
SD	Standard Deviation
SDS	Sodium Dodecyl Sulfate
SE	Standard Error
TAE	Tris-Acetate-EDTA
T-DNA	Transfer-DNA
ddH ₂ O	double distilled water
DEPC	Diethylpyrocarbonate
DMSO	Dimethyl sulfoxide
DNA	Deoxyribonucleic Acid
dNTPs	Deoxynucleotide-5'-triphosphates
DTT	Dithiothreitol
EDTA	Ethylene Diamine Tetra-acetic Acid
FT-ICR MS	Fourier transform ion cyclotron resonance mass spectrometry
kb	Kilo base pair
kDa	Kilo Dalton
d	day
h	hour
s	second
min	minute
RT	room temperature
UV	Ultraviolet
FW	fresh weight

FIGURES AND TABLES

FIGURES

Figure 1. Model of SA synthesis and SA signal transduction.....	4
Figure 2. Model of biosynthesis and signal transduction of JA and ET.	9
Figure 3. Interactions between the SA and the JA /ET pathways.	12
Figure 4. Scheme of reactions catalyzed by UGTs and physiological functions in <i>Arabidopsis</i>	15
Figure 5. Model of the involvement of <i>UGT76B1</i> as a novel mediator in SA- and JA- dependent regulation of defense responses.	16
Figure 6. Pathogen susceptibility is positively correlated with <i>UGT76B1</i> expression	18
Figure 7. SA and JA marker genes expression in <i>UGT76B1</i> overexpression and knockout lines after introgression into <i>sid2</i> , <i>NahG</i> , <i>npr1</i> and <i>jar1</i>	23
Figure 8. The impact of <i>UGT76B1</i> expression on the onset of senescence is dependent on <i>SID2</i> and <i>NPR1</i> , but independent from <i>JAR1</i>	23
Figure 9. JA wounding response in <i>Arabidopsis</i> lines with different <i>UGT76B1</i> expression levels.....	25
Figure 10. Transcriptional reprogramming of genes by <i>UGT76B1</i> expression or ILA treatment.....	27
Figure 11. Pie chart analysis of genes regulated by ILA and <i>UGT76B1</i> according to GO enrichment.....	28
Figure 12. Analysis of biotic stress relevance on genes regulated by ILA and alteration of <i>UGT76B1</i> expression.	31
Figure 13. Venn diagrams of transcriptome analysis on action of ILA and the altered <i>UGT76B1</i> expression.	32
Figure 14. Gene co-expression network for <i>EARLII</i> (At4g12480).	49
Figure 15. Defense marker gene expression altered by <i>UGT76B1</i> expression and ILA treatment.....	51
Figure 16. Effect of exogenously applied ILA on susceptibility towards avirulent <i>Pseudomonas syringae</i> infection.....	52
Figure 17. Isoleucic acid treatment in <i>ugt76b1-1</i> and <i>UGT76B1-OE-7</i>	53
Figure 18. Effect of ILA in <i>ugt76b1 sid2</i> and <i>NahG</i> on activation of defense genes	54
Figure 19. Defense marker genes expression by ILA treatment in lines deficient in SA (<i>sid2</i> , <i>NahG</i> , <i>npr1</i>), JA (<i>jar1</i>) and ET (<i>etr1</i>) pathways.....	58
Figure 20. Time-course of marker genes expression in SA and JA pathways and <i>UGT76B1</i> after ILA treatment.....	61
Figure 21. Free SA and conjugated SA levels in 4-week-old seedlings of water-treated Col-0, ILA-treated Col-0 and leucic acid-treated Col-0.....	62
Figure 22. The measurement of JA-related metabolites.	63
Figure 23. Direct effects of exogenously applied ILA.....	65
Figure 24. ILA perception by roots in lines deficient in SA, JA and ET pathways and <i>cpr5</i> ..	66
Figure 25. Root growth inhibition by ILA inversely correlates with GOX3 expression.	67
Figure 26. Intensity of mass peaks corresponding to ILA- and valic acid-glucoside in different plant species.	69
Figure 27. Direct impact of ILA on plant defense in barley.	70
Figure 28. Direct effect of analogues of ILA on root growth.	72
Figure 29. Valic acid and leucic acid, putative additional substrates of <i>UGT76B1</i>	75
Figure 30. The expression of defense genes mediated by analogues of ILA.....	77
Figure 31. Defense marker gene expression after ILA, acetic acid and lactic acid application.	78

Figure 32. Defense marker gene expression induced by acetic acid application in comparison with ILA.	79
Figure 33. Model of the involvement of <i>UGT76B1</i> as a mediator in defense responses (SA mediated response, JA mediated response and other defense responses).	81
Figure 34. Model of the involvement of ILA as a mediator in defense responses (SA mediated response, JA mediated response and other defense responses).	86
Figure 35. The workflow for microarray processing and data analysis	112
Figure 36. Pairs plots of microarray data for samples.	114

TABLES

Table 1. Comparison of genes oppositely regulated in <i>ugt76b1</i> knockout and <i>UGT76B1</i> overexpression relative to Col-0 with microarray data sets published in Genevestigator.	33
Table 2. Comparison of genes oppositely regulated in <i>ugt76b1</i> knockout and <i>UGT76B1</i> overexpression relative to Col-0 with microarray data sets published in Genevestigator.	34
Table 3. Overlapping genes consistently regulated by ILA, <i>ugt76b1</i> knockout and <i>UGT76B1</i> overexpression.	37
Table 4. Comparison of genes, upregulated in <i>ugt76b1</i> knockout and by ILA application relative to Col-0 with microarray data sets published in Genevestigator.	39
Table 5. Comparison of genes, up-regulated in the <i>ugt76b1</i> knockout and by ILA application relative to mock-treated Col-0 (\log_2 -transformed value ≥ 1 equal to twofold) with microarray data sets published in Genevestigator.	42
Table 6. Functional classification of genes induced more than twofold by ILA, but not induced, however, in the <i>ugt76b1</i> knockout, according to TAIR ontology.	46
Table 7. Sixty two genes were induced only by ILA (Figure 13 A).	46
Table 8. Measurement of branched-chain amino acids after treatment of ILA, leucic acid and valic acid in Col-0.	68
Table 9. <i>Arabidopsis</i> mutants and overexpression lines used in this project.	98

1. INTRODUCTION

1.1. Different layers of pathogen recognition in plants

During their whole life plants face a vast set of challenges from pathogen infection, and have therefore evolved very complex defense mechanisms, which can be classified into different layers. Similar to animals, plants develop a first line of innate defense response by recognizing conserved pathogen associated molecular patterns (PAMP) *via* pattern recognition receptors (PRRs) inducing PAMP-triggered immunity (PTI). Most of these PRRs are leucine rich repeat receptor kinases (LRR-RKs), belonging to a big family of over 600 members (Shiu and Bleeker, 2001). In *Arabidopsis*, flg22, a 22-amino-acid peptide from bacterial flagellin, the elongation factor EF-Tu and chitin were found to be detected by FLAGELLIN-SENSING 2 (FLS2), the Elongation Factor-TU RECEPTOR (EFR) and CHITIN ELICITOR RECEPTOR KINASE 1 (CERK1) respectively (Zipfel et al., 2006; Chinchilla et al., 2007; Miya et al., 2007; Wan et al., 2008). During the long-term battle with plants, pathogens have evolved a mechanism to directly inject virulence effectors, mainly recreated by a type III secretion system to overcome unspecific PTI. To fight the virulence of effectors from pathogens, plants have in turn established effector-triggered immunity (ETI) by recognizing virulence effectors *via* corresponding receptor (R) proteins dependent on a specific gene-to-gene manner. This is commonly accompanied by a hypersensitive response (HR) in the form of rapid cell death limiting the spread of the pathogen from its infection site (Jones and Dangl, 2006). The key hormones salicylic acid (SA), jasmonic acid (JA) and ethylene (ET) interactively play crucial roles downstream of PTI and ETI to defend against different pathogens (Dodds and Rathjen, 2010). According to the life style, pathogens can be divided into biotrophic pathogens and necrotrophic pathogens (Glazebrook, 2005). The defense against biotrophic pathogens, deriving nutrients from living tissues *via* feeding structures, depends mainly on the SA pathway. Biotrophic pathogens can be divided into virulent lines and avirulent lines. Virulent lines cause compatible plant-pathogen interactions and very aggressive pathogen attack, whereas avirulent lines lead to incompatible plant-pathogen interactions due to the recognition of virulence effectors in plants triggering ETI, accompanied by hypersensitive response (HR). The SA pathway was reported to play a positive role in regulating HR response (Jones and Dangl, 2006). Necrotrophic pathogens, killing the host tissues through producing cell-wall-degrading enzyme and feeding on the remains, are mainly fended off by JA/ET pathways. Furthermore, necrotrophic pathogens can be fended off by camalexin, a major phytoalexin. Consistently, the increased susceptibility of

the mutant *pad3* (of *PHYTOALEXIN DEFICIENT 3*) towards *Alternaria brassicicola* was caused by a defect of camalexin biosynthesis (Thomma et al., 1999).

1.2. The SA pathway in plant defense

1.2.1. The regulation of the SA pathway

The plant hormone SA takes an important role in defense mainly against biotrophs. The precursor chorismate can be converted to the phenolic compound SA *via* two different enzymatic pathways. One is metabolized by PHENYLALANINE AMMONIA LYASE (PAL), while the other involves ISOCHORISMATE SYNTHASE 1/SALICYLIC ACID INDUCTION DEFICIENT 2 (ICS1/SID2). SID2 is mainly responsible for the stress-induced SA accumulation as in *sid2* mutants the level of SA is only 5-10% of control values after infection or UV stress (Figure 1A) (Nawrath and Metraux, 1999; Dewdney et al., 2000). Most of the SA is converted to SA O- β -glucoside (SAG) by SA glucosyltransferases and subsequently transported to vacuoles for storage. Small amounts of SA are converted by conjugation to form salicyloyl glucose ester (SGE) and methyl salicylate (MeSA). MeSA is an inactive form, but plays a role as a long distance signal in transferring SAR in tobacco and *Arabidopsis* (Park et al., 2007; Vlot et al., 2009). The conjugation of SA to amino acids may affect SA action as well. Overexpression of acyl-adenylate/thioester-forming enzyme (GH3.5), which is involved in conjugating amino acids to SA, causes increased SA response. Interestingly, another conjugating enzyme AVRPPHB SUSCEPTIBLE 3 (PBS3)/acyl-adenylate/thioester-forming enzyme (GH3.12) which shows conjugation activity on 4-substituted benzoates but not SA, acts as a positive regulator upstream of SA synthesis. ENHANCED DISEASE SUSCEPTIBILITY 1 (EDS1) and PHYTOALEXIN DEFICIENT 4 (PAD4) are involved in upregulating SA synthesis (Vlot et al., 2009). NON-EXPRESSOR OF PR GENES1 (NPR1) is a key regulator of SA-mediated responses (Cao et al., 1997). In non-challenged cells, NPR1 exists in the cytoplasm of the cell as oligomers, linked *via* intermolecular disulfide bonds. Upon stress, SA-triggered cellular redox change induces the monomerization of NPR1 *via* thioredoxins TRX-H3 and TRX-H5 (Tada et al., 2008). Conversely, the S-nitrosylation of NPR1 regulated by S-nitrosoglutathione (GSNO) facilitates its oligomerization, which maintains protein homeostasis upon SA induction (Lindermayr et al., 2005; Tada et al., 2008). After the import of monomers of NPR1 to the nucleus, NPR1 interacts with a class of positive TGA transcriptional factors to positively regulate the SA-responsive genes such as PATHOGENESIS-RELATED (PR) proteins including PR1, PR2

and PR5 (Figure 1B). Some PR-genes, encode many antimicrobial proteins such as PR2 and PR5. *PR1*, *PR2* and *PR5* are characterized as marker genes of SA response; however, the biological function of *PR1* remains elusive (van Loon et al., 2006). Many negatively regulatory proteins of the SA pathway can be found to interact with NPR1 such as the NPR1-interacting proteins NIM1-INTERACTING 1 (NIMIN1), 2, and 3, and SUPPRESSOR OF *npr1* INDUCIBLE1 (SNI1). These NIMINs play roles in inhibiting promoter activity of defense genes likely *via* influencing TGA transcription factors (Figure 1B). The binding partner and regulation mechanism of SNI1 is still unclear. The *snl* mutant was identified in a screen to rescue SA response in the *npr1* mutant, suggesting an NPR1 independent response (Mosher et al., 2006). In addition, the constitutively enhanced SA response in *suppressor of SA insensitivity 2* (*ssi2*) was confirmed to be partially dependent on SA, but not NPR1. The NPR1-independent pathway may require WHIRLY (WHY) transcription factor family. Probably, NPR1 regulates the downstream SA response, independent from, but in concert with WHY transcription factors (Vlot et al., 2009) (Figure 1B). The synthetic elicitor 3,5-dichloroanthranilic acid (DCA) can induce both NPR1-dependent and NPR1-independent mechanisms of disease resistance in *Arabidopsis*. In the *npr1* mutant, DCA-induced resistance was only mildly affected (Knoth et al., 2009). This was in contrast to the complete block of activation of resistance by SA, functional analogues of SA, 2,6-dichloroisonicotinic acid (INA) and acibenzolar-S-methyl benzo(1,2,3)thiadiazole-7-carbothioic acid S-methyl ester (BTH) in *npr1* (Lawton et al., 1996; Dong, 2004).

Many loss-of-function mutants leading to retarded SA response accompanied by reduced resistance to biotrophic pathogens were thus identified to positively regulate the SA pathway. For instance, genes in mitogen-activated protein kinase signaling such as *ERD1*, *MPK3* and *MPK6*, probably act upstream of SA synthesis (Frye et al., 2001; Asai et al., 2002; Tang et al., 2005; Qiu et al., 2008; Rasmussen et al., 2012). NUCLEOSIDE DIPHOSPHATE LINKED TO SOME MOIETY X 6 (NUDT6) was reported to positively regulate the SA pathway dependent on NPR1 *via* changing NADH metabolism *in vivo* (Ishikawa et al., 2010). In contrast, many mutants constitutively activating SA response have been found displaying elevated SA accumulation and expression of *PR* genes. Well-characterized mutants include the *mpk4*, *acd*, *lsd*, *cpr* mutants, *mlo*, *hrl1*, *hlm1*, *snl* and *ssi1* (Greenberg et al., 1994; Li et al., 1999; Shah et al., 1999; Petersen et al., 2000; Devadas et al., 2002; Balague et al., 2003; Lorrain et al., 2003; Consonni et al., 2006; Journot-Catalino et al., 2006).

Via genetic analysis a group of WRKY transcription factor genes such as *WRKY70*, *WRKY33* and *WRKY18* were found to modulate the SA pathway. *WRKY70*, *WRKY50* and *WRKY51* positively regulate the SA pathway, whereas *WRKY33* negatively regulate the SA pathway (Li et al., 2004; Pandey et al., 2010; Gao et al., 2011; Birkenbihl et al., 2012). Many WRKY transcription factors are induced after nuclear translocation of NPR1 monomers (Wang et al., 2006).

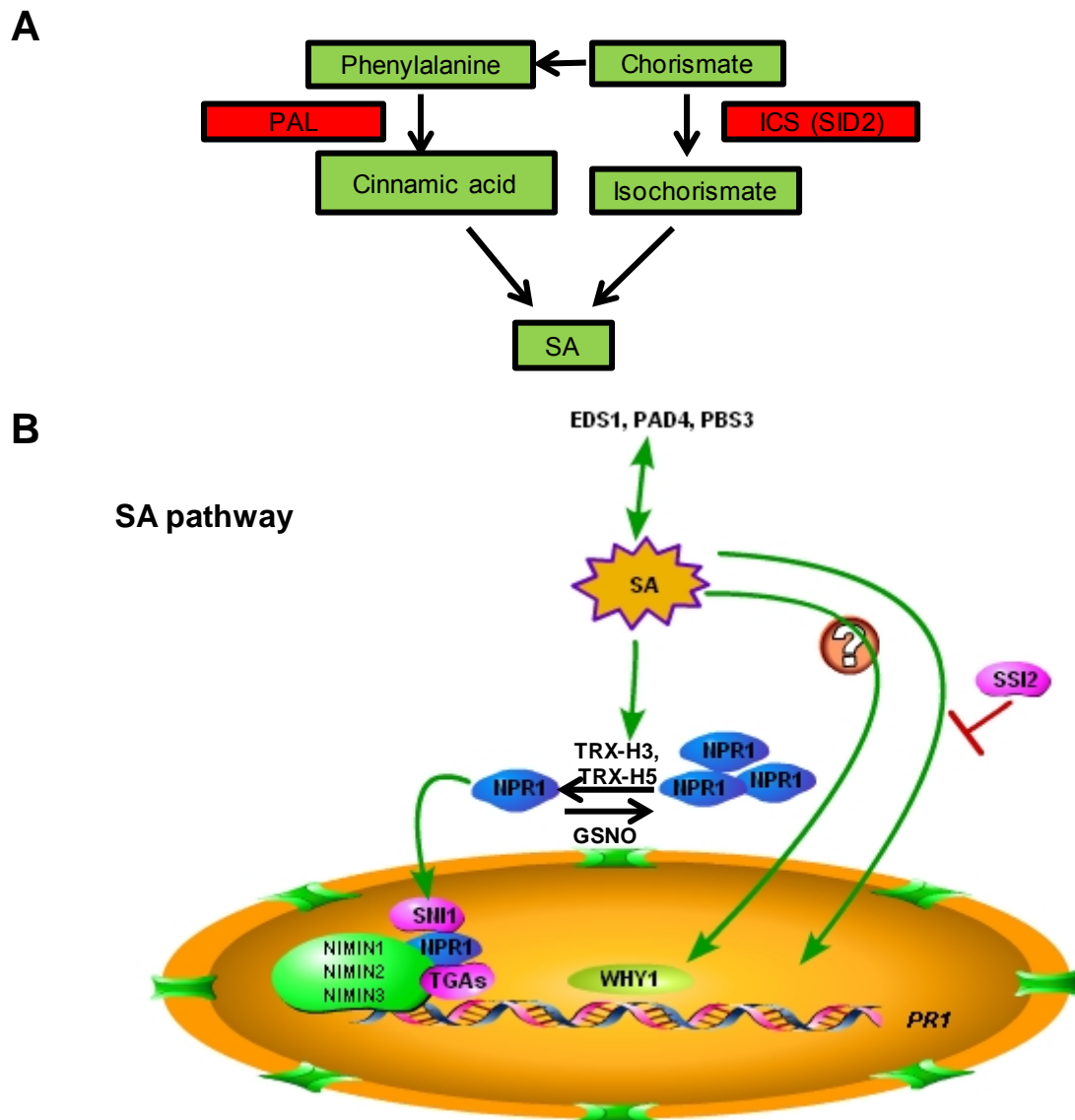


Figure 1. Model of SA synthesis and SA signal transduction.

(A) There are two SA biosynthetic pathways: the isochorismate (IC) pathway and phenylalanine ammonia-lyase (PAL) pathway. Both start from chorismate. (B) *EDS1*, *PAD4* and *PBS3* are involved upstream of SA synthesis and can be induced by positive SA feedback. The redox state alteration caused by SA burst leads to the monomerization of NPR1. The monomerization of NPR1 by thioredoxins (TRXs) such as TRX-H3 and TRX-H5 cause the translocation of NPR1 in nucleus and subsequent interaction with positive transcription activators TGAs, negative regulators NIM1-

interacting proteins (NIMINs) and SNI1. S-nitrosoglutathione (GSNO) can facilitate the oligomerization of NPR1. The transcription factor WHY1 is probably involved in NPR1-independent SA response. SSI2 is a negative regulator, independent on NPR1 to regulate SA-mediated response. *PR1*, *PR2* and *PR5* are SA-responsive marker genes. Activation (closed arrowhead), suppression (\perp) and important genes are indicated.

1.2.2. Defense response regulated by the SA pathway

Chemical elicitors can induce defense responses mediated by the SA pathway. The chemical defense activators can be classified into two groups: one group constitutively activates defense response, such as SA functional analogues INA and BTH, and the other group cannot trigger defense response directly, protect plants, however *via* priming. Priming is considered to be a condition, in which defense can be activated more rapidly and robustly upon infection. Chemicals such as β -aminobutyric acid (BABA), azelaic acid (AzA) or pipecolic acid (Pip) can induce priming (Ryals et al., 1996; Jung et al., 2009; Navarova et al., 2012). Systemic acquired resistance (SAR) is another important aspect of plant defense. It elicits broad-spectrum resistance against pathogens that occurs at systemic leaves induced by a local infection in developmentally older leaves. The local infection produces signals such as SA, AzA, glycerol-3-phosphate (G3P) or Pip, leading to the activation or priming of pathogen-related genes in systemic leaves. SA and NPR1 are known to play key roles in SAR (Zheng and Dong, 2013).

Plant senescence is a natural age-dependent cell death program, facilitating the redistribution of resources from senescing leaves into young leaves, which is at least partially SA dependent (Yoshida et al., 2001; Buchanan-Wollaston et al., 2005). Senescence can be visualized by yellowing of the leaves caused by chlorophyll degradation. Senescence marker genes such as *SENESCENCE ASSOCIATED GENE 13* (*SAG13*) and *YELLOW LEAF-SPECIFIC GENE9* (*YSL9*) can be measured as the indicators of the onset of senescence before a visible phenotype is observed (Miller et al., 1999; Yoshida et al., 2001).

1.3. JA pathway in plant defense

The JA pathway mainly protects plants against necrotrophic pathogens and wounding. The plant hormone JA is a lipid-derived compound and is synthesized through the oxylipin biosynthetic pathway. The JA synthesis starts from the precursor α -linolenic acid, released from membrane lipids in chloroplast. The key synthetic enzymes include a 13-lipoxygenase (13-LOX), a 13-allene oxide synthase (13-AOS), an allene oxide cyclase (AOC) and an OPDA-specific reductase (OPR3) (Figure 2A, left). There are many conjugation forms of JA

JA-Ile, MeJA, JA-ACC, JA-Glc and 12-HSO₄-JA. However, there is evidence showing that only MeJA and JA-Ile are the active forms (Miersch et al., 2008). Upon stress JA can be rapidly conjugated to amino acids such as isoleucine by JASMONATE RESISTANT (JAR1), leading to the major biologically active form JA-Ile. JA-Ile can then bind to the F-box protein CORONATINE INSENSITIVE 1 (COI1) leading to the conformation change of COI1. This conformation changes allow the association of COI1 with the JASMONATE ZIM (JAZ) domain transcriptional repressor proteins. INOSITOLPENTAKISPHOSPHATE (InsP5) acts as a co-receptor for JA-Ile to stabilize the association of JAZ-COI1 (Sheard et al., 2010). COI1, functions in the E3-ligase SKP1-Cullin-F-box complex SCF^{COI1} and directs the degradation of JAZs, causing the activation of JA response. In *Arabidopsis*, there are 12 JAZ members (JAZ1-JAZ12). Under normal conditions, JAZ proteins repress the activity of positive transcriptional regulators by binding to them. Co-repressors are recruited to coordinate the suppression with JAZ proteins. The recruitment of TOPLESS (TPL) is achieved through NOVEL INTERACTOR of JAZ (NINJA) containing an ERF-associated amphiphilic repression (EAR) motif (Figure 2B). TPL has been shown to interact with HISTONE DEACETYLASES (HDCAs) to deacetylate histones at promoters or interrupt the Mediator-RNA polymerase II complex, thus leading to the suppression of transcription (Kazan and Manners, 2012) (Figure 2B).

There are two major branches of JA signaling downstream of JAZ repressors: the MYC branch, responsible for the wounding response and the ERF branch, associated with necrotrophic pathogen resistance (Figure 2B). The MYC branch, controlled by MYC-type transcriptional factors, directs wounding responses including the expression of *VEGETATIVE STORAGE PROTEIN2* (*VSP2*), the JA-responsive marker gene. MYC2 recruits MED25, one subunit of the plant mediator complex to initiate transcription (Chen et al., 2012). MYC2 is the major transcription factor regulating the JA pathway while MYC3 and MYC4 activate JA response additively to MYC2, though it is still unclear how MYC3 and MYC4 modulate the JA pathway (Fernandez-Calvo et al., 2011). MYC2 prefers binding for the G-box sequence (5'-CACGTG-3'). Consistently, the G-box sequence of the promoter is required for the induction of early responsive JA response gene *JAZ2*, regulated by MYC2. The ERF branch containing ETHYLENE RESPONSE FACTOR 1 (ERF1) and OCTADECANOID-RESPONSIVE ARABIDOPSIS AP2 59 (ORA59) controls the JA-responsive marker gene *PLANT DEFENSIN1.2* (*PDF1.2*), usually regulated by the ET pathway in response to necrotrophic pathogen infection (Figure 2B). Interestingly, the MYC branch and ERF branch were found to be antagonistic to each other. The *myc2* mutant was more resistant to the

infection of the necrotrophic pathogen *Alternaria brassicicola*, probably due to the enhanced ERF response. When the MYC branch was suppressed by *ORA59* overexpression, plants were more susceptible to *P. rapae* larvae, which feed on the plants, causing wounding response (Verhage et al., 2011). MYC2 negatively regulates genes in the other JA-responsive branch including *ERF1*, *ORA59* and *PDF1.2*. However, the suppression mechanism is still unclear. Interestingly, MYC2 regulates some NAC-domain containing TF genes *ANAC109* and *ANAC055*, which have been shown to positively regulate *VEGETATIVE STORAGE PROTEIN* (*VSP*) genes, but negatively regulate *PDF1.2* (Bu et al., 2008). Recently, upstream of *ERF1* and *ORA59*, two transcription factors ETHYLENE INSENSITIVE 3 (*EIN3*) and *EIN3*-LIKE 1 (*EIL1*) were found to be the synergistic convergence knot, regulated by both the JA and ET pathways (Figure 2B). *EIN3* and *EIL1* are activated by the release of repression from JAZ and HDA6 in the JA pathway; however they are positively regulated by the essential regulator ETHYLENE INSENSITIVE 2 (*EIN2*) in the ET pathway. *EIN2* can stabilize *EIN3* and *EIL1*, via preventing them to be degraded by *EIN3*-BINDING F BOX PROTEIN 1 and 2 (*EBF1* and *EBF2*). *EBF1* and *EBF2* are two F-box proteins mediating the proteasome degradation (Zhu et al., 2011) (Figure 2B).

1.4. Ethylene pathway in plant defense

The plant hormone ET is a gaseous hormone, playing key roles in many physiological processes. The biosynthesis of ET originates from S-adenosyl methionine (SAM), which is produced by SAM synthetase from methionine and ATP. 1-aminocyclopropane-1-carboxylic acid (ACC), the precursor of ET can be synthesized by ACC oxidase from SAM and converted to ET (Figure 2A, right). It induces the ripening of the fruits or leaf abscission. However, ET also plays an active role in plant defense. For example, in *Arabidopsis*, ET potentiates the expression of *PR1* via an unknown mechanism (De Vos et al., 2006) (Figure 3). There are five ethylene-responsive receptors, which can be divided into two subgroups: the first group contains ETHYLENE RESPONSE1 (*ETR1*) and ETHYLENE RESPONSE SENSOR1 (*ERS1*), characterized by His kinase activity; the second group contains *ETR2*, *ERS2* and *EIN4*, characterized by Ser/Thr kinase activity *in vitro* (Moussatche and Klee, 2004). These five ethylene receptors are localized on the ER membrane and play redundant roles in recognizing ET (Figure 2B). In resting cells, these receptors without ET ligands can activate CONSTITUTIVE TRIPLE RESPONSE 1 (*CTR1*), which negatively regulates *EIN2* by phosphorylation (Santner and Estelle, 2009). *EIN2* can stabilize *EIN3* and *EIL1* positive transcription factors which regulates *ORA59* and *ERF1*. Upon ethylene binding, the lost

activation of CTR1 by ethylene receptors such as ETR1 causes the degradation of EIN3 and EIL1 by EBF1 and EBF2 (Figure 2B). The JA pathway and ET pathways share the same signaling, starting from EIN3 and EIL1. EIN3 and EIL1 can be regulated by both the JA and the ET pathways and therefore are synergistic knots of the JA and ET pathways (Figure 2B) (Zhu et al., 2011). The mutant *cev1* of gene *CONSTITUTIVE EXPRESSION OF VSP 1* constitutively activates JA and ET signaling, suggesting a common regulation of both pathways (Ellis and Turner, 2001). ET can act on the ERF branch of the JA pathway, but antagonizes the MYC branch. Pathogenesis-related proteins *PR3* and *PR4* are the marker genes of the ET response. *PDF1.2* requires both JA and ET pathways to be induced and therefore is a marker gene of both pathways.

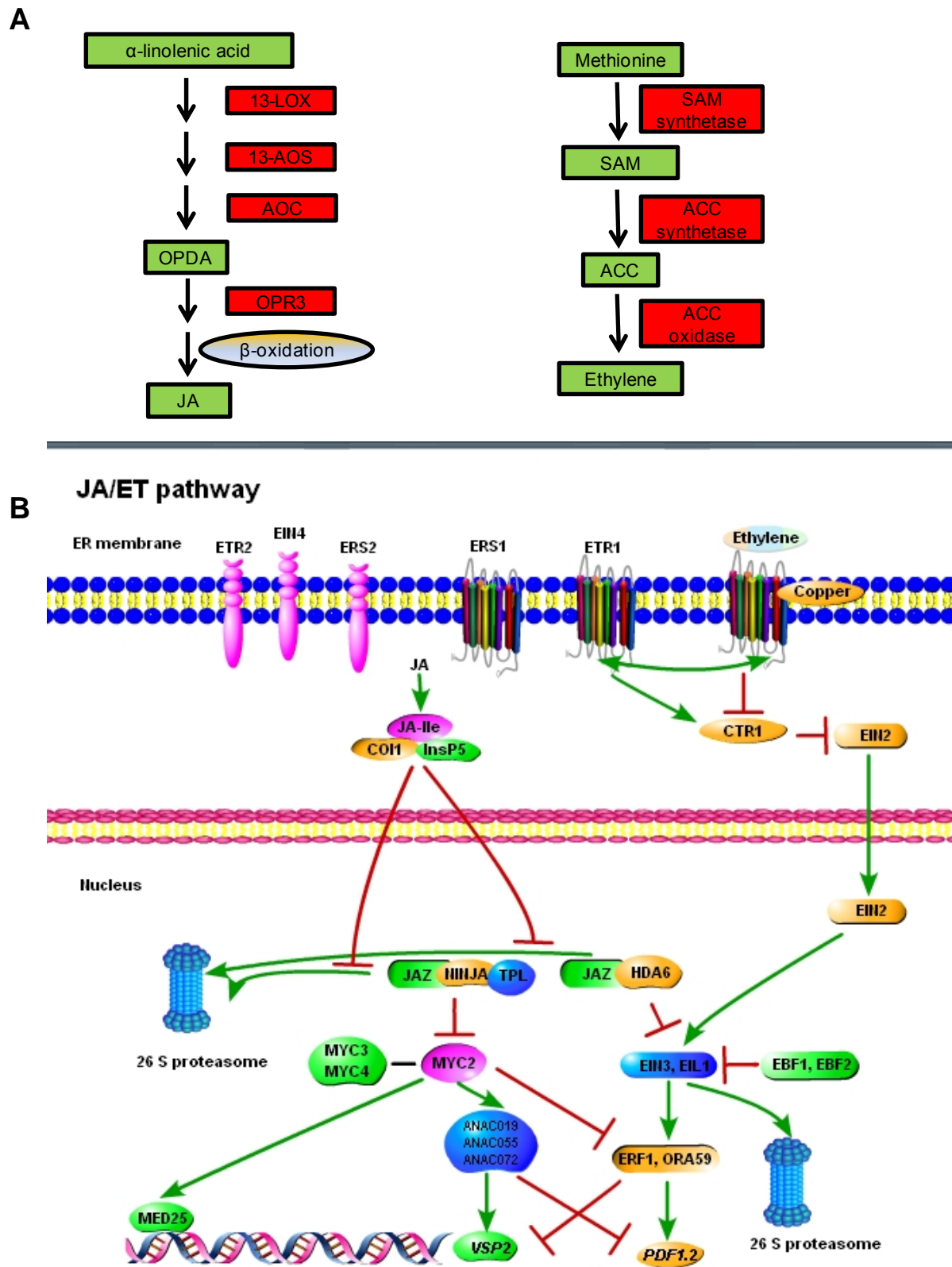


Figure 2. Model of biosynthesis and signal transduction of JA and ET.

(A) JA is synthesized from α -linolenic acid from the chloroplast membrane. The activity of a 13-lipoxygenase (13-LOX), a 13-allene oxide synthase (13-AOS) and an allene oxide cyclase (AOC) leads to the production of 12-oxo-phytodienoic acid (OPDA). Then OPDA is reduced by OPDA-reductase (OPR3) and subjected to an β -oxidation to synthesize JA. The synthesis of ET originates

from methionine. S-AdoMet is converted by S-AdoMet (SAM) synthetase. ACC, the precursor of ET can be synthesized by ACC oxidase and converted to ET. (B) JA and ET can synergistically activate EIN3 and EIL1, positive regulators of ERF1 and ORA59, leading to the induction of PDF1.2. The active form JA-Ile can be recognized by COI1 and co-receptor InsP5, causing the degradation of JAZs. There are two antagonistic branches in JA response: MYC branch and ERF branch. JAZ proteins can suppress the activity of MYC2, the positive regulator of VSP2, by enrolling the negative regulator TPL *via* MINJA. MYC2 can directly interact with MED25, an subunit of the mediator. MYC2 can activate the expression of ANACs to up-regulate VSP2. MYC3 and MYC4 can activate JA response additively with MYC2. In the ERF branch, JAZs can inhibit the activity of EIN3 and EIL1 by direct association with them and enrollment of HDA6. In the ET pathway, there are five ethylene receptors localized in the ER membrane. By binding to ET, CTR1 is deactivated by ET receptors. CTR1 can inhibit EIN2, which activates EIN3 and EIL1 by preventing the degradation of them *via* EBF1 and EBF2. Activation (closed arrowhead), suppression (\perp) and important genes are indicated.

1.5. SA-JA/ET cross-talk

1.5.1. Antagonistic interactions of SA-JA pathways

The mutually antagonistic effect between the SA and JA pathways is quite well-known (Glazebrook, 2005; Vlot et al., 2009). NPR1 acts as a crucial modulator in SA-mediated suppression of JA signaling. It has been reported that nuclear localization of NPR1 is required for activation of SA response, but not for SA-mediated suppression, however, of JA response (Spoel et al., 2003). This indicates that cytosolic NPR1 is capable of suppressing the JA pathway. Furthermore, nuclear NPR1 is required for expression of transcription (co)factors that suppress JA-dependent gene expression such as *GLUTAREDOXIN 480* (*GRX480*), *TGAs*, and *WRKYs* (Spoel et al., 2003; Li et al., 2004; Ndamukong et al., 2007) (Figure 3), suggesting suppression on JA response also in a NPR1 nucleus-dependent manner. *GRX480* plays a role in SA-JA cross-talk, by suppressing JA-mediated response, in an NPR1-dependent manner (Ndamukong et al., 2007). Additionally, expression of marker gene *PDF1.2* in the mutant *npr1*, after pharmacological application of SA and MeJA, showed that SA suppression on the JA pathway is dependent on NPR1 (Leon-Reyes et al., 2009).

Many other regulators have been reported to play roles in cross-talk of SA and JA pathways such as MYC2 and the WRKY TFs WRKY70, WRKY50, WRKY51 and WRKY33 which exert antagonistic influences on SA-JA communication (Laurie-Berry et al., 2006; Li et al., 2006; Vlot et al., 2009; Gao et al., 2011; Birkenbihl et al., 2012). Among them, WRKY70, WRKY50 and WRKY51 show suppression of the JA response through an NPR1-independent mechanism (Gao et al., 2011) (Figure 3), even though they can be regulated by NPR1. Interestingly, ET can bypass NPR1-dependency to render suppression of SA on JA (Leon-Reyes et al., 2009).

The suppression of the JA pathway by the SA pathway was localized downstream of JA synthesis, JAR1 and SCF^{COI1}, which targets JAZs for degradation (Leon-Reyes et al., 2010; Van der Does et al., 2013). The suppression of the JA pathway by the SA pathway is exerted *via* inhibiting the expression of the transcriptional activator ORA59, which targets GCC-box motifs in JA-responsive promoters (Van der Does et al., 2013), though it is unclear whether or not it is dependent on NPR1.

The inhibition of SA pathway by JA pathway is through the activation of three homologous NAC TF genes *ANAC019*, *ANAC055* and *ANAC072* (Figure 3). These can also be activated by the phytotoxin coronatine (COR), which requires SCF^{COI1} and MYC2. These TFs exert an inhibitory effect *via* suppressing ICS1, a positive regulator of SA synthesis, and activate BASAL TRANSCRIPT LEVEL OF THE SA METHYL TRANSFERASE 1 (BSMT1), which transforms SA to the inactive SA ester (Figure 3). Additionally, *ANAC019*, *ANAC055* and *ANAC072* can be activated by ABA application, suggesting a role in the antagonism of ABA pathway on SA pathway (Zheng et al., 2012) (see below). Consistent with this, the up-regulation of *ANAC019* and *ANAC055* by both MeJA and ABA was dependent on MYC2 (Bu et al., 2008).

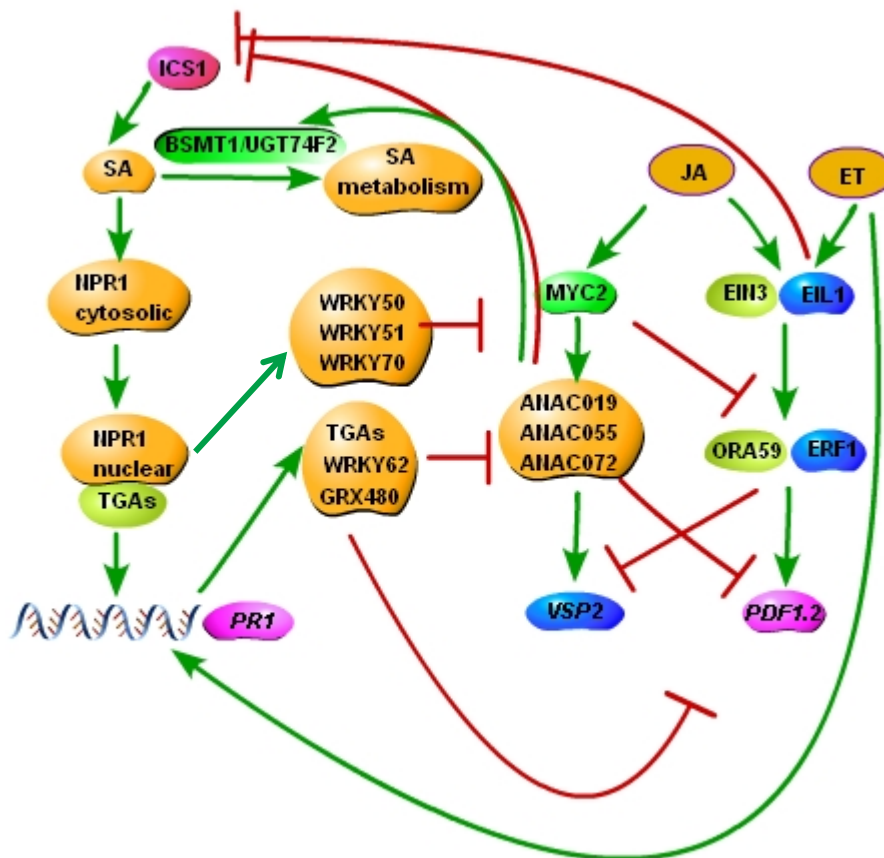


Figure 3. Interactions between the SA and the JA /ET pathways.

ET can synergistically induce PR1 *via* an unknown mechanism. SA and JA/ET are mostly antagonistic to each other. On the left-hand (SA) side, cytosolic localization of NPR1 is sufficient for suppression on JA/ET response. Some components regulated by NPR1 such as WRKY62, TGAs and GRX480 can confer the suppression on JA response. Some WRKYs such as WRKY50, WRKY51 and WRKY70 can suppress JA response independent from NPR1. The suppression of the JA pathway by the SA pathway is downstream of JA synthesis having no influence on JAZes accumulation, but, however, results in the degradation of ORA59. On the right-hand (JA) side, JA can suppress the SA response by inducing ANACs, regulated by MYC2. ANACs can inhibit ICS1 however enhance the BSMT1 and UGT74F2 to elevate SA accumulation. Furthermore, EIN3 and EIL1 can suppress ICS1 activity by directly binding to the promoter of *ICS1*. Activation (closed arrowhead), suppression (\perp), hypothesis activation (dashed line) and important genes are indicated.

1.5.2. Synergistic interaction of SA and JA pathways

Despite the well-known antagonistic effect, synergistic actions of SA and JA pathways have also been frequently reported (Schenk et al., 2000; van Wees et al., 2000; Spoel et al., 2003; Mur et al., 2006; Hebelstrup et al., 2012; Buxdorf et al., 2013). It has been reported that both SA- and JA-mediated responses are activated by the epiphytic fungus *Pseudozyma aphidis* (Buxdorf et al., 2013). A low light ratio of low red: far-red light compromises both SA and JA-dependent responses in *Arabidopsis*, though the mechanism is still unclear (de Wit et al., 2013). In the *edr1 gsl5* double mutant, SA and JA marker genes were synergistically activated, though the single gene mutations *edr1* and *gsl5* only prime the SA response (Wawrzynska et al., 2010). Exogenous application of low concentrations of both SA and JA can synergistically up-regulate both SA and JA pathways (Mur et al., 2006).

ROS, NO, and mediator, which is a multiprotein complex that functions as a transcriptional coactivator in all eukaryotes, are believed to positively regulate both SA and JA pathways. NO was established to have positive influence on defense against both biotrophic and necrotrophic pathogens. Ozone exposure to plants generated reactive oxygen species (ROS) and could trigger all SA, JA and ET responses. ET synthesis preceded both SA and JA production (Wang et al., 2002). The loss of function of *GLB1*, encoding haemoglobin, led to the enhanced resistance to both biotrophs and necrotrophs, concomitant with elevated NO accumulation after both infections (Mur et al., 2012). The mutation of Mediator subunit 16 (MED 16) blocked both the induction of JA and SA responses (Zhang et al., 2012). Furthermore, flg22, regulating PTI, can enhance SA, JA and ET pathways (Zipfel et al., 2004; Tsuda et al., 2008). Despite the progress made in exploring the convergence of SA and JA pathways, the regulation of the SA-JA equilibrium is still unclear yet. The overall fitness of

plants is costly impaired, concomitant with the activation of defense responses. The equilibrium of both pathways requires to be tightly controlled (Figure 3).

1.6. Non SA, JA, ET-mediated responses

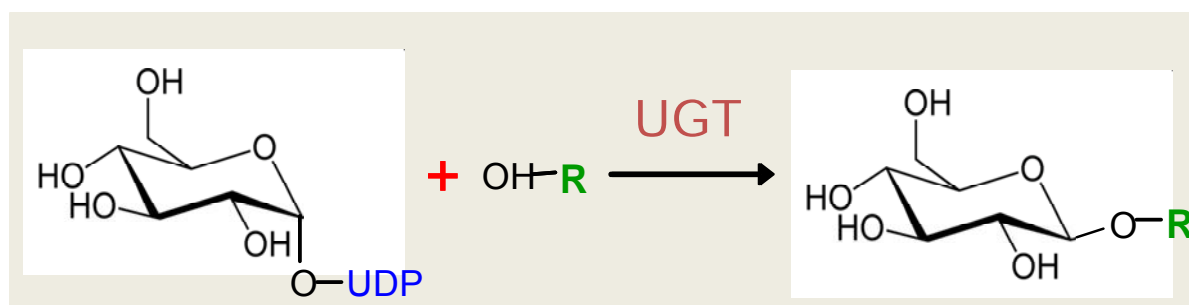
In addition to the major roles of SA, JA and ET pathways in plant defense, other hormone pathways can mediate plant defense as well. ABA signaling was found to antagonize the plant immunity by suppressing SA-dependent defenses. Furthermore, after wounding or herbivory, ABA can act synergistically with the JA pathway, through positively regulating the MYC branch of the JA response. Auxin, a major phytohormone operating plant development, can manipulate plant defense by suppressing SA levels and signaling. In turn, SA signaling can repress the auxin pathway. However, how auxin and SA interact is still unknown. Cytokinins (CKs), which affect plant growth and development, can modulate plant immunity, probably by synergistically influencing the SA response. Gibberellins (GAs) are yet another class of hormones that control plant growth; GA signaling leads to the degradation of growth-repressing DELLA proteins. Interestingly, DELLA proteins have been shown to interact with JAZ proteins to hinder JAZ from inhibiting the activity of transcriptional factors. Thus, GAs negatively influence the JA pathway by the regulation of DELLA degradation (Robert-Seilanianantz et al., 2011).

1.7. Plant UDP-glycosyltransferase modulates plant defense *via* interacting with SA and JA pathways

1.7.1. UDP-glycosyltransferase

In plants, more than 100,000 compounds are produced through secondary metabolism. The majority of them are modified *via* hydroxylation, methylation, acylation or attachment to small molecules. Among them, glycosylation is one of the most common modifications, transferring glucose to small organic molecules to form glucosides, thereby regulating the bioactivity, solubility or stability (Gachon et al., 2005). Plant UDP-glycosyltransferases (UGTs) accept UDP-activated carbohydrates at a conserved carboxy-terminal domain and recognize diverse substrates by a more variable amino terminal region. UGTs play important roles in the regulation of activity of signaling molecules and defense compounds, modification of secondary metabolites and detoxification of xenobiotics (Jones and Vogt, 2001) (Figure 4). The amino acid length of UGTs varies from 400 to 500, with a variable similarity from 30 % identity to 95 % identity. UDP-Glucuronosyltransferases, the main

UDP-glycosyltransferases of mammalian cells, catalyze the conjugation of glucuronic acid from UDP-glucuronic acid as the sugar donor to internal or external aglycons. Despite the well-known localization of mammalian UGTs in the endoplasmic reticulum, plant UGTs are widely believed to localize in the cytoplasm (Radomska-Pandya et al., 1999). Many compounds were identified as substrates of UGTs by systematic recombinant protein assay, including many endogenous compounds, like auxin, abscisic acid, flavonoids, lignin precursors, hydroxybenzoic acids and xenobiotics such as herbicides. In spite of the broad substrate acceptance of UGTs *in vitro*, there is limited knowledge about their physiological roles in plants. So far, there is only evidence showing *Arabidopsis* UGT enzymes to have effects on flavonoids, SA, indole-3-acetic acid, glucosinolates and brassinosteroids. There are 122 UGT isoforms in *Arabidopsis*. However, most of them are orphan enzymes without known *in vivo* substrates and physiological roles (Bowles et al., 2005) (Figure 4).



UGTs

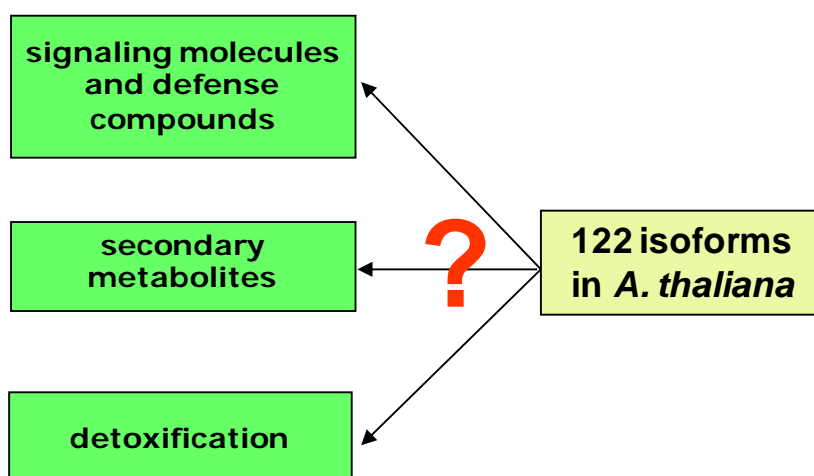


Figure 4. Scheme of reactions catalyzed by UGTs and physiological functions in *Arabidopsis*.

UGTs transfer a sugar moiety from UDPG to small organic molecules. 122 UGT isoforms exist in *Arabidopsis*. This glycosylation can regulate signaling molecules and defense compounds, secondary metabolites as well as detoxification.

1.7.2. UGTs and plant defense

Several *UGT* genes are induced by abiotic and biotic stresses. *UGT73B3* and *UGT73B5* have been reported to be required for resistance to *Pseudomonas syringae* in *Arabidopsis* (Langlois-Meurinne et al., 2005). *UGT84A2/BRT1* has recently been reported to be required for non-host resistance to the Asian soybean pathogen *Phakopsora pachyrhizi* (Langenbach et al., 2013). In *Arabidopsis*, *UGT74F1*, *UGT74F2* and *UGT75B1* can recognize SA as the substrate *in vitro* (Lim et al., 2002). However, only the loss-of-function of *UGT74F1* can enhance the resistance to pathogen infection probably due to the glycosylation of SA (Noutoshi et al., 2012).

The stress-responsiveness of the whole *Arabidopsis* family has been screened based on the public expression data, showing that *UGT76B1* is among the top-stress induced UGTs, highly responsive to both abiotic and biotic cues. Based on our previous results, *UGT76B1* is a novel player in SA-JA cross-talk, suppressing SA marker genes, for instance *PRI*, but enhancing the JA pathway, for instance *VSP2* (von Saint Paul, 2010) (Figure 5). SA marker genes were enhanced while JA marker genes were suppressed in the *ugt76b1* mutant. The loss function of *UGT76B1* showed enhanced resistance to the biotrophic pathogen *Pseudomonas syringae* and early senescence, accompanied by elevated SA levels. The *UGT76B1* overexpression line showed opposite phenotypes. However, the susceptibility towards necrotrophic pathogens was not tested. The transcription factor *WRKY70* is a known player, positively regulating the SA pathway but suppressing the JA pathway (Li et al., 2004). The expression of *WRKY70* was negatively correlated with *UGT76B1* expression, suggesting that *UGT76B1* might overrule the effects of *WRKY70*. Isoleucic acid, an amino acid related molecule, was identified as a substrate of *UGT76B1* through ultra-high-resolution mass spectrometric analysis in combination with *in vitro* recombinant enzyme tests. This study first identified ILA as a substrate of *UGT76B1* by a non-targeted metabolomic analysis. The role of *UGT76B1* in plant defense indicates that ILA may play a role in plant defense and requires further research (von Saint Paul, 2010) (Figure 5).

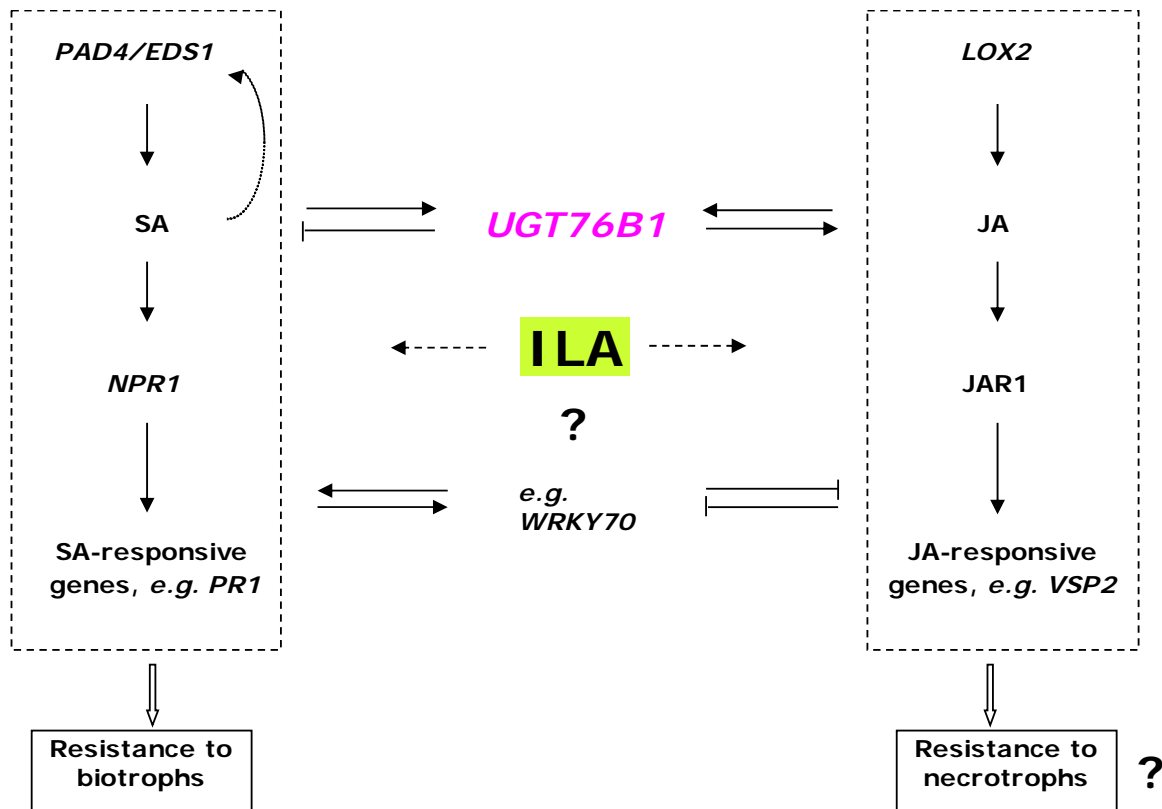


Figure 5. Model of the involvement of *UGT76B1* as a novel mediator in SA- and JA-dependent regulation of defense responses.

UGT76B1 induces the JA response and represses the SA pathway, having a negative influence on the resistance to *P. syringae*. The enhancement of JA pathway by *UGT76B1* indicates that *UGT76B1* may regulate defense against necrotrophs. *ILA* as the substrate of *UGT76B1* may also have influence on defense. Key steps of both pathways are shown. Signaling molecules (bold), enzymatic transformations (pointed and open arrowhead), activation (closed arrowhead), suppression (\perp) and important genes are indicated.

1.8. Aim of this work

Based on previous results from Veronica von Saint Paul in our laboratory, *UGT76B1* is a novel player in SA- and JA- mediated defense response and ILA has been identified as an endogenous substrate of UGT76B1. The goal of this project was to further explore the role of UGT76B1 and ILA in plant defense.

The first aim was to understand how and where UGT76B1 is integrated into the SA and JA crosstalk. This included the question whether the antagonistic effect of UGT76B1 on the SA-JA cross-talk could be also reflected in the susceptibility of lines with the altered *UGT76B1* expression towards necrotrophic pathogens. Extensive genetic studies on mutants in *Arabidopsis* have revealed many crucial components of both SA and JA pathways (see above). This will allow a genetic strategy to introgress such lines into plants with altered *UGT76B1* expression to study the impact on the SA and JA pathways.

The second aim was to explore how ILA can impact plant defense. In general, the strategy was to investigate the effect of ILA on defense through analysis of defense marker genes in various genetic backgrounds, non-targeted microarray analysis of gene expression patterns, and finally the role in protecting plants against pathogen infection.

The third aim was to study the connection of UGT76B1 and ILA in activating plant defense. Therefore the gene expression profiles in response to ILA *vs.* *UGT76B1* expression were compared using non-targeted microarray analysis. Furthermore, another strategy was adopted to compare the defense response of mutants deficient in SA and JA pathways in response to ILA application and the alteration of *UGT76B1* expression.

2. RESULTS

2.1. *UGT76B1* expression positively correlates with resistance against necrotrophic pathogen infection

UGT76B1 is highly responsive to biotic stresses based on public expression data. Previously, the negative correlation of *UGT76B1* expression and resistance to the biotrophic pathogen *Pseudomonas* has been found. Additionally, *UGT76B1* expression positively regulates JA-mediated response, which is mainly responsible for defense against necrotrophic pathogens (von Saint Paul, 2010).

To assess whether the altered expression of *UGT76B1* can also influence the susceptibility towards necrotrophic pathogens, the infection symptoms were observed after droplet inoculation by the necrotrophic fungus *Alternaria brassicicola* in *ugt76b1-1*, *UGT76B1-OE-7* and Col-0. Whole leaves infected with *Alternaria brassicicola* in *ugt76b1-1* became yellow, whereas leaves of the control Col-0 showed only small yellowish parts. However, leaves of *UGT76B1-OE-7* showed nearly no symptoms after the same infection (Figure 6). This indicated that the mutant *ugt76b1-1* exhibited enhanced susceptibility, whereas the *UGT76B1* overexpression line was more resistant to *A. brassicicola*. Thus, *UGT76B1* expression positively correlates with resistance against necrotrophic pathogen infection.

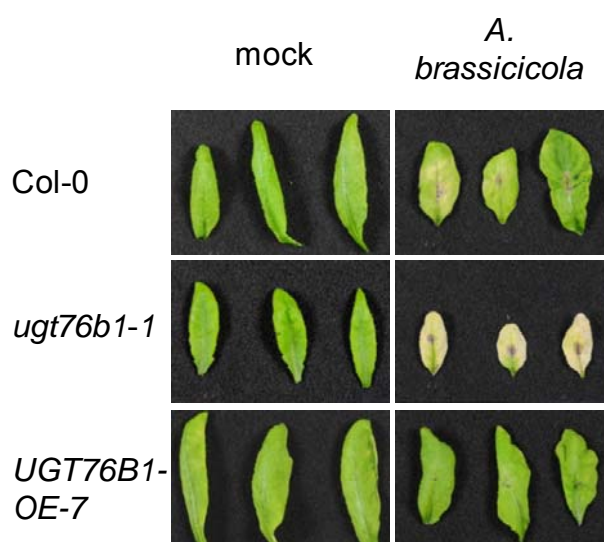


Figure 6. Pathogen susceptibility is positively correlated with *UGT76B1* expression

Enhanced/decreased resistance of *UGT76B1-OE-7/ugt76b1-1* lines to *Alternaria brassicicola*. Four-week-old plants were infected with 7.5×10^3 spores (see Methods). Pictures were taken 13 days after infection. Twelve plants were infected for each line. The experiments were repeated several times with similar results.

2.2. Integration of *UGT76B1* into SA and JA pathways

2.2.1. Dependence of *UGT76B1*-mediated response on SA and JA pathway

Previously, *UGT76B1* has been shown to be a regulator in SA-JA cross-talk, suppressing SA pathway and activating JA pathway (von Saint Paul, 2010).

To elucidate how *UGT76B1* integrates into SA and JA pathways, both *ugt76b1-1* and *UGT76B1-OE-7* were introgressed in lines deficient in either SA or JA pathways. The *NahG* overexpression lines completely block SA accumulation by introducing a bacterial *NahG* gene, encoding a hydrolase activity towards SA (Gaffney et al., 1993). The *sid2* mutant leads to the loss of stress-induced SA synthesis, where only a basal level of 5-10% SA remains (Nawrath and Metraux, 1999). The *npr1* mutation causes the loss-of-function of a major positive regulator activating the SA pathway through interaction with TGA transcription factors (Cao et al., 1997). The mutant *jar1* blocks JA pathway due to inability to synthesize bioactive JA-Ile conjugates (Berger, 2002).

Marker genes of SA or JA pathways were measured by RT-qPCR to evaluate SA or JA-mediated response. Marker genes for SA pathway include *PR1*, *EDS1* (Figure 1), *SAG13*, and *WRKY70* (Figure 3), while marker genes for JA pathway are *PDF1.2* and *VSP2* (Figure 2).

The induction of *PR1* and *SAG13* by *ugt76b1-1* was completely abolished in *ugt76b1 NahG* with the same background expression level as in *NahG*, suggesting that induction of both genes in *ugt76b1* was dependent on SA levels. However, *PR1* and *SAG13* can still be effectively induced by *ugt76b1* in a *sid2* background, independent from *SID2*. Overexpression of *UGT76B1* was still effective to suppress expression of *PR1* and *SAG13* in *sid2* indicating that the suppression of *PR1* and *SAG13* expression by *UGT76B1* overexpression was independent from *SID2* (Figure 7A). On the other hand, the expression of the JA marker *VSP2* in *ugt76b1 NahG* was enhanced to the same level as in *NahG*, indicating that the suppression of the JA pathway by *ugt76b1-1* was dependent on SA levels. *UGT76B1* was effective to induce *VSP2* expression in a *sid2* background, suggesting that the *UGT76B1*-dependent enhancement of *VSP2* was independent from *SID2* (Figure 7A). However, the loss-of-function of *UGT76B1* could not further suppress *VSP2* expression in *sid2*. Notably, *VSP2* was only suppressed by the *ugt76b1* mutant around twofold, much less than the change of more than tenfold induction by *UGT76B1* overexpression. This suggested that *VSP2* was less sensitive to the regulation by *ugt76b1* than to the regulation by *UGT76B1* overexpression. Since basal

UGT76B1 expression was quite low in Col-0 whereas *UGT76B1* overexpression greatly increased the expression of *UGT76B1*, the different sensitivities of *VSP2* in response to the *ugt76b1* knockout and the *UGT76B1* overexpression could be explained. Thus, the lack of regulation of *VSP2* in response to loss-of-function of *UGT76B1* in *sid2* could be also due to the lower sensitivity. Therefore the positive regulation of *VSP2* by *UGT76B1* might be independent from *SID2*.

The activation of *PR1* and *SAG13* by *ugt76b1* was still effective in *npr1* (Figure 7B), suggesting an *NPR1*-independent manner of induction. In agreement, overexpression of *UGT76B1* was also effective to suppress *PR1* and *SAG13*. Thus, *UGT76B1* could regulate expression of *PR1* and *SAG13* independent from *NPR1*. The suppression of *EDS1* and *WRKY70* by *UGT76B1* overexpression was also effective in *npr1*, suggesting a regulation of *EDS1* and *WRKY70* independent from *NPR1*. In contrast, the expression of *EDS1* and *WRKY70* in *ugt76b1 npr1* was the same as in *npr1*. Though the loss-of-function of *UGT76B1* seemed not to regulate *EDS1* and *WRKY70* in *npr1*, it at least did not contradict the effect of *UGT76B1* overexpression. *EDS1* and *WRKY70* were only slightly induced in the *ugt76b1* knockout whereas they were much stronger suppressed by *UGT76B1* overexpression as compared to Col-0 (Figure 7B). This suggested that the regulation of *EDS1* and *WRKY70* was not sensitive to the loss-of-function of *UGT76B1*, probably because the basal expression of *UGT76B1* in Col-0 was already very low. The *UGT76B1* overexpressor greatly increased *UGT76B1* expression and activated *EDS1* and *WRKY70* effectively. Therefore, *UGT76B1* mostly likely negatively regulated *EDS1* and *WRKY70* independent from *NPR1* (Figure 7B). The constitutive expression of *UGT76B1* effectively increased *VSP2* expression in the *npr1* background suggesting that the *UGT76B1*-dependent enhancement of *VSP2* was independent from *NPR1*. In contrast, the loss-of-function of *UGT76B1* seemed to induce *VSP2* in *npr1* also, suggesting the negative regulation of *VSP2* expression by *UGT76B1* in *npr1* background, contrary to the positive regulation of *VSP2* expression by *UGT76B1* in Col-0. This might suggest that the loss-of-function of *UGT76B1* had a direct negative role in regulating *VSP2* in the *npr1* background whereas the positive regulation of *UGT76B1* on *VSP2* in Col-0 was mostly coming from the SA pathway *via* SA and JA cross-talk.

The *jar1* mutant did not influence expression of *PR1* and *SAG13* in *ugt76b1-1*. The *jar1* mutant compromised in the JA pathway probably resulted in reduction of suppression on the SA pathway by the JA pathway. It is reasonable that in the *jar1* mutant, SA-mediated responses (*PR1* and *SAG13*) could be activated relative to Col-0. However, *PR1* and *SAG13*

were still suppressed by *UGT76B1-OE-7* in combination with *jar1* (Figure 7C). Therefore the suppression of *PR1* and *SAG13* by *UGT76B1* was directly due to the SA pathway but not the antagonism of the JA pathway *via* cross-talk. The enhancement of *VSP2* in *UGT76B1-OE-7* was eliminated by *jar1*, suggesting the activation of JA response by *UGT76B1-OE-7* was dependent on *JAR1*.

Thus, both the enhancement of SA and suppression of JA pathways by *ugt76b1-1* were dependent on SA. *UGT76B1* might regulate SA marker genes (*PR1*, *SAG13*, *EDS1* and *WRKY70*) and JA maker gene (*VSP2*) independent from both *SID2* and *NPRI*.

SAG13 is a senescence marker gene and at least partially SA-dependent (Miller et al., 1999; Yoshida et al., 2001). Both the early senescence in *ugt76b1-1* and delayed senescence in *UGT76B1-OE-7* have been reported to be consistent with induction of *SAG13* in *ugt76b1-1* and suppression of *SAG13* in *UGT76B1-OE-7* relative to Col-0 (von Saint Paul, 2010). The expression of *SAR13* was lower in both the *ugt76b1 sid2* and *ugt76b1 npr1* double mutants than in Col-0 (Figure 7A and B). In contrast, *SAG13* expression in *ugt76b1-1* was not influenced by the mutation of *JAR1* at all (Figure 7C). This suggested that senescence marker gene *SAG13* expression was dependent on SA and *NPRI*, but not *JAR1*. To investigate whether an early senescence phenotype developed in *ugt76b1-1* was dependent on SA and JA pathways, I observed the senescence development in the *ugt76b1 sid2*, *ugt76b1 npr1*, *ugt76b1 NahG* and *ugt76b1 jar1* double mutants. The early senescence phenotype was abolished in the *ugt76b1 sid2*, *ugt76b1 npr1* and *ugt76b1 NahG* double mutants, suggesting that the early senescence developed in *ugt76b1-1* was dependent on SA and *NPRI*. However the double mutant *ugt76b1 jar1* still developed the early senescence phenotype as *ugt76b1-1*, indicating the early senescence phenotype of *ugt76b1* was independent from *JAR1*. Interestingly, the retarded growth of the *jar1* mutant was gone in both *ugt76b1 jar1* and *UGT76B1-OE-7 jar1*. No obvious growth difference was observed in *UGT76B1-OE-7* with or without combination with *jar1*, *sid2* and *npr1* (Figure 8).

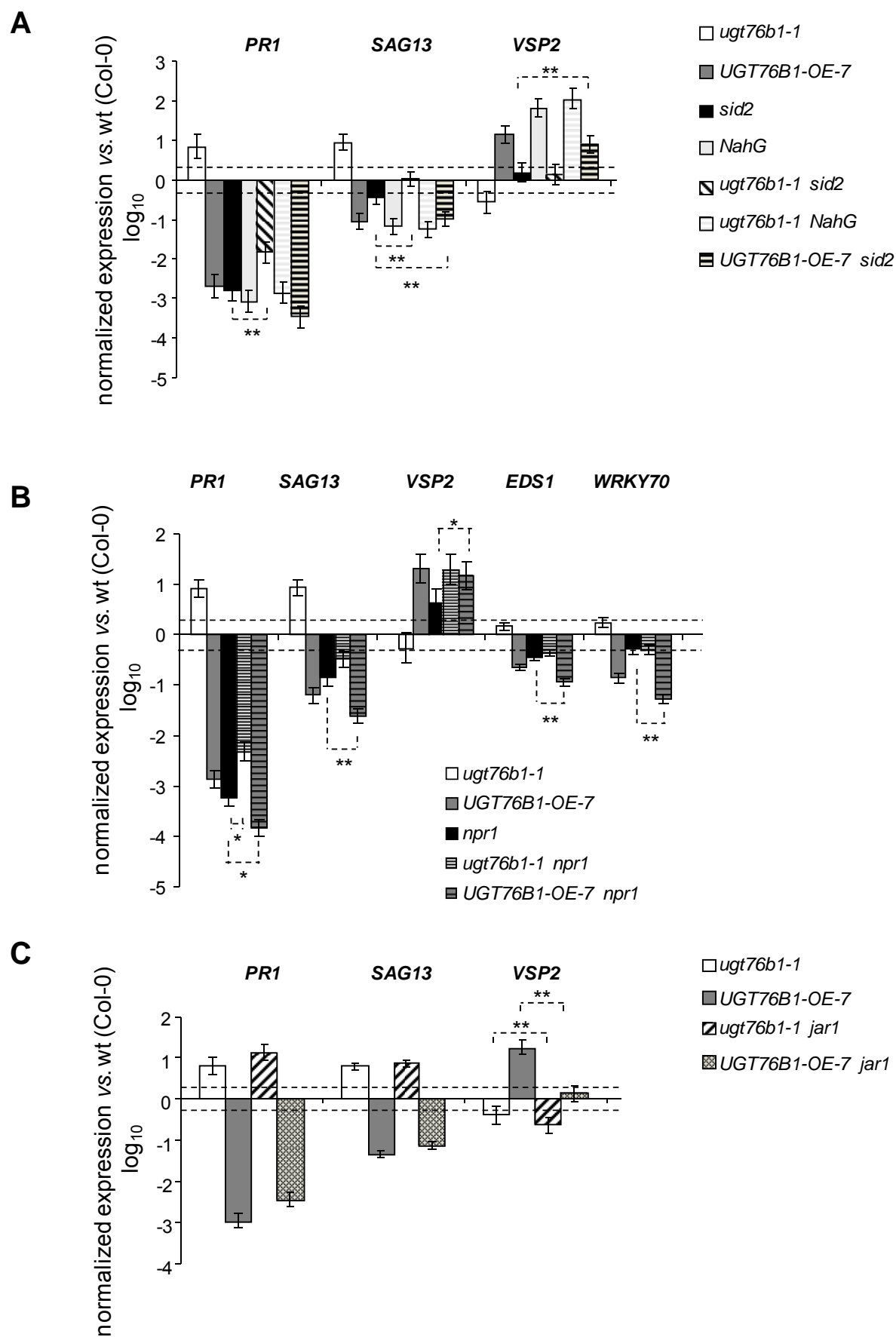


Figure 7. SA and JA marker genes expression in *UGT76B1* overexpression and knockout lines after introgression into *sid2*, *NahG*, *npr1* and *jar1*.

Gene expression of *PR1*, *SAG13*, *VSP2*, *EDS1* and *WRKY70* in 4-week-old *ugt76b1-1*, *UGT76B1-OE-7* and double mutants (with: (A) *sid2* and *NahG*, (B) *npr1*, (C) *jar1*) was measured by RT-qPCR. Expression levels were normalized to *UBIQUITIN5* and *S16* transcripts; levels relative to Col-0 plants are displayed. Arithmetic means and standard errors from log₁₀-transformed data of at least 4 independent replicates from two separate experiments were calculated using ANOVA. The significance for the difference of *PR1*, *SAG13*, *VSP2*, *EDS1* and *WRKY70* expression was measured, compared between lines (*ugt76b1 NahG*, *UGT76B1 NahG*, *ugt76b1 sid2*, *UGT76B1 SID2*, *ugt76b1 npr1* and *UGT76B1 npr1*) and corresponding single mutants *sid2*, *NahG* (A), *npr1* (B) and *jar1* (C) respectively. Stars indicated the significance of the difference between the two bars connected by the dotted line: ** p-value ≤ 0.01 , * p-value ≤ 0.05 .

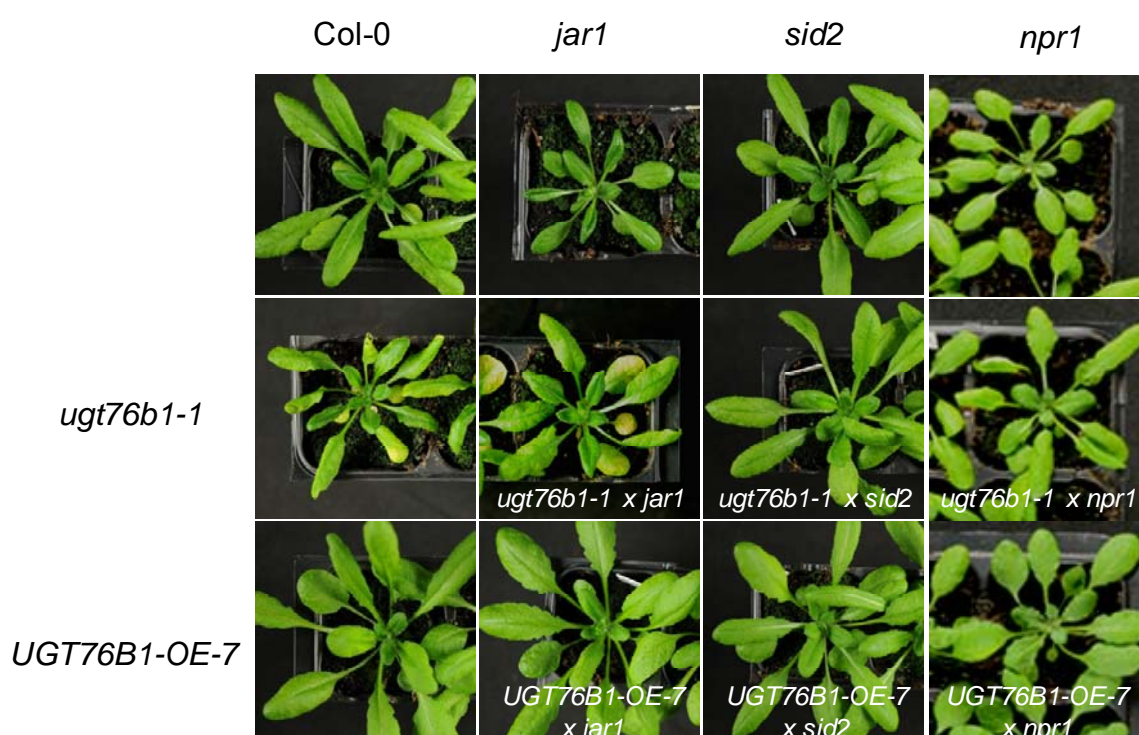


Figure 8. The impact of *UGT76B1* expression on the onset of senescence is dependent on *SID2* and *NPRI*, but independent from *JARI*.

Pictures were taken from four-week-old *Arabidopsis* plants.

2.2.2. *UGT76B1* impact on JA pathway is independent from JA synthesis

UGT76B1 has been previously shown to be a novel player in SA-JA crosstalk, suppressing SA response while enhancing JA response. This is accompanied by elevated SA levels in *ugt76b1-1* and slightly decreased SA levels in *UGT76B1-OE-7*, indicating an impact of *UGT76B1* on SA synthesis (von Saint Paul, 2010). It has been demonstrated that the activation of *VSP2* by *UGT76B1* overexpression is dependent on *JARI*, responsible for

synthesizing the bioactive compound JA-isoleucine (Figure 7C). Nevertheless the impact of *UGT76B1* on JA biosynthesis is still unknown.

To test whether *UGT76B1* influences JA biosynthesis, JA-related metabolites JA, JA-Ile and OPDA were measured. However, all three metabolites were below the detection limit in Col-0, *ugt76b1-1* and *UGT76B1-OE-7*, suggesting no obvious impact of *UGT76B1* on JA synthesis.

Since wounding can trigger JA synthesis, JA-related metabolites were also addressed in Col-0, *ugt76b1-1* and *UGT76B1-OE-7*, 30 min after wounding to analyze whether *UGT76B1* could influence JA synthesis after this exogenous stimulus. In parallel, the expression of marker genes from SA pathway (*EDS1* and *PR1*) and JA pathway (*PDF1.2*, *VSP2*, *JAR1* and *JAZ1*) were measured by RT-qPCR after wounding. After wounding, JA, JA-Ile and OPDA accumulated to a slightly higher level in *ugt76b1-1* and to a slightly lower level in *UGT76B1-OE-7* in comparison to wild type (Figure 9A), although the naïve knockout line had suppressed and the constitutive overexpression had upregulated the JA pathway. *JAZ1* is an early JA-responsive marker gene. *JAZ1* was induced to a high level after wounding without any difference among Col-0, *ugt76b1-1* and *UGT76B1-OE-7* (Figure 9B). This suggested that the activation of *JAZ1* was independent from the synthesis of JA-related metabolites which at least showed a tendency to be regulated by *UGT76B1* expression after wounding. This inconsistent situation was similar to cases of the *wrky33* and *ssi1* mutants, where the final JA response was suppressed despite enhancement of JA synthesis (Kachroo et al., 2003; Birkenbihl et al., 2012). Thus, after wounding the impact of *UGT76B1* on activation of *JAZ1* should be independent from JA synthesis. Furthermore, 30 minutes after wounding, SA marker genes *EDS1* and *PR1* were still induced in *ugt76b1-1*, but suppressed, however, in *UGT76B1-OE-7* relative to Col-0, suggesting no influence of wounding on the SA pathway, 30 minutes after wounding. *PDF1.2* was quite variable. However, *VSP2* could be induced by wounding (Figure 9B). *VSP2*, as a late wounding marker gene, usually responds 6 h after wounding. Consistently 30 min after wounding *VSP2* was only slightly induced in Col-0 still showing suppression in *ugt76b1-1* and induction in *UGT76B1-OE-7* relative to Col-0 after wounding. It is possible that since the JA response may be activated higher by *UGT76B1* overexpression, less JA synthesis would be required for the activation in *UGT76B1* overexpression.

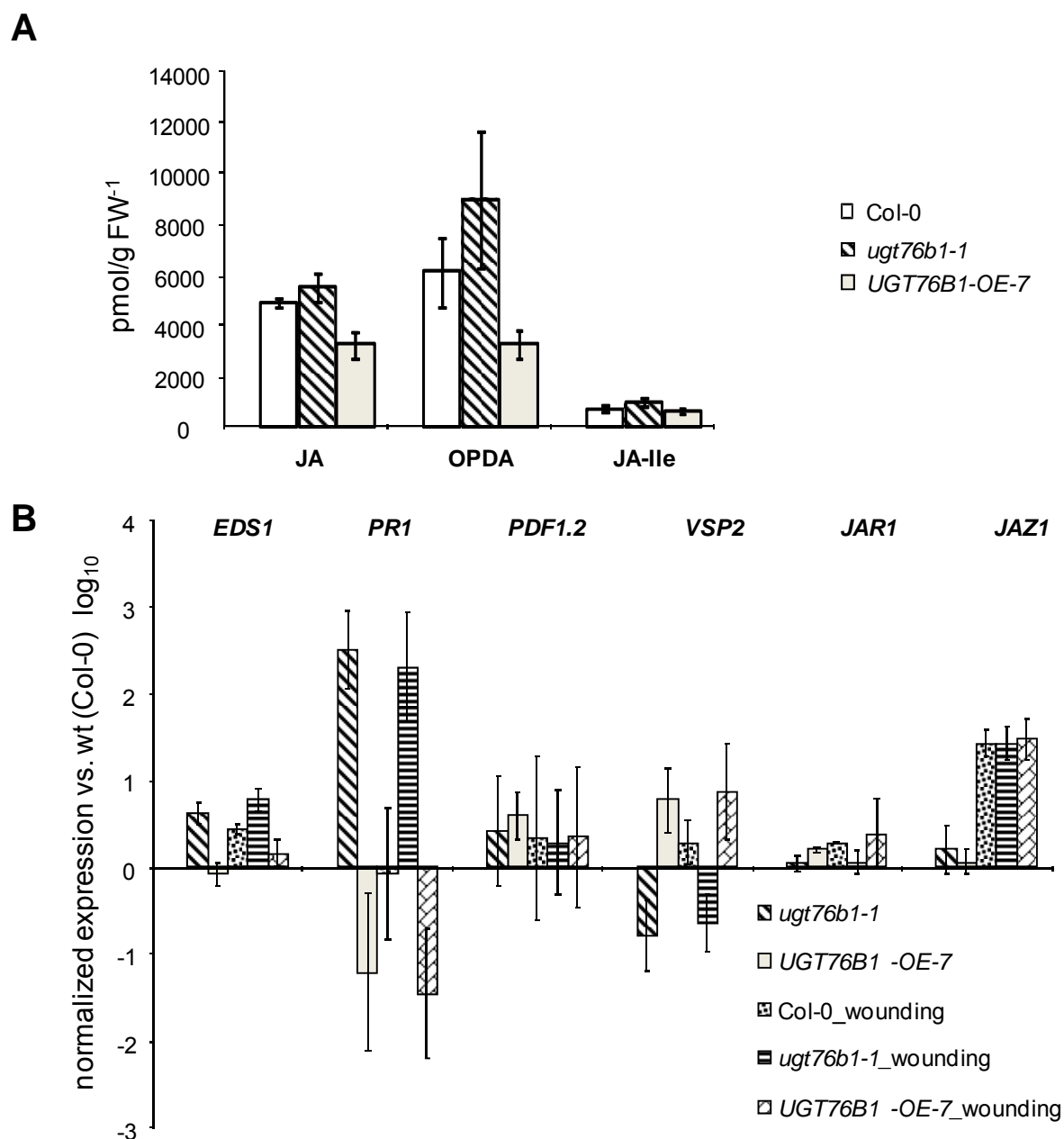


Figure 9. JA wounding response in *Arabidopsis* lines with different *UGT76B1* expression levels.

(A) The JA-related metabolites JA, OPDA and JA-Ile were measured in 4-week-old plants 30 minutes after wounding. The measurement was repeated with similar results. (B) Transcript levels of *EDS1*, *PR1*, *PDF1.2*, *VSP2*, *JAR1* and *JAZ1* were measured by RT-qPCR in leaves of 4-week-old plants directly or 30 minutes after wounding. Expression levels are normalized to *UBIQUITIN5* and *S16* transcripts; levels relative to Col-0 plants are displayed. Arithmetic means and standard errors of log₁₀-transformed data are calculated from three replicates.

2.3. Non-targeted microarray analysis

Veronica von Saint Paul (2010) has shown that the loss-of-function of *UGT76B1* can activate defense against the biotrophic pathogen *Pseudomonas*, accompanied by elevated expression of the defense marker genes *PR1* and *SAG13*. Additionally, ILA has been found to be a

substrate of UGT76B1 *in vivo* (von Saint Paul, 2010). Thus, one might speculate that the enhancement of defense in the *ugt76b1* mutant might be at least partially due to the lost activity of UGT76B1 to glucosylate ILA.

To further understand how ILA and *UGT76B1* impact on pathogen resistance and to address a potential connection of ILA and *UGT76B1* in plant defense, a transcriptome analysis was performed to compare expression patterns of *ugt76b1-1*, *UGT76B1-OE-7* and ILA-treated wild type (Col-0) relative to naïve Col-0. ILA was applied by spraying a 1 mM solution in water onto the leaves; all non-treated plants were sprayed with water as a mock control to allow a side-by-side comparison.

Four-week-old *Arabidopsis* plants were used for the experiments, since no visible, major developmental phenotype can be observed among *ugt76b1-1*, *UGT76B1-OE-7* and Col-0 at this stage. Whole transcriptome microarrays (Agilent) were used for the expression analyses. The data were evaluated and genes with more than twofold changes and a corrected p-value ≤ 0.05 were identified (Methods). According to these criteria, 769 genes were altered in *ugt76b1-1* with 539 genes being up- and 230 genes being downregulated in comparison to the wild type. Two hundred thirty three genes changed more than twofold in *UGT76B1-OE-7* with 64 genes being up- and 169 genes being downregulated. Eventually, 236 genes were altered by ILA with 212 being up- and 24 being downregulated (Figure 10). As a first analysis, a functional classification was performed utilizing functional categorization provided at TAIR (www.arabidopsis.org) among genes altered more than twofold in three comparisons respectively (ILA vs. Col, *ugt76b1-1* vs. Col and *UGT76B1-OE-7* vs. Col). It revealed that the enrichment pattern in three overrepresented classes of genes was quite similar: *response to stress*, *response to abiotic stress* or *biotic stress* and *signaling transduction*, suggesting that similar processes were mainly influenced by ILA and the altered *UGT76B1* expression levels in *Arabidopsis* (Figure 11). To further check whether any genes, and which genes, regulated by ILA or *UGT76B1* were directly related to pathogen defense or affected other processes in more detail, genes altered in the three comparisons (ILA vs. Col, *ugt76b1-1* vs. Col and *UGT76B1-OE-7* vs. Col) were analyzed for the genes annotation by MapMan (<http://mapman.gabipd.org/web/guest/mapman>). The detailed results are integrated below.

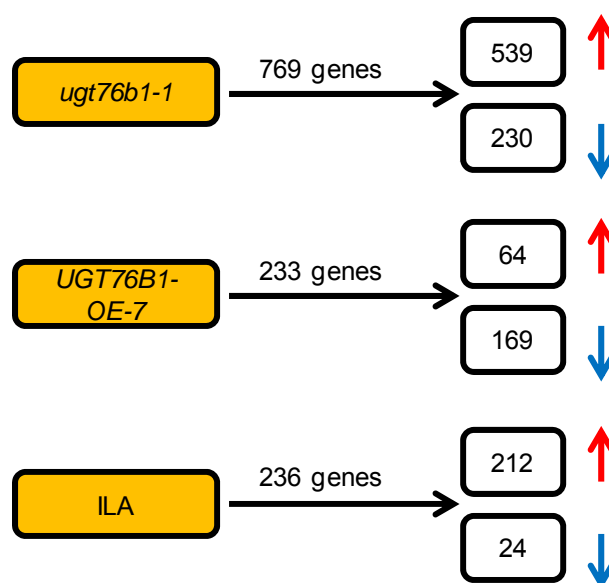


Figure 10. Transcriptional reprogramming of genes by *UGT76B1* expression or ILA treatment.

Microarray was performed using *Arabidopsis* Genechip from Agilent. Microarray analysis was compared among mock-treated (water) *ugt7b1-1*, mock-treated *UGT76B1-OE-7* and ILA-treated Col-0 relative to mock-treated Col-0. Differentially expressed genes by loss-of-function, overexpression of *UGT76B1* or ILA (twofold or more, $p \leq 0.05$) are indicated above the black arrow. Genes induced or suppressed more than twofold are indicated as “red arrow” and “blue arrow” respectively.

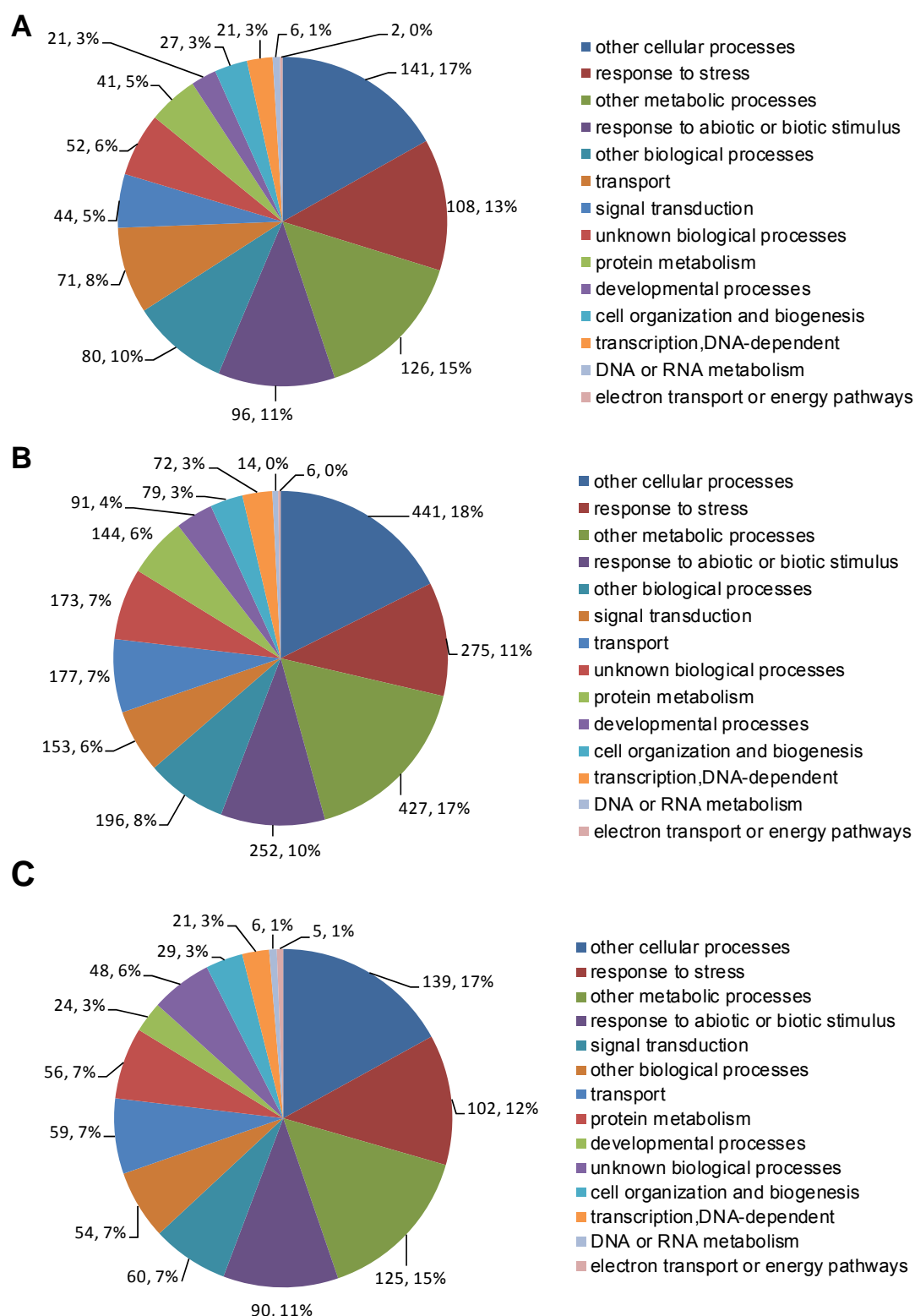


Figure 11. Pie chart analysis of genes regulated by ILA and *UGT76B1* according to GO enrichment.

(A) 236 genes, induced or suppressed more than twofold by ILA, were analyzed. (B) Seven hundred and sixty nine genes, induced or suppressed more than twofold by loss-function-of *UGT76B1*, were analyzed. (C) Two hundred thirty three genes, induced or suppressed more than twofold by gain-function-of *UGT76B1*, were analyzed.

2.3.1. *UGT76B1* expression negatively regulates SA-mediated response

UGT76B1 has been shown to antagonistically impact on SA and JA pathways. To further identify genes regulated by different *UGT76B1* expression levels, differential gene expressions were compared in *ugt76b1-1* and *UGT76B1-OE-7* relative to the wild type, Col-0. In *ugt76b1-1* expression of a total of 769 genes was altered twofold or more ($P \leq 0.05$) as compared to Col-0. Among 769 genes, 539 genes were upregulated and 230 genes were downregulated (Figure 10). According to MapMan more than 250 out of 769 genes were related to *pathogen defense response*, most of which were induced in *ugt76b1-1* (Figure 12 B). In *UGT76B1-OE-7* expressions of 233 genes were changed twofold or more ($P \leq 0.05$) compared with mock-treated Col-0. Among 233 genes, 64 genes were induced, whereas 169 genes were suppressed (Figure 10). About 90 out of 233 genes were related to defense response, most of which were suppressed by the constitutive expression of *UGT76B1* (Figure 12C). A total of 97 genes were oppositely regulated by loss-of-function and ectopic expression of *UGT76B1*; the vast majority, 94 genes, were upregulated in the *ugt76b1* knockout and downregulated by the *UGT76B1* overexpression (Figure 13A). Only 3 genes were induced by overexpression of *UGT76B1* but suppressed by the loss-of-function of *UGT76B1* (Figure 13C). Surprisingly, 21 genes were induced in both lines with different *UGT76B1* expression; however zero suppressed in both instances (data now shown). This strongly suggests that *UGT76B1* has a function mainly in suppressing a set of defense-responsive genes.

Different *UGT76B1* expression has been shown to manipulate SA metabolism, elaborated by elevated free SA in *ugt76b1-1*, but decreased free SA in *UGT76B1-OE-7* (von Saint Paul et al., 2011). To explore whether the 94 genes negatively correlated with *UGT76B1* expression respond to SA or JA stimuli or to infection by *P. syringae*, their expression in response to virulent *Pseudomonas syringae* pv. *tomato* DC3000 infection of wild type (vs. mock), *Pseudomonas syringae* pv. *maculicola* infection of *npr1-1* or *sid2* (vs. infected Col-0) or after treatment of Col-0 with BTH, SA or MeJA was extracted from the public database Genevestigator (<https://www.genevestigator.com/gv/plant.jsp>) (Zimmermann et al., 2005). Sixty six genes could match the corresponding probes, since different platforms and annotations had been employed in these and my studies. These 66 genes were divided into two classes, sorted by less than twofold change (Table 1) vs. a higher extent in response to SA treatment (Table 2). Very few genes were induced lower than twofold in response to SA treatment, among which the responsiveness of *RLP28* and *RLP43*, belonging to receptor-like

proteins was less than twofold to any elicitation from Genevestigator (Table 1). In contrast, *RLP28* and *RLP43* were more than twofold induced in *ugt76b1*, but suppressed in *UGT76B1* overexpression (Table 1). This indicated that *RLP28* and *RLP43* might only be specifically regulated by *UGT76B1*, but not responsive to treatment with SA and BTH as well as *Pseudomonas* infection. Most of the *UGT76B1*-dependent genes can be induced by *Pseudomonas* infection as well as by BTH and SA stimuli (Table 2). The induction of most of them showed *SID2* and *NPR1* dependence when infected with *Pseudomonas syringae* pv. *maculicola*, as compared to *Pseudomonas syringae* pv. *maculicola* infection of Col-0. Furthermore, about one half of these sixty six genes were repressed by MeJA (Table 1 and 2). Thus, *UGT76B1* had a major role in suppressing a set of SA-responsive genes, which could be regulated via *SID2* and *NPR1* (Table 1 and 2).

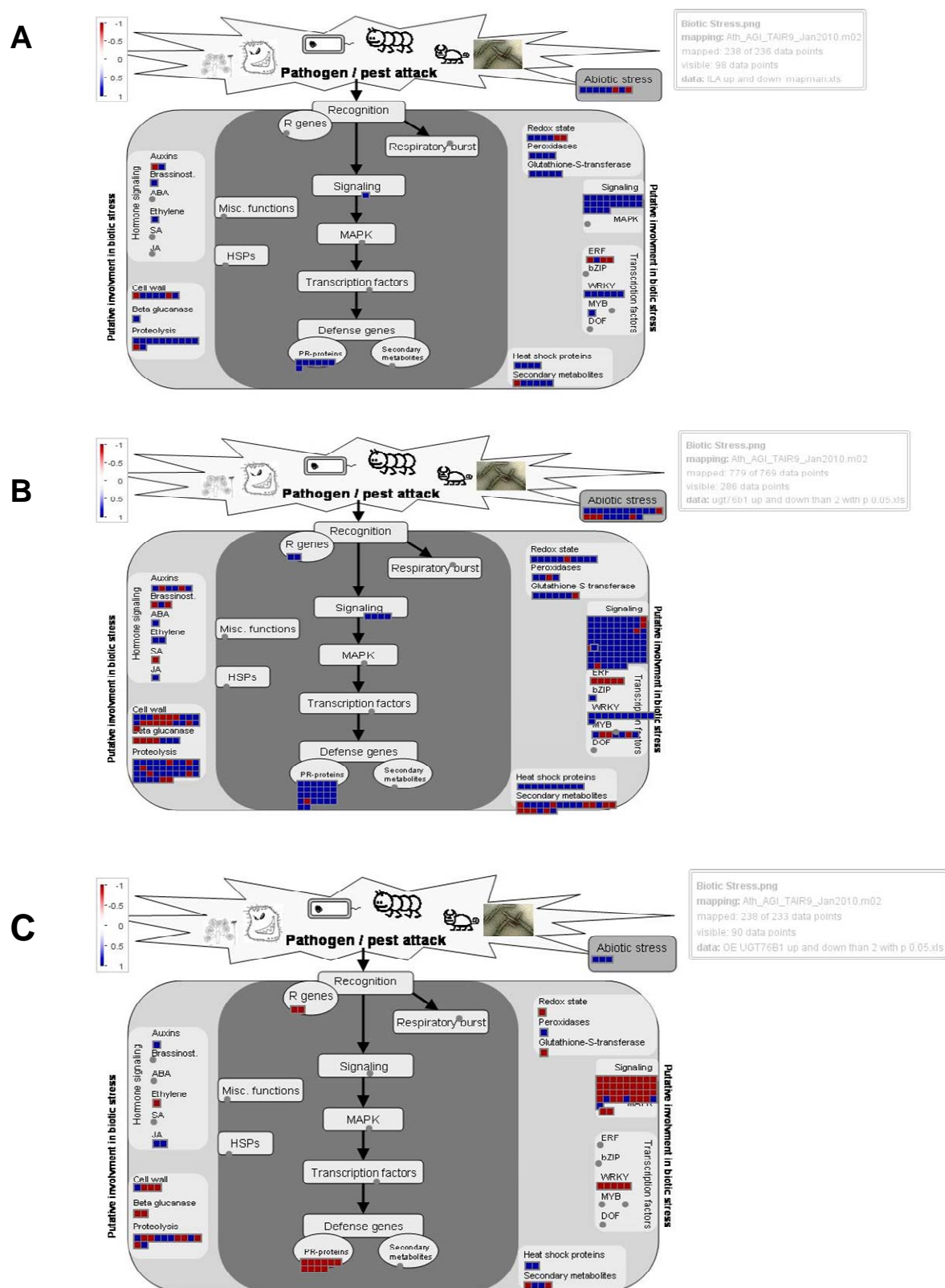


Figure 12. Analysis of biotic stress relevance on genes regulated by ILA and different *UGT76B1* expression.

(A) Two hundred thirty six genes, induced or suppressed more than twofold by ILA, were analyzed. (B) Seven hundred sixty nine genes, induced or suppressed more than twofold by loss-of-function of *UGT76B1*, were analyzed. (C) Two hundred thirty three genes, induced or suppressed more than twofold by constitutive overexpression of *UGT76B1*, were analyzed.

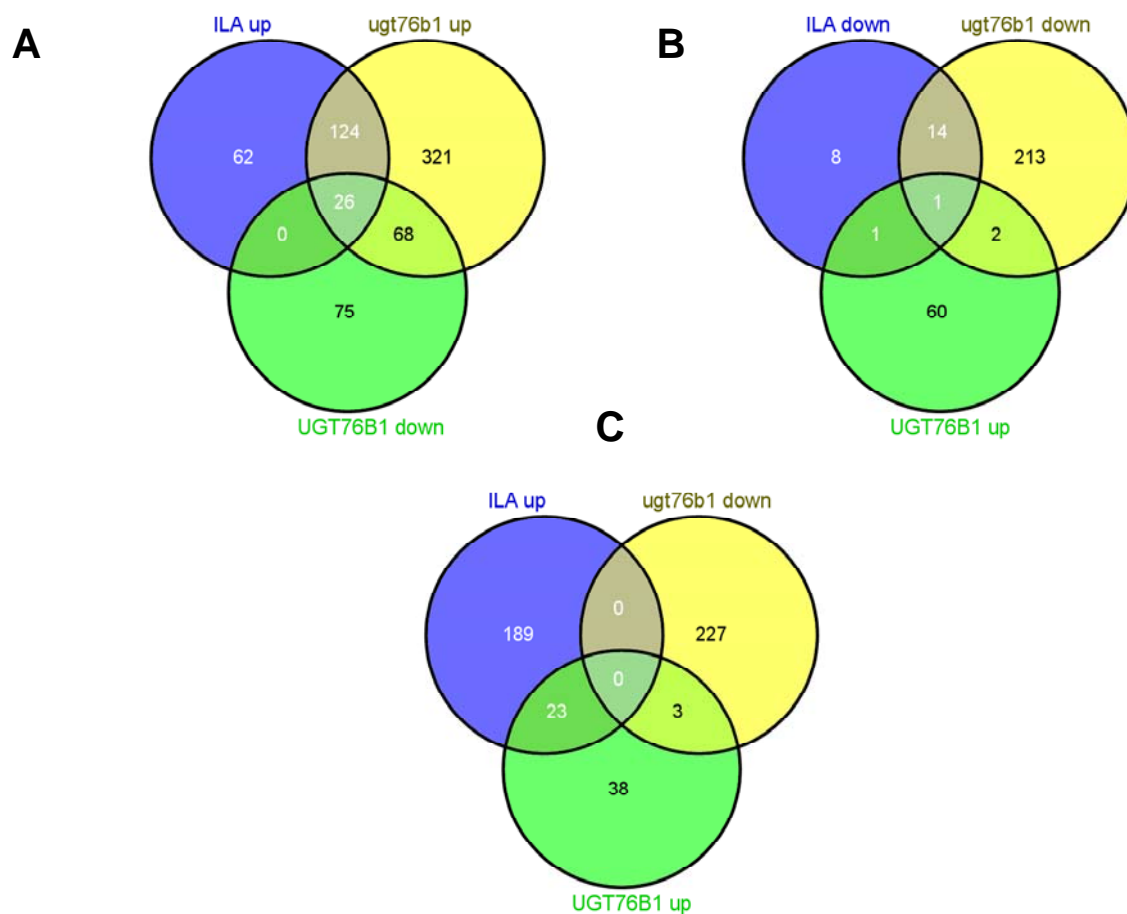


Figure 13. Venn diagrams of transcriptome analysis on action of ILA and different *UGT76B1* expression.

(A) Expression patterns were compared among ILA-induced, *ugt76b1*-induced and *UGT76B1*-suppressed gene lists. (B) Expression patterns were compared among ILA-suppressed, *ugt76b1*-suppressed and *UGT76B1*-induced gene lists. (C) Expression patterns were compared among ILA-induced, *ugt76b1*-suppressed and *UGT76B1*-induced gene lists.

Table 1. Comparison of genes oppositely regulated in *ugt76b1* knockout and *UGT76B1* overexpression relative to Col-0 with microarray data sets published in Genevestigator.

Ninety four genes induced in *ugt76b1* knockout but suppressed in *UGT76B1* overexpression, however, were uploaded to Genevestigator. Among 94 genes, 66 matched the Affymetrix probes, which were classified into two groups according to the fold change in response to SA treatment. The first group of genes, which has been induced less than twofold in response to SA treatment, is shown here. Genes induced more than twofold (\log_2 -transformed value ≥ 1) are indicated in “blue”, whereas genes suppressed more than twofold are highlighted in “red” (\log_2 -transformed value ≤ -1).

AGI	Fold change (\log_2 -transformed data)								fluorescence in WT ⁹	Annotation (TAIR 10)
	<i>P. syringae</i> ¹	BTH ²	SA ³	MeJA ⁴	<i>npr1-1</i> ⁵	<i>sid2</i> ⁶	<i>ugt76b1-1</i> ⁷	<i>UGT76B1-OE-7</i> ⁸		
AT2G33080	-0.02	0.17	0.14	-0.15	-0.65	-0.30	3.78	-1.41	5.14	RPL28
AT3G28890	0.65	0.79	0.60	0.06	-0.08	-0.65	2.28	-2.51	7.39	RPL43
AT5G52740	-0.24	3.04	0.29	-0.07	0.02	-0.14	2.36	-1.17	4.76	Copper transport protein family
AT3G20960	0.36	0.09	0.54	-0.10	-1.10	-0.94	1.25	-1.17	6.99	CYP705A33A
AT1G20350	0.25	1.22	0.59	0.07	-0.22	0.23	3.00	-1.08	6.28	TIM17-1
AT2G21850	0.38	0.20	0.89	-0.41	-1.46	-1.29	1.73	-1.19	5.22	Cysteine/Histidine-rich C1 domain family protein
AT3G04720	-0.11	1.83	0.97	-4.30	-0.01	0.78	1.50	-1.04	11.77	PR-4
AT2G15390	1.65	1.22	0.97	-1.27	-0.79	-0.38	1.88	-1.15	7.00	FUT4

¹ From GEO accession # GSE 5520. *Arabidopsis* leaf samples were inoculated with *Pseudomonas syringae* pv. *tomato* DC3000 for 24 h before harvesting.

² From GEO accession # GSE9955. Whole *Arabidopsis* Col-0 plants were treated with the salicylic acid analog benzothiadiazole (BTH) for 24 h before harvesting.

³ From GEO accession #GSE34047. Leaf samples of Col-0 were sprayed with 1 mM salicylic acid and incubated for 6 h before collecting samples.

⁴ From GEO accession #GSE17464. Leaf disc samples were collected from five-week-old *Ler* plants grown under short day (8 h light / 16 h dark, 120 $\mu\text{mol s}^{-1} \text{m}^{-2}$) conditions, sprayed with 10 μM MeJA, covered with plastic bags and kept for one hour.

^{5 and 6} From GEO accession # GSE 18978. Leaves of *npr1*, *sid2* and Col-0 (control) in *Arabidopsis* were injected with *Pseudomonas syringae* pv. *maculicola* for 24 h before collecting samples.

^{7 and 8} Leaves of *ugt76b1* knockout and *UGT76B1* overexpression lines in Col-0 background were sprayed with water, compared with Col-0 sprayed with water via microarray.

⁹ The average fluorescence of three biological replicates water-treated Col-0 from 7 and 8 in microarray analysis. The \log_2 -transformed fluorescence of any sample in this assay is from 4 to 20.

Table 2. Comparison of genes oppositely regulated in *ugt76b1* knockout and *UGT76B1* overexpression relative to Col-0 with microarray data sets published in Genevestigator.

Ninety four genes induced in *ugt76b1* knockout but suppressed in *UGT76B1* overexpression, however, were analyzed using Genevestigator for expression after the indicated treatments. Out of 94 genes 66 matched the Affymetrix probes, which were classified into two groups according to fold change in response to SA treatment. The second group of genes, which were induced more than twofold (\log_2 -transformed value ≥ 1) in response to SA treatment, was sorted according to the suppression by MeJA. Genes induced more than twofold are indicated in “blue”, whereas genes suppressed more than twofold (\log_2 -transformed value ≤ -1) are indicated in “red”. The description of experiments is the same as in Table 1.

AGI	Fold change (\log_2 -transformed data)								fluorescence in WT ⁹	Annotation (TAIR 10)
	<i>P. syringae</i> ¹	BTH ²	SA ³	MeJA ⁴	<i>npr1-1</i> ⁵	<i>sid2</i> ⁶	<i>ugt76b1-1</i> ⁷	<i>UGT76B1-OE-7</i> ⁸		
AT5G45380	0.30	2.71	2.01	-4.43	-1.06	-2.37	2.04	-1.60	8.36	DUR3, solute:sodium symporters
AT1G51800	1.18	0.81	2.80	-4.14	-3.06	-3.14	2.83	-1.18	5.97	Leucine-rich repeat protein kinase family protein
AT4G01700	1.77	3.17	3.31	-4.03	-0.61	-1.53	1.88	-1.08	9.90	Chitinase family protein
AT1G10340	1.85	2.13	2.38	-3.94	-2.30	-1.90	3.63	-1.26	6.73	Ankyrin repeat family protein
AT3G26210	1.26	3.93	3.27	-3.93	-0.82	-0.48	1.85	-2.02	9.48	CYP71B23
AT3G47480	2.49	3.19	2.13	-3.83	-0.71	-0.72	3.44	-1.89	9.76	Calcium-binding EF-hand family protein
AT3G13950	2.06	2.31	1.46	-3.72	-1.09	-0.69	4.35	-1.03	4.16	unknown protein
AT3G28540	1.87	2.77	2.91	-3.38	-1.91	-2.33	2.22	-1.22	10.85	P-loop containing nucleoside triphosphate hydrolases superfamily protein
AT3G51330	1.13	3.33	2.75	-3.28	-2.09	-2.13	2.15	-1.41	6.23	Eukaryotic aspartyl protease family protein
AT3G26220	0.66	2.37	1.02	-3.23	-1.10	-0.44	1.58	-1.09	8.93	CYP71B3
AT1G03850	1.37	5.63	4.37	-2.84	-2.79	-2.75	1.92	-1.03	9.43	Glutaredoxin family protein
AT5G42830	0.39	1.92	1.68	-2.72	-2.21	-1.70	2.53	-1.75	6.69	HXXXD-type acyl-transferase family protein
AT4G25110	0.74	1.76	2.68	-2.69	-2.08	-2.44	1.90	-3.23	9.27	AtMC2,metacaspase 2
AT5G67450	0.72	1.38	2.38	-2.55	-2.02	-1.95	1.39	-1.07	5.54	AZF1, ZF1, zinc-finger protein 1
AT1G35710	2.87	3.38	2.14	-2.40	-1.09	-1.71	2.36	-1.78	6.55	Protein kinase family protein with leucine-rich repeat domain
AT2G04450	1.68	4.23	2.82	-2.29	-1.75	-1.91	3.74	-2.08	7.91	NUDT6, nudix hydrolase homolog 6
AT1G30900	2.08	3.71	3.00	-2.23	-2.36	-2.50	2.52	-1.77	7.51	VACUOLAR SORTING RECEPTOR 6
AT4G23610	2.01	3.03	1.88	-2.17	-1.88	-1.76	1.84	-1.93	7.33	Late embryogenesis abundant (LEA) hydroxyproline-rich glycoprotein family
AT4G20110	2.10	2.74	2.92	-2.06	-1.11	-1.33	2.05	-2.28	9.22	VSR7, VACUOLAR SORTING RECEPTOR 7
AT5G20400	0.35	1.48	1.58	-1.79	-1.06	-1.15	1.30	-1.66	7.58	2-oxoglutarate (2OG) and Fe(II)-dependent oxygenase superfamily protein
AT2G47130	2.24	3.97	3.22	-1.71	-1.44	-1.60	1.89	-2.52	7.57	NAD(P)-binding Rossmann-fold superfamily protein
AT1G13470	2.38	5.16	3.62	-1.41	-2.72	-2.67	2.57	-4.75	10.76	Protein of unknown function (DUF1262)
AT5G59680	0.49	1.61	1.50	-1.29	-1.37	-1.35	1.61	-2.33	7.50	Leucine-rich repeat protein kinase family protein
AT4G11890	2.32	4.46	3.34	-1.07	-1.01	-0.93	2.78	-1.61	6.08	Protein kinase superfamily protein
AT1G73805	2.41	2.38	2.42	-1.04	-1.52	-1.94	2.33	-1.98	9.21	Calmodulin binding protein-like
AT5G10760	0.97	4.88	1.90	-1.00	-1.78	-2.06	4.02	-2.45	9.31	Eukaryotic aspartyl protease family protein
AT5G24210	1.12	1.76	3.10	-1.00	-1.34	-1.27	1.81	-1.07	11.78	alpha/beta-Hydrolases superfamily protein
AT1G34420	2.44	0.93	1.20	-0.98	-0.44	-0.30	2.10	-2.20	7.79	leucine-rich repeat transmembrane protein kinase family protein
AT5G59670	1.64	3.36	2.82	0.03	-1.47	-1.94	1.21	-2.22	11.50	Leucine-rich repeat protein kinase family protein
AT5G60900	3.21	2.52	2.73	-0.82	-0.49	-0.81	1.36	-2.65	10.85	RLK1, receptor-like protein kinase 1
AT2G32680	0.96	3.55	2.29	0.35	-0.77	-0.54	3.80	-1.61	6.41	RLP23, receptor like protein 23
AT3G25010	1.90	3.80	2.16	-0.29	-0.29	-0.93	4.04	-1.44	6.26	RLP41, receptor like protein 41

AT3G25020	0.82	1.34	1.90	-0.17	-0.93	-1.26	2.58	-1.04	7.34	RLP42, receptor like protein 42
AT4G23220	1.68	2.94	2.75	0.22	-0.84	-0.96	1.32	-1.20	9.52	CRK14
AT3G45860	0.43	3.94	1.60	0.40	-1.20	-1.92	2.92	-1.78	5.66	CRK4, cysteine-rich RLK (RECEPTOR-like protein kinase) 4
AT4G23150	2.22	3.13	2.70	0.29	-1.08	-0.91	4.62	-1.77	5.99	CRK7, cysteine-rich RLK (RECEPTOR-like protein kinase) 7
AT5G45000	1.80	2.45	2.57	-0.63	-2.91	-3.24	1.24	-2.70	7.63	Disease resistance protein (TIR-NBS-LRR class) family
AT1G21250	2.28	3.51	2.89	0.05	-0.75	-1.10	1.56	-2.17	11.25	PRO25, WAK1, cell wall-associated kinase
AT5G24530	2.01	4.61	2.85	-0.07	-1.71	-2.59	2.56	-3.04	11.35	DMR6, 2-oxoglutarate (2OG) and Fe(II)-dependent oxygenase superfamily protein
AT4G10500	2.49	4.83	3.55	0.20	-2.02	-2.71	6.38	-1.99	5.88	2-oxoglutarate (2OG) and Fe(II)-dependent oxygenase superfamily protein
AT5G05460	1.41	1.72	2.10	-0.64	-1.37	-1.69	1.18	-1.85	8.04	Glycosyl hydrolase family 85
AT3G50480	1.10	3.08	2.47	0.11	-1.14	-0.70	2.42	-1.69	8.98	HR4, homolog of RPW8 4
AT5G09290	1.31	0.57	1.17	-0.01	-1.82	-2.03	3.45	-1.24	5.28	Inositol monophosphatase family protein
AT2G39210	1.17	1.79	2.85	-0.86	-1.27	-1.51	1.31	-1.33	10.07	Major facilitator superfamily protein
AT2G26560	0.37	3.60	2.02	-0.36	-1.30	-0.74	1.96	-1.95	10.60	PLA IIA, PLA2A, phospholipase A 2A
AT2G26440	2.12	3.87	3.27	0.23	-1.73	-2.68	1.50	-2.73	11.61	Plant invertase pectin methylesterase inhibitor superfamily
AT2G32160	0.53	1.70	1.43	0.34	-1.45	-1.49	1.10	-1.68	7.63	S-adenosyl-L-methionine-dependent methyltransferases superfamily protein
AT5G07770	0.83	0.68	1.10	-0.06	-1.29	-1.56	1.05	-1.01	8.39	Actin-binding FH2 protein
AT4G03450	0.94	2.42	2.46	0.99	-1.34	-1.09	1.95	-2.68	8.08	Ankyrin repeat family protein
AT1G24150	1.38	1.65	1.77	0.24	-1.01	-0.87	1.24	-1.05	7.69	FH4, formin homologue 4
AT5G22570	3.77	5.35	4.71	-0.51	-5.12	-5.24	2.82	-3.15	3.42	WRKY38
AT3G57260	2.91	5.10	1.64	0.13	0.14	-0.19	5.38	-2.04	9.81	BG2,PR2
AT3G57240	1.32	4.76	3.74	-0.43	-1.91	-1.72	2.29	-2.37	4.65	BG3, beta-1,3-glucanase 3
AT5G55450	1.62	5.02	2.60	0.00	-0.44	-0.34	2.09	-2.06	5.93	Bifunctional inhibitor/lipid-transfer protein
AT2G34940	1.68	1.48	2.84	-0.30	-1.86	-1.92	1.30	-2.51	6.99	BP80-3;2, VSR3;2, VSR5, VACUOLAR SORTING RECEPTOR 5
AT5G52760	3.63	4.64	2.08	0.05	-1.10	-1.15	3.11	-1.61	8.07	Copper transport protein family
AT1G23840	1.29	2.13	2.12	-0.83	-1.39	-1.36	1.55	-1.33	9.45	unknown protein
AT3G48640	2.34	2.20	2.18	-0.37	-1.81	-1.70	2.00	-1.00	5.39	unknown protein

2.3.2. Microarray analysis indicates a negative correlation of *UGT76B1* expression and ILA action

To investigate the effect of ILA at transcription level, gene expression was measured after ILA treatment of Col-0 compared to non-treated Col-0. After ILA application, expression of 236 genes was significantly altered ($P \leq 0.05$) at least twofold with 212 genes being induced and 24 genes being downregulated (Figure 10). More than 90 out of 236 genes were related to *pathogen defense response* according to MapMan analysis (Figure 12A). ILA is an *in vivo* substrate of *UGT76B1* in *Arabidopsis* and *UGT76B1* is closely associated with plant defense. To investigate the potential connection of ILA-mediated responses and *UGT76B1* expression, the expression patterns of ILA-treated Col-0 and *ugt76b1-1* were compared. Out of the 212 ILA-upregulated transcripts 70 % (150 genes) overlap with genes constitutively enhanced in *ugt76b1-1*. Similarly, 24 genes were suppressed by ILA more than twofold, among which 15 genes (> 60%) overlap with genes constitutively suppressed in *ugt76b1-1* (Figure 13A and B). Two other opposite comparisons (genes induced by ILA vs. genes suppressed in *ugt76b1*

knock out and genes suppressed by ILA vs. genes enhanced in *ugt76b1* knockout) were also performed. However, in both cases no overlapping genes were identified (data not shown). Thus, there is only considerable positive correlation of the effects provoked by exogenous ILA application and the *ugt76b1-1* knockout.

The considerable overlap of genes regulated in the same manner in ILA-treated wild-type plants and the *ugt76b1-1* mutant raised the question whether genes of this group were also included in genes oppositely regulated by constitutive *UGT76B1* overexpression. Indeed, 26 genes were commonly induced by ILA and *ugt76b1-1*, yet suppressed by *UGT76B1-OE-7*, suggesting their close correlation in response to ILA and to the expression of *UGT76B1* (Figure 13A and Table 3). Similarly, only one gene (At1g70640) showed the opposite behavior, *i.e.* it was suppressed by ILA and in *ugt76b1-1*, however induced in *UGT76B1-OE-7* (Figure 13B). Importantly, there are only sixteen genes that exhibited a parallel regulation among all three scenarios (data now shown). Thus, a strong preference for the overlap of genes regulated in an opposite manner by ILA application and *UGT76B1* expression level (as tested by loss-of-function and ectopic overexpression) was found. Among the 26 ILA-upregulated genes, many genes belong to kinase- and receptor-like proteins including At4g23140, At4g23150, At1g56120, At3g47480, At2g32680, At2g33080, At3g25010 and At3g25020. Furthermore, another single gene, *NUDT6* encoding a protein with NADH pyrophosphatase activity affecting defense *via* regulation of *NPRI* (Ishikawa et al., 2010) was significantly induced by ILA and the *ugt76b1* knockout, but suppressed, however, by *UGT76B1* overexpression.

Table 3. Overlapping genes consistently regulated by ILA, *ugt76b1* knockout and *UGT76B1* overexpression.

Twenty six genes were induced by ILA and *ugt76b1*, however suppressed upon *UGT76B1* overexpression more than twofold.

AGI	<i>ugt76b1-1</i> ¹	<i>UGT76B1-OE-7</i> ²	ILA ³	fluorescence in WT ⁴	TAIR 10
AT4G02520	1.84	-1.16	1.27	13.52	GSTF2
AT2G04450	3.74	-2.08	2.17	7.91	NUDT6
AT4G23140	4.11	-1.98	1.40	7.65	CRK6
AT4G23150	4.62	-1.77	1.79	5.99	CRK7
AT1G56120	2.37	-1.71	1.02	7.22	Leucine-rich repeat transmembrane protein kinase
AT3G47480	3.44	-1.89	1.95	9.76	Calcium-binding EF-hand family protein
AT2G32680	3.80	-1.61	1.56	6.41	RLP23
AT2G33080	3.78	-1.41	1.43	5.14	RLP28
AT3G25010	4.04	-1.44	1.89	6.26	RLP41
AT3G25020	2.58	-1.04	1.11	7.34	RLP42
AT5G26170	3.47	-1.54	1.62	5.92	WRKY50
AT5G26690	2.96	-2.07	1.56	6.95	Heavy metal transport
AT5G52740	2.36	-1.17	1.54	4.76	Copper transport protein family
AT5G52760	3.11	-1.61	1.34	8.07	Copper transport protein family
AT1G14880	3.04	-2.71	1.30	11.93	PCR1
AT1G14870	2.78	-1.43	1.25	10.45	PCR2
AT3G04720	1.50	-1.04	1.79	11.77	PR4
AT3G57260	5.38	-2.04	2.44	9.81	PR2
AT4G01700	1.88	-1.08	1.00	9.90	Chitinase family protein
AT3G28540	2.22	-1.22	1.00	10.85	P-loop containing nucleoside triphosphate hydrolases superfamily protein
AT5G10760	4.02	-2.45	1.62	9.31	Eukaryotic aspartyl protease family protein
AT3G51330	2.15	-1.41	1.13	6.23	Eukaryotic aspartyl protease family protein
AT1G10340	3.63	-1.26	1.92	6.73	Ankyrin repeat family protein
AT4G10500	6.38	-1.99	2.47	5.88	2-oxoglutarate (2OG) and Fe(II)-dependent oxygenase superfamily protein
AT5G09290	3.45	-1.24	1.70	5.28	Inositol monophosphatase family protein
AT3G13950	4.35	-1.03	2.45	4.16	unknown

¹, ² and ³ Leaves of *ugt76b1* knockout and *UGT76B1* overexpression lines in Col-0 background were sprayed with water, whereas leaves of Col-0 were sprayed with 1 mM ILA, compared with Col-0 sprayed with water. The value of log₂-transformed fold changes relative to Col-0 is shown.

⁴ The average fluorescence of three biological replicates of water-treated Col-0 from the experiment “7 and 8” in microarray analysis (The description for experiment “7 and 8” is the same as the description in legend of Table 1).

2.3.3. Genes induced by both ILA and loss-of-function of *UGT76B1* can be separated into two classes depending on their responsiveness to SA

To explore whether genes commonly induced by ILA and the *ugt76b1* knockout respond to JA or SA stimuli or to infection by *P. syringae*, their expression in response to virulent *Pseudomonas syringae* pv. *tomato* DC3000 infection of wild type (vs. mock), *Pseudomonas syringae* pv. *maculicola* infection of *npr1-1* or *sid2* (vs. infected Col-0) or after treatment with BTH, SA or MeJA was extracted from Genevestigator (referred to the description in 2.3.1) (Zimmermann et al., 2005). One hundred and twenty five genes out of 150 genes could match the corresponding probes from the different microarray platforms used. They were separated into two groups dependent on being less than twofold upregulated by SA and non-responsive to SA (Table 4), or being more than twofold activated by SA (Table 5).

The expression of 46 genes was upregulated less than twofold in response to SA treatment, among which 15 genes were suppressed more than twofold by MeJA (Table 4). Twenty one genes were neither responsive to *Pseudomonas syringae* pv. *tomato* DC3000 infection, BTH, SA treatment or JA treatment in wild type, nor responsive to *Pseudomonas syringae* pv. *maculicola* infection in *npr1-1* or *sid2*. There is no obvious enrichment among these genes. However, some are apparently related to nuclear functions such as At4g26630 (DEK domain-containing chromatin associated protein), At2g31970 (*RAD50*, DNA repair-recombination protein), At1g79280 (*TPR*, NUA, nuclear pore anchor), At5g55040 (DNA-binding bromodomain-containing protein), At5g04560 (*DME*, HhH-GPD base excision DNA repair family protein), At1g67230 (*LINC1*, LITTLE NUCLEI1) and At1g68790 (*LINC3*, LITTLE NUCLEI3). This indicates that nuclear and DNA-related processes might be commonly affected by ILA and the loss-of-function of *UGT76B1*, which are not related to SA- or JA-mediated responses.

Table 4. Comparison of genes upregulated in *ugt76b1* knockout and by ILA application relative to Col-0 with microarray data sets published in Genevestigator.

One hundred and fifty genes induced in *ugt76b1* knockout and by ILA application were analyzed using Genevestigator for comparing with the gene expression pattern in response to JA or SA stimuli or to infection by *P. syringae*. Among the 150 genes 125 probes matched with the Affymetrix-based data, which were classified into two groups according to their fold change in response to SA treatment. The first group of genes, which were induced less than twofold in response to SA treatment, was sorted according to the change after MeJA treatment in *Ler*. Genes induced more than twofold (\log_2 -transformed value ≥ 1) by *Pseudomonas*, BTH and SA are indicated in “blue” whereas genes suppressed more than twofold (\log_2 -transformed value ≤ -1) in response to *Pseudomonas* infection in *npr1* and *sid2* relative to Col-0; MeJA treatment in *Ler* are indicated in “red”. The description of experiments is the same as Table 1, except 8. ⁸ Leaves of Col-0 were sprayed with 1mM ILA, compared with Col-0 *via* microarray analysis.

AGI	Fold change (\log_2 -transformed data)								fluorescence in WT ⁹	Annotation (TAIR 10)
	<i>P. syringae</i> ¹	BTH ²	SA ³	MeJA ⁴	<i>npr1-l</i> ⁵	<i>sid2</i> ⁶	<i>ugt76b1-l</i> ⁷	ILA ⁸		
AT2G37130	-0.69	0.67	0.57	-5.91	0.51	0.27	1.98	2.18	8.59	Peroxidase superfamily protein
AT2G45220	0.85	-0.05	0.33	-5.66	-1.56	-0.82	2.59	2.71	5.40	Plant invertase/pectin methylsterase inhibitor superfamily
AT4G15610	-0.25	0.12	0.09	-5.47	-0.39	0.41	1.38	1.96	6.97	Uncharacterised protein family (UPF0497)
AT2G42360	1.10	0.55	0.92	-4.63	-1.33	-0.35	2.83	1.48	4.95	RING/U-box superfamily protein
AT3G04720	-0.11	1.83	0.97	-4.30	-0.01	0.78	1.50	1.79	11.77	HEL, PR-4, PR4, pathogenesis-related 4
AT4G23700	1.38	0.08	0.80	-4.23	-1.80	-0.67	3.10	1.80	3.42	CHX17, cation/H ⁺ exchanger 17
AT3G21080	1.06	0.11	0.58	-3.61	-1.91	-0.79	1.99	1.96	5.15	ABC transporter-related
AT4G24450	0.91	-0.05	-0.07	-1.85	1.09	0.09	1.25	1.44	7.40	ATGWD2, GWD3, PWD, phosphoglucan, water dikinase
AT2G46150	0.17	0.62	0.90	-1.63	-1.73	-2.22	1.49	1.12	5.35	Late embryogenesis abundant (LEA) hydroxyproline-rich glycoprotein family
AT1G33030	0.90	0.32	0.87	-1.55	-0.41	0.15	1.70	1.31	5.09	O-methyltransferase family protein
AT3G28580	1.25	0.02	0.62	-1.24	-0.12	0.02	3.58	2.44	5.43	P-loop containing nucleoside triphosphate hydrolases superfamily protein
AT5G01550	0.26	-0.26	0.25	-1.19	-2.12	-2.25	2.09	1.18	4.46	LECRKA4.2, lectin receptor kinase a4.1
AT3G09270	0.86	0.09	0.88	-1.15	-1.10	-0.37	3.21	2.21	5.10	GSTU8, glutathione S-transferase TAU 8
AT2G47190	1.58	0.54	0.42	-1.04	-0.31	0.24	2.06	1.02	3.80	MYB2, myb domain protein 2
AT4G21850	4.65	1.98	0.80	-1.01	0.46	0.33	3.98	2.13	8.17	MSRB9, methionine sulfoxide reductase B9
AT4G26630	0.14	-0.08	-0.34	-0.41	0.15	-0.04	1.25	1.23	10.49	DEK domain-containing chromatin associated protein
AT1G06670	0.39	0.01	0.05	-0.32	0.01	-0.10	1.22	1.13	6.80	NIH, nuclear DEIH-boxhelicase
AT2G31970	0.49	0.15	0.61	-0.12	-0.28	-0.15	1.57	1.11	6.45	DNA repair-recombination protein (RAD50)
AT1G79280	0.59	-0.05	0.45	0.07	-0.04	-0.25	1.92	1.84	8.45	TPR, NUA, nuclear pore anchor
AT5G55040	0.44	0.04	0.07	0.16	-0.31	-0.38	1.14	1.07	1.59	DNA-binding bromodomain-containing protein

AT5G04560	0.56	-0.13	0.24	0.63	-0.79	-0.99	1.63	1.50	7.95	DME, HhH-GPD base excision DNA repair family protein
AT1G67230	0.60	-0.10	0.24	0.90	0.02	0.05	1.13	1.23	9.91	LINC1, little nuclei1
AT1G68790	0.31	-0.05	-0.34	-0.26	0.51	0.31	1.20	1.16	9.08	LINC3, little nuclei3
AT2G33080	-0.02	0.17	0.14	-0.15	-0.65	-0.30	3.78	1.43	5.14	RLP28, receptor like protein 28
AT3G24982	2.84	0.17	0.00	-0.11	0.30	0.29	2.42	3.89	3.66	RLP40, receptor like protein 40
AT3G26470	1.85	0.44	0.15	-0.12	0.03	0.06	2.54	1.90	4.90	Powdery mildew resistance protein, RPW8 domain
AT2G40740	0.04	0.11	0.37	-0.10	-0.58	-0.21	3.10	1.02	4.22	WRKY55, WRKY DNA-binding protein 55
AT5G16680	1.04	0.35	0.43	-0.18	-0.19	-0.24	1.14	1.02	9.25	RING/FYVE/PHD zinc finger superfamily protein
AT4G14630	0.23	0.07	-0.02	-0.71	-1.46	-0.21	2.35	2.06	2.51	GLP9, germin-like protein 9
AT2G37080	-0.16	0.37	0.57	-0.66	0.07	-0.22	2.31	1.36	7.97	RIP3, ROP interactive partner 3
AT1G67120	0.26	0.27	0.83	-0.54	-0.07	-0.21	1.63	1.15	6.04	ATPases;nucleotide binding;ATP binding
AT2G28290	0.50	-0.15	0.23	0.04	-0.38	-0.44	1.40	1.22	9.12	CHR3, SYD, P-loop containing nucleoside triphosphate hydrolases superfamily protein
AT5G41790	0.83	-0.78	0.06	-0.37	0.05	-0.10	1.61	1.43	9.31	CIP1, COP1-interactive protein 1
AT4G18600	0.29	-0.13	-0.04	-0.14	0.02	-0.15	1.15	1.22	6.97	SCAR-LIKE, SCARL, WAVE5, SCAR family protein
AT5G52740	-0.24	3.04	0.29	-0.07	0.02	-0.14	2.36	1.54	4.76	Copper transport protein family
AT1G04600	-0.15	0.06	0.14	-0.04	0.12	-0.02	3.84	1.20	3.14	XIA, myosin XI A
AT5G23020	1.12	-0.03	-0.20	0.21	0.83	0.61	1.84	1.27	7.97	IMS2, MAM-L, MAM3
AT2G45460	0.53	-0.07	0.16	0.28	0.02	-0.04	1.20	1.16	6.73	SMAD/FHA domain-containing protein
AT2G43150	-0.14	-0.19	-0.23	0.28	0.06	-0.09	1.22	1.12	10.61	Proline-rich extensin-like family protein
AT4G27860	4.32	0.42	0.81	1.36	0.01	-0.61	1.69	1.44	5.43	vacuolar iron transporter (VIT) family protein
AT4G27500	1.25	0.75	0.95	1.46	-0.34	-0.38	1.61	1.36	11.12	PP1I, proton pump interactor 1
AT5G04020	0.20	0.32	0.55	1.47	-0.41	-0.06	1.14	1.11	7.95	calmodulin binding
AT1G68620	2.18	0.00	0.33	1.81	-0.35	-0.04	1.84	1.90	5.99	alpha/beta-Hydrolases superfamily protein
AT3G56410	0.57	0.63	0.99	0.61	-0.30	-0.20	1.14	1.13	2.82	Protein of unknown function (DUF3133)
AT5G40450	0.86	-0.34	-0.90	0.34	0.92	0.80	1.78	1.85	10.98	unknown protein
AT1G76960	0.64	2.10	0.72	-0.02	-0.51	-0.63	3.53	2.19	10.51	unknown protein

Among genes commonly induced by ILA and *ugt76b1* knockout, expression of 79 genes was more than twofold upregulated in response to SA treatment, most of which were more than twofold suppressed by MeJA. To investigate whether these ILA and *ugt76b1*-induced as well as SA responsive genes are regulated by *NPRI*, the key positive regulator in SA pathway, they were further sorted from smallest to largest expression in response to *Pseudomonas* infection in *npr1-1* and grouped into two classes: (i) being more than twofold downregulated and (ii) the genes being less than twofold downregulated, not responsive or upregulated. Upon

infection with *Pseudomonas syringae* pv. *maculicola* many genes showed expression reduction in *npr1-1* relative to Col-0. Furthermore, among them most genes showed an expression decrease in *sid2* relative to Col-0 upon infection with *P. syringae*. Thus they showed a dependence on *NPR1* and *SID2* to be induced upon infection with *Pseudomonas syringae* pv. *maculicola*. However, upon infection by *P. syringae*, a certain number of genes did not show expression reduction in *npr1-1* or *sid2* mutants, suggesting independence of *NPR1* or *SID2* to be induced upon *P. syringae* infection. Therefore, among genes commonly induced by ILA and loss-of-function of *UGT76B1*, both responsiveness and non-responsiveness to regulation by *NPR1* and *SID2* after *P. syringae* infection were found (Table 5).

Table 5. Comparison of genes up-regulated in the *ugt76b1* knockout and by ILA application relative to mock-treated Col-0 (log₂-transformed value ≥ 1 equal to twofold) with microarray data sets published in Genevestigator.

One hundred and fifty genes induced in *ugt76b1* knockout and by ILA application were analyzed using Genevestigator for comparing with the gene expression pattern in response to JA or SA stimuli or to infection by *P. syringae*. Among the 150 genes, 125 probes matched with the Affymetrix-based data, which were classified into two groups according to their fold change in response to SA treatment. The second group of genes, which were induced more than twofold in response to SA treatment, was sorted according to the change in *npr1-1* in response to *Pseudomonas* infection. Genes induced more than twofold (log₂-transformed value ≥ 1) by *Pseudomonas*, BTH and SA are indicated as “blue”. Genes suppressed more than twofold (log₂-transformed value ≤ -1) in response to *Pseudomonas* infection in *npr1-1* and *sid2* relative to Col-0 and MeJA treatment in *Ler* are indicated as “red”. The description of experiments is the same as Table 1 and Table 3. ⁸ Leaves of Col-0 were sprayed with 1 mM ILA, compared with Col-0 sprayed with water *via* microarray.

	Fold change (log ₂ -transformed data)									
AGI	<i>P. syringae</i> ¹	BTH ²	SA ³	MeJA ⁴	<i>npr1-1</i> ⁵	<i>sid2</i> ⁶	<i>ugt76b1-1</i> ⁷	ILA ⁸	fluorescence in WT ⁹	Annotation (TAIR 10)
AT3G28510	1.35	0.76	3.69	-0.56	-5.74	-5.87	6.31	3.26	3.89	P-loop containing nucleoside triphosphate hydrolases superfamily protein
AT2G19190	0.16	0.18	2.88	-5.70	-3.83	-3.86	3.96	2.22	5.26	FRK1, FLG22-induced receptor-like kinase 1
AT2G14610	1.35	6.16	2.52	-1.38	-3.34	-3.15	6.46	4.84	5.51	ATPR1, PR 1, PR1
AT5G11920	2.18	1.04	2.11	-3.14	-3.12	-3.25	4.54	2.25	5.01	cwINV6, 6-&1-fructan exohydrolase
AT4G35180	3.56	2.07	4.48	-0.42	-2.69	-4.53	3.10	1.38	4.52	LHT7
AT1G10340	1.85	2.13	2.38	-3.94	-2.30	-1.90	3.63	1.92	6.73	Ankyrin repeat family protein
AT3G51330	1.13	3.33	2.75	-3.28	-2.09	-2.13	2.15	1.13	6.23	Eukaryotic aspartyl protease family protein
AT5G46050	1.32	1.81	2.26	-5.63	-2.05	-2.67	2.53	1.60	7.31	PTR3, peptide transporter 3
AT4G10500	2.49	4.83	3.55	0.20	-2.02	-2.71	6.38	2.47	5.88	2-oxoglutarate (2OG) and Fe(II)-dependent oxygenase superfamily protein
AT3G28540	1.87	2.77	2.91	-3.38	-1.91	-2.33	2.22	1.00	10.85	P-loop containing nucleoside triphosphate hydrolases superfamily protein
AT3G18250	0.92	1.95	1.89	-4.72	-1.89	-1.39	3.70	2.81	5.46	Putative membrane lipoprotein
AT2G35980	0.37	0.34	1.12	-0.29	-1.84	-0.51	3.40	3.05	4.19	NHL10, YLS9
AT5G09290	1.31	0.57	1.17	-0.01	-1.82	-2.03	3.45	1.70	5.28	Inositol monophosphatase family protein
AT5G10760	0.97	4.88	1.90	-1.00	-1.78	-2.06	4.02	1.62	9.31	Eukaryotic aspartyl protease family protein
AT2G04450	1.68	4.23	2.82	-2.29	-1.75	-1.91	3.74	2.17	7.91	NUDT6
AT4G00700	1.84	2.08	2.53	-0.89	-1.69	-1.69	5.02	2.41	3.35	C2 calcium/lipid-binding plant phosphoribosyltransferase family protein
AT1G51890	0.80	0.78	2.57	-5.71	-1.67	-1.27	3.83	2.55	4.04	Leucine-rich repeat protein kinase family protein
AT1G65690	0.91	1.49	1.27	-3.30	-1.64	-0.78	2.89	1.99	6.66	Late embryogenesis abundant (LEA) hydroxyproline-rich glycoprotein family
AT4G18250	1.47	1.04	2.18	-1.99	-1.59	-1.13	3.17	1.62	2.26	receptor serine/threonine kinase, putative
AT5G60280	0.98	0.85	1.62	-1.72	-1.58	-1.45	2.57	1.28	1.90	Concanavalin A-like lectin protein kinase family protein
AT4G23210	1.50	0.20	1.13	-4.87	-1.51	-0.90	1.70	1.46	4.67	CRK13, cysteine-rich RLK (RECEPTOR-like protein kinase) 13

AT1G72060	-0.59	3.35	2.05	-2.44	-1.47	-1.05	2.04	1.10	8.63	serine-type endopeptidase inhibitors
AT5G44570	1.41	0.39	1.38	-3.08	-1.24	-1.88	1.52	1.77	4.05	unknown protein
AT5G02490	0.99	0.99	2.88	-1.20	-1.24	-1.17	2.75	1.28	8.65	Heat shock protein 70 (Hsp 70) family protein
AT1G33960	3.10	1.98	2.37	-5.11	-1.16	-0.88	4.19	3.08	4.61	AIG1, P-loop containing nucleoside triphosphate hydrolases superfamily protein
AT3G21520	0.15	0.61	1.26	-0.82	-1.16	-0.88	3.63	1.85	3.16	DMP1, DUF679 domain membrane protein 1
AT4G21120	1.41	0.20	1.83	-4.45	-1.16	-1.14	2.80	1.59	5.68	AAT1, CAT1, amino acid transporter 1
AT1G26420	0.64	0.57	1.58	-3.26	-1.15	-0.52	2.82	1.67	4.84	FAD-binding Berberine family protein
AT1G74590	0.60	0.61	1.40	-1.29	-1.14	-0.66	3.14	2.51	3.72	GSTU10, glutathione S-transferase TAU 10
AT5G52760	3.63	4.64	2.08	0.05	-1.10	-1.15	3.11	1.34	8.07	Copper transport protein family
AT3G13950	2.06	2.31	1.46	-3.72	-1.09	-0.69	4.35	2.45	4.16	unknown protein
AT4G23150	2.22	3.13	2.70	0.29	-1.08	-0.91	4.62	1.79	5.99	CRK7, cysteine-rich RLK (RECEPTOR-like protein kinase) 7
AT3G25010	1.90	3.80	2.16	-0.29	-0.29	-0.93	4.04	1.89	6.26	RLP41, receptor like protein 41
AT3G25020	0.82	1.34	1.90	-0.17	-0.93	-1.26	2.58	1.11	7.34	RLP42, receptor like protein 42
AT1G74360	1.94	0.58	2.04	-1.79	-0.83	-0.62	2.49	1.12	6.10	Leucine-rich repeat protein kinase family protein
AT4G23310	0.36	0.90	1.29	-0.34	-0.72	-0.55	4.57	1.36	4.09	CRK23, cysteine-rich RLK (RECEPTOR-like protein kinase) 23
AT4G04490	2.11	1.98	2.18	-2.05	-0.60	-0.48	3.05	1.33	5.91	CRK36, cysteine-rich RLK (RECEPTOR-like protein kinase) 36
AT1G21240	0.76	0.45	1.87	0.10	-0.68	-0.29	3.71	2.05	2.77	WAK3, wall associated kinase 3
AT2G43000	-0.12	0.53	1.10	0.07	-0.91	0.28	2.93	1.88	5.16	anac042, NAC042, NAC domain containing protein 42
AT2G46400	3.29	1.54	2.32	-1.07	-0.98	-0.78	2.86	1.26	7.87	WRKY46, WRKY DNA-binding protein 46
AT2G25000	0.69	2.14	2.22	-4.54	-0.93	-1.17	1.70	1.41	8.75	WRKY60, WRKY DNA-binding protein 60
AT2G29350	2.26	1.72	1.35	-4.26	-0.09	0.13	3.55	3.30	6.89	SAG13, senescence-associated gene 13
AT3G57260	2.91	5.10	1.64	0.13	0.14	-0.19	5.38	2.44	9.81	BG2, BGL2, PR-2, PR2, beta-1,3-glucanase 2
AT4G39030	2.73	0.88	1.36	1.56	-0.64	-0.63	1.87	1.19	6.72	EDS5, SID1, MATE efflux family protein
AT2G43570	2.57	4.20	1.78	-1.42	-0.58	-0.41	5.56	3.53	6.80	CHI, chitinase, putative
AT4G01700	1.77	3.17	3.31	-4.03	-0.61	-1.53	1.88	1.00	9.90	Chitinase family protein
AT3G22600	1.26	2.34	1.68	-1.02	-0.80	-0.35	2.08	2.46	8.10	Bifunctional inhibitor/ lipid-transfer protein/ seed storage 2S albumin superfamily protein
AT2G30770	1.73	1.46	2.93	-0.75	-0.28	0.20	2.02	2.70	5.21	CYP71A13, cytochrome P450
AT3G26830	3.12	1.60	3.91	-1.35	0.01	0.38	3.19	2.99	6.08	CYP71B15, PAD3
AT1G57630	3.66	2.85	2.15	-0.23	-0.66	-0.37	3.97	2.33	6.46	Toll-Interleukin-Resistance (TIR) domain family protein
AT4G24190	0.51	3.25	2.14	-1.91	-0.15	-0.48	2.33	1.22	9.16	HSP90.7, SHD, Chaperone protein htpG family protein
AT4G16660	1.33	2.31	2.14	-1.17	-0.09	-0.29	1.74	1.04	7.49	heat shock protein 70 (Hsp 70) family protein
AT1G04980	0.41	3.13	2.65	-3.20	-0.16	-0.48	2.43	1.10	7.94	PDI10, PDIL2-2, PDI-like 2-2
AT4G38560	1.51	0.61	1.17	-1.69	-0.72	-0.84	3.31	1.31	6.50	Arabidopsis phospholipase-like protein (PEARLI 4) family

AT1G45145	3.01	2.28	1.58	-0.27	-0.29	-0.21	2.02	1.04	12.40	LIV1, TRX5, thioredoxin H-type 5
AT3G51860	1.05	1.77	1.34	-1.43	0.11	0.29	5.29	1.84	4.46	ATHCX1, CAX1-LIKE, CAX3, cation exchanger 3
AT3G50930	3.03	0.95	2.01	1.12	0.54	0.37	3.69	1.36	7.23	BCS1, cytochrome BC1 synthesis
AT3G47480	2.49	3.19	2.13	-3.83	-0.71	-0.72	3.44	1.95	9.76	Calcium-binding EF-hand family protein
AT5G39670	3.25	2.46	1.36	-2.36	-0.42	-0.14	3.44	1.80	7.78	Calcium-binding EF-hand family protein
AT3G50770	3.41	0.71	1.04	-2.40	-0.18	0.07	3.68	2.58	6.33	CML41, calmodulin-like 41
AT5G18470	0.95	3.32	2.42	-1.08	-0.74	-0.56	3.38	1.54	8.35	Curculin-like (mannose-binding) lectin family protein
AT4G38540	1.24	0.37	1.72	-2.98	0.24	0.79	1.56	1.10	7.04	FAD/NAD(P)-binding oxidoreductase family protein
AT1G61800	4.31	-0.24	1.43	1.34	-0.80	-0.18	2.39	2.39	2.58	GPT2, glucose-6-phosphate phosphate translocator 2
AT5G60800	2.24	1.40	1.64	-0.52	-0.77	-0.80	2.19	1.07	7.87	Heavy metal transport/ detoxification superfamily protein
AT3G16530	-0.65	0.26	1.64	-2.61	2.11	2.54	1.36	1.02	10.39	Legume lectin family protein
AT3G23550	0.49	0.32	1.12	-0.47	1.32	2.56	1.71	2.24	5.75	MATE efflux family protein
AT3G09940	5.28	1.55	1.84	-1.22	-0.17	-1.06	3.62	1.53	3.80	MDAR2, MDAR3, MDHAR, monodehydroascorbate reductase
AT1G60730	0.77	0.08	1.30	-0.14	-0.05	0.22	1.18	1.18	7.54	NAD(P)-linked oxidoreductase superfamily protein
AT1G77510	0.77	3.79	2.58	-2.97	-0.21	-0.41	2.13	1.14	9.03	PDI6, PDIL1-2, PDI-like 1-2
AT1G43910	4.88	1.71	1.81	-2.37	-0.61	-0.58	2.81	1.58	5.95	P-loop containing nucleoside triphosphate hydrolases superfamily protein
AT1G13340	4.49	1.06	1.44	-1.84	-0.68	-0.25	3.04	1.11	6.95	Regulator of Vps4 activity in the MVB pathway protein
AT5G10380	0.77	1.88	1.13	-0.39	-0.61	-0.75	3.16	1.29	11.27	RING1, RING/U-box superfamily protein
AT5G64000	0.99	2.55	1.79	-1.93	-0.39	-0.04	4.04	1.27	7.66	SAL2, Inositol monophosphatase family protein
AT1G67810	1.49	1.57	2.93	-1.78	0.08	0.76	1.94	1.31	6.63	SUFE2, sulfur E2
AT3G26440	1.07	1.15	1.16	-2.74	-0.65	-0.23	2.89	1.84	5.14	Protein of unknown function (DUF707)
AT5G22530	2.82	1.48	1.79	0.11	-0.74	-0.53	2.45	1.43	2.67	unknown protein
AT2G18690	1.62	2.14	2.36	-1.59	-0.60	-0.07	3.07	1.06	2.24	unknown protein
AT3G14280	0.85	1.08	1.84	-2.88	-0.22	0.08	2.31	1.43	7.26	unknown protein

2.3.4. Specific ILA effect on the JA response

Sixty two genes were specifically induced more than twofold by ILA, but not induced in the *ugt76b1* knockout (Figure 13A). To get a hint on the functional characteristics of these genes in plants, the BioMaps service (<http://www.virtualplant.org>) was used to analyze the enrichment pattern. BioMaps categorizes genes based on Gene Ontology (GO) terms and identifies GO-terms that are over-represented in the dataset. A significant over-represented category was indicated by a p-value of less than 0.01. Fifty three genes were assigned with the function annotation. Nineteen genes out of 53 were associated with the category “response to stimulus” (p=0.00253). In this group, responses to biotic stimuli, fungal stimuli, wounding and JA/ET-dependent resistance were overrepresented (Table 6). Additionally the category “lipid transport” was enriched in ILA-induced genes. In the classification of GO cellular component, the overrepresentation of the category “cell wall” was also enriched (Table 6). The fold change induction by ILA was listed together with the fluorescence signal value of the control (Col-0). The fluorescence signal value can be used to judge the confidence of the induction. *ORA59*, a key positive transcriptional regulator of JA/ET signaling transduction, as well as *PDF1.2* and *PDF1.4*, marker genes of the JA/ET pathway were among these 62 genes (Table 7). Furthermore, two WRKY transcriptional factors *WRKY28* and *WRKY8* were induced by ILA more than twofold. *WRKY28* is involved in SA biosynthesis (van Verk et al., 2011). *WRKY8* is a negative regulator of SA-mediated resistance against *P. syringae* and positive regulator of JA-mediated resistance against *B. cinerea*, which can be induced by wounding (Chen et al., 2010a).

Table 6. Functional classification of genes induced more than twofold by ILA, but not induced in the *ugt76b1* knockout, according to TAIR ontology.

Sixty two genes upregulated only by ILA (Figure 13) were tested for over-representation against *Arabidopsis thaliana* ATH1 (23,334 genes) background population by using the BioMaps tool at VirtualPlant (<http://virtualplant.bio.nyu.edu/cgi-bin/vpweb/>). Categories enriched at $p < 0.01$ are listed here. The method used to calculate p-values of over-representation was hypergeometric distribution *. Nine genes were not assigned and hence total number of genes considered was reduced to fifty three.

Term	Observed Frequency	Expected Frequency	p-value
GO Biological Process			
response to stimulus	19 out of 53 genes, 35.8%	3689 out of 24961 genes, 14.8%	0.00253
response to biotic stimulus	12 out of 53 genes, 22.6%	610 out of 24961 genes, 2.4%	2.52E-07
defense response	11 out of 53 genes, 20.8%	747 out of 24961 genes, 3%	1.05E-05
defense response to fungus	7 out of 53 genes, 13.2%	131 out of 24961 genes, 0.5%	5.95E-07
jasmonic acid and ethylene-dependent systemic resistance	2 out of 53 genes, 3.8%	7 out of 24961 genes, 0%	0.00281
response to wounding	4 out of 53 genes, 7.5%	145 out of 24961 genes, 0.6%	0.00414
lipid transport	4 out of 53 genes, 7.5%	146 out of 24961 genes, 0.6%	0.00414
GO Cellular Component			
cell wall	7 out of 53 genes, 13.2%	553 out of 22480 genes, 2.5%	0.0059
endomembrane system	18 out of 53 genes, 34%	3499 out of 22480 genes, 15.6%	0.0088

Table 7. Sixty two genes were induced only by ILA (Figure 13A).

¹ Leaves of Col-0 were sprayed with 1 mM ILA, compared with Col-0 sprayed with water *via* microarray. The value is \log_2 -transformed fold change. ²The average fluorescence of three biological replicates of water-treated Col-0 in microarray analysis. The value of \log_2 -transformed fluorescence is from 4 to 20.

AGI	ILA ¹	fluorescence in WT ²	Annotation (TAIR 10)
AT5G44420	3.12	10.69	LCR77, PDF1.2, PDF1.2A, plant defensin 1.2
AT1G19610	1.77	8.00	LCR78, PDF1.4, Arabidopsis defensin-like protein
AT1G06160	1.83	5.09	ORA59, ERF 59
AT2G43590	1.45	8.99	Chitinase family protein
AT2G43620	1.44	8.26	Chitinase family protein
AT4G37990	1.87	4.91	CAD8, CAD-B2, ELI3, ELI3-2, elicitor-activated gene 3-2
AT2G36080	1.06	6.30	AP2/B3-like transcriptional factor family protein
AT4G18170	1.22	6.51	WRKY28
AT5G46350	1.48	6.41	WRKY8
AT1G06230	1.04	9.21	GTE4, global transcription factor group E4
AT4G12480	2.73	1.61	pEARLI 1, Bifunctional inhibitor/lipid-transfer protein/seed storage 2S albumin superfamily protein
AT4G12490	3.75	8.68	Bifunctional inhibitor/lipid-transfer protein/seed storage 2S albumin superfamily protein
AT4G12500	3.34	5.47	Bifunctional inhibitor/lipid-transfer protein/seed storage 2S albumin superfamily protein
AT3G22620	1.86	7.62	Bifunctional inhibitor/lipid-transfer protein/seed storage 2S albumin superfamily protein
AT2G43510	2.44	8.74	ATT11, T11, trypsin inhibitor protein 1
AT2G38870	1.38	11.53	Serine protease inhibitor, potato inhibitor I-type family protein
AT2G30750	1.86	2.71	CYP71A12, cytochrome P450, family 71, subfamily A, polypeptide 12

AT5G53320	1.10	3.92	Leucine-rich repeat protein kinase family protein
AT2G25470	1.47	2.13	RLP21, receptor like protein 21
AT1G76930	3.23	3.63	EXT1, EXT4, ORG5, extensin 4
AT5G05340	2.41	4.33	Peroxidase superfamily protein
AT5G64120	1.90	8.60	Peroxidase superfamily protein
AT4G08770	1.21	4.79	Peroxidase superfamily protein
AT5G52390	2.08	6.29	PAR1 protein
AT3G27400	1.35	8.23	Pectin lyase-like superfamily protein
AT1G75310	1.02	8.67	AUL1, auxin-like 1 protein
AT1G74010	1.87	4.96	Calcium-dependent phosphotriesterase superfamily protein
AT5G44800	1.27	7.19	CHR4, PKR1, chromatin remodeling 4
AT5G43310	1.18	8.63	COP1-interacting protein-related
AT2G17740	1.44	1.89	Cysteine/Histidine-rich C1 domain family protein
AT1G79400	1.05	2.42	CHX2, cation/H ⁺ exchanger 2
AT3G59220	1.03	6.58	PIRIN1, PRN, PRN1, pirin
AT1G34355	1.03	2.63	PS1, forkhead-associated (FHA) domain-containing protein
AT2G37770	1.73	3.36	NAD(P)-linked oxidoreductase superfamily protein
AT5G12420	1.57	1.71	O-acyltransferase (WSD1-like) family protein
AT3G62150	1.09	8.41	PGP21, P-glycoprotein 21
AT5G57480	1.03	7.01	P-loop containing nucleoside triphosphate hydrolases superfamily protein
AT1G15125	1.89	6.74	S-adenosyl-L-methionine-dependent methyltransferases superfamily protein
AT1G26390	2.78	2.55	FAD-binding Berberine family protein
AT1G30700	1.55	3.30	FAD-binding Berberine family protein
AT1G80810	1.17	3.79	Tudor/PWWP/MBT superfamily protein
AT5G40340	1.04	9.29	Tudor/PWWP/MBT superfamily protein
AT5G46070	1.20	9.26	Guanylate-binding family protein
AT5G61890	1.32	6.65	Integrase-type DNA-binding superfamily protein
AT5G05390	1.01	4.30	LAC12, laccase 12
AT1G15415	1.35	2.64	Encodes protein phosphatase 2A (PP2A) B'gamma subunit
AT2G39350	1.12	7.26	ABC-2 type transporter family protein
AT2G39030	3.21	7.72	Acyl-CoA N-acyltransferases (NAT) superfamily protein
AT1G76810	1.07	9.07	eukaryotic translation initiation factor 2 (eIF-2) family protein
AT3G02885	1.80	3.92	GASA5, GAST1 protein homolog 5
AT4G10120	1.24	10.41	SPS4F, Sucrose-phosphate synthase family protein
AT1G79830	1.02	8.51	GC5, golgin candidate 5
AT2G41800	2.25	8.17	Protein of unknown function, DUF642
AT3G47200	1.68	2.55	Plant protein of unknown function (DUF247)
AT5G16730	1.38	9.10	Plant protein of unknown function (DUF827)
AT5G44574	1.40	5.26	unknown protein
AT3G14060	1.35	2.99	unknown protein
AT1G03820	1.30	9.80	unknown protein
AT4G39675	1.06	1.83	unknown protein
AT1G28400	1.06	2.46	unknown protein
AT5G44575	1.05	8.16	unknown protein
AT3G14172	1.19	6.15	function unknown

Three genes belonging to peroxidase superfamily proteins encoded by At5g05340, At5g64120 and At4g08770 were also induced by ILA. Many studies provided evidence that plant

peroxidases participate in many cellular processes such as lignification, suberization, auxin catabolism, wound healing and defense against pathogens (Hiraga et al., 2001).

Four lipid transfer proteins (LTPs), *EARLII* (At4g12480), At4g12490, At4g12500 and At3g22620 were induced by ILA. LTPs transfer phospholipids between membranes *in vitro* and there are at least 15 LTP genes in the *Arabidopsis* genome. LTPs show diverse functions and some exhibit regulation of defense resistance. DEFECTIVE IN INDUCED RESISTANCE 1 (DIR1) promotes systemic acquired resistance probably *via* binding a lipid molecule (Maldonado et al., 2002). The mutation of AZELAIC ACID INDUCED 1 (AZI1), another lipid transfer protein, is compromised in the priming of resistance by Azelaic acid (Jung et al., 2009). *EARLII* together with At4g12490, At4g12500 and At4g12470 are closely related in the phylogenetic tree based on the homology of proteins, which can be all responsive to the same stimulus cold stress (Vogel et al., 2005). Three members of this family, *i.e.* *EARLII* (At4g12480), At4g12490 and At4g12500, are induced in by ILA. Interestingly the tight co-expression pattern of *EARLII* (At4g12480), At4g12490 and At4g12500 together with *AZII* was found by checking the co-expression pattern of *EARLII* using the public database ATTED (Figure 14). Another defense marker gene *PDF1.4* was tightly co-expressed with *EARLII* as well. Therefore, ILA might also activate defense *via* these LTPs.

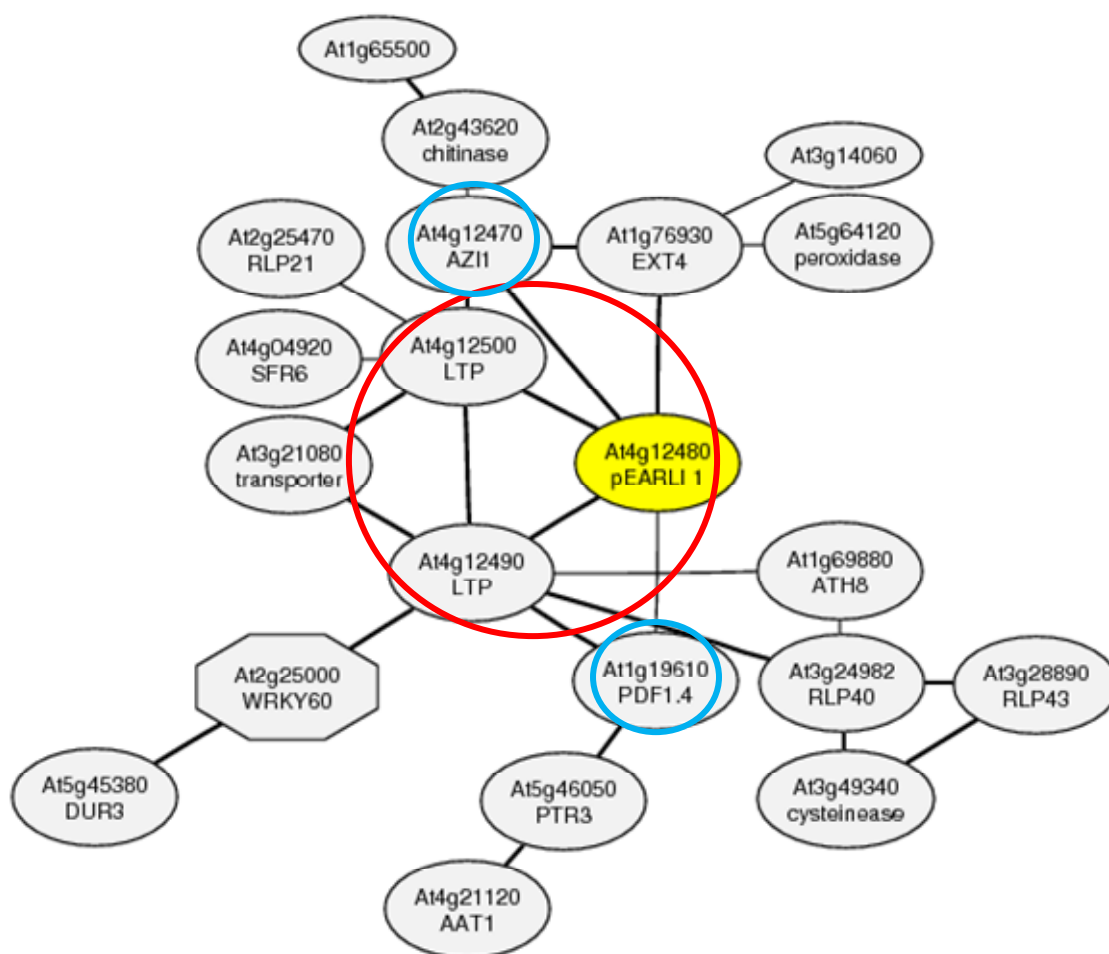


Figure 14. Gene co-expression network for *EARLII* (At4g12480).

Co-expression analysis was performed using the ATTED co-expression tool (<http://atted.jp/>)

2.3.5. Validation of the negative correlation of ILA application and the *UGT76B1* expression level in regulating defense-responsive genes

The above microarray analysis indicated a reverse correlation of *UGT76B1* expression and exogenous ILA application in mediating defense gene expression. From microarray data, *SAG13*, *YSL9*, *AIG1*, *CYP71A13*, *PAD3* and *NUDT6* were among the gene lists commonly induced by ILA and the *ugt76b1* knockout (Table 5). *SAG13* and *YSL9* are senescence marker genes. *CYP71A13* and *PAD3* are camalexin synthesis-related genes. *NUDT6* encoding an ADP-ribose/NADH pyrophosphohydrolase is a positive regulator of SA pathway, which modulates *NPR1* activity (Ishikawa et al., 2010). *AIG1* is the expression marker after infection with *Pseudomonas syringae* pv *maculicola* strain ES4326 carrying *avrRpt2*, dependent on the avirulent effector *avrRpt2* (Reuber and Ausubel, 1996). *PR3* and *PR4* are the marker genes of ET pathway.

In order to validate the negative correlation of ILA and *UGT76B1* in regulating defense responsive genes, these genes together with *FMO1*, which is required for SAR, *PBS3*, a positive regulator of SA synthesis, as well as ET marker genes (*PR3* and *PR4*), were measured after ILA treatment and in lines with different *UGT76B1* expression by RT-qPCR.

SAG13, *YSL9*, *FMO1*, *AIG1*, *PAD3* and *CYP71A13* can be significantly induced by ILA and in *ugt76b1-1* to similar degrees, but tended to be suppressed, however, in *UGT76B1-OE-7* (Figure 15A). *NUDT6* was the only gene which was both significantly upregulated by ILA and in *ugt76b1-1* and significantly suppressed in *UGT76B1-OE-7* (Table 3 and Figure 15A), suggesting that *NUDT6* expression was very sensitive to and more robustly responding to *UGT76B1*/ ILA regulation. *PBS3*, involved in SA synthesis, was significantly induced in *ugt76b1-1*, however tended to be slightly induced by ILA. *PR4* was significantly induced by ILA more than twofold. Thus, the negative correlation of *UGT76B1* and ILA in mediating defense response was confirmed.

Previously it had been shown that the SA marker gene *PR1* was induced in *ugt76b1-1*, but suppressed in *UGT76B1-OE-7*. On the other hand, the JA/ET marker gene *PDF1.2* was suppressed in *ugt76b1-1*, but activated in *UGT76B1-OE-7* (von Saint Paul, 2010). Thus they were not included in the genes mentioned above. To further investigate the impact of ILA activity on their expression, *PR1* and *PDF1.2* were measured 24 h after ILA treatment. *PR1* was induced by ILA in a concentration dependent manner (Figure 15B), suggesting a positive effect of ILA on it. *PDF1.2* was significantly induced by ILA application (Figure 15B and Figure 32). Notably, ILA and the *ugt76b1* mutant showed opposite regulation on *PDF1.2* expression, demonstrating that exogenously applied ILA exerted some unique regulation different from the *ugt76b1* knockout. However, *VSP2*, a JA-dependent marker gene of wounding response, was not altered by ILA treatment (Figure 15B). It has been shown that JA response contains two branches: the *ERF*-mediated branch and the *MYC2*-mediated branch. The *ERF*-mediated branch regulates *PDF1.2* expression and resistance against necrotrophic pathogens (see introduction). The *MYC2*-mediate branch regulates *VSP2* expression and response to wounding and herbivores. Hence, ILA could activate *PDF1.2* expression mediated by *ERF* branch, opposite to the downregulation of *PDF1.2* by the *ugt76b1* knockout scenario.

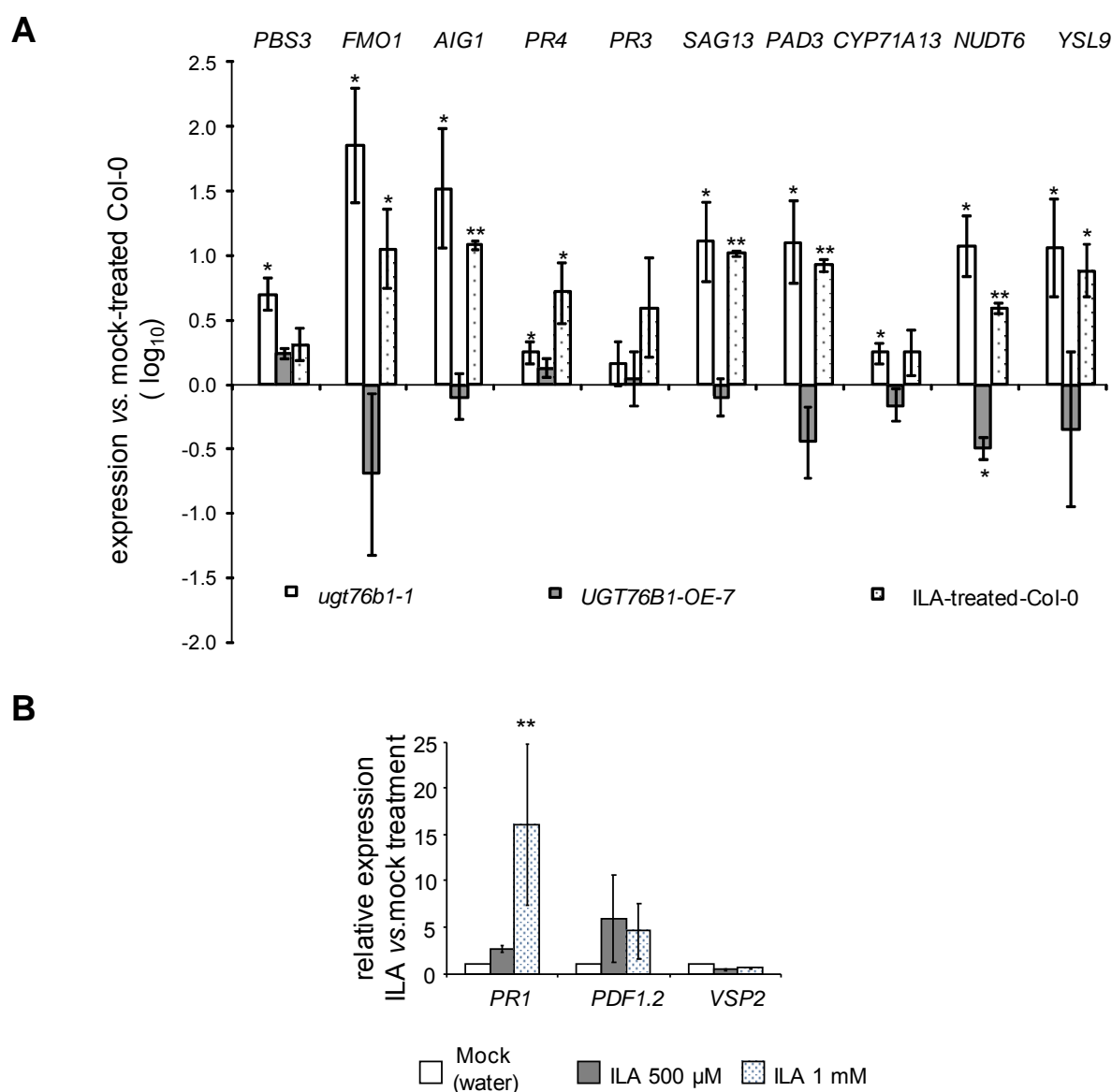


Figure 15. Defense marker gene expression altered by *UGT76B1* expression and ILA treatment.

(A) Gene expression of *PBS3*, *FMO1*, *AIG1*, *PR4*, *PR3*, *SAG13*, *PAD3*, *CYP71A13*, *NUDT6* and *YSL9* in 4-week-old plants measured by RT-qPCR. Col-0 was treated with 1 mM ILA; the *ugt76b1-1* and *UGT76B1-OE-7* overexpression lines were treated with sterile distilled water (mock). (B) Defense marker gene expression in Col-0 plants after ILA treatment. Transcript levels of *PR1*, *PDF1.2* and *VSP2* in leaves of four-week-old plants 24 h after ILA or water treatment measured by RT-qPCR. Values are relative to expression 24 h after mock (water) treatment. Expression levels are normalized to *UBIQUITIN5* and *S16* transcripts; levels relative to mock-treated Col-0 plants (water) are displayed. Arithmetic means and standard errors were derived from \log_{10} -transformed data of three replicates. Stars indicate significance of the difference compared to mock-treated Col-0 calculated by T-test (unpaired). ** p-value ≤ 0.01 , * p-value < 0.05 .

2.4. ILA activity

2.4.1. ILA enhances resistance against *Pseudomonas* infection

From the above study (results from 2.3) it can be concluded that ILA activates the expression of many defense genes. To test whether the activation of defense genes by ILA could be transformed to pathogen resistance, the susceptibility towards the biotrophic avirulent pathogen *P. syringae* strain DC3000 *AvrRpt2* was tested after ILA application. Plants were pretreated with 1 mM ILA 24 h prior to inoculation. In contrast to the mock-sprayed plants, ILA-treated plants showed less bacterial growth both 1 d and 3 d after inoculation suggesting a consistent resistance induced by ILA (Figure 16). Therefore, ILA directly activates resistance against pathogen infection.

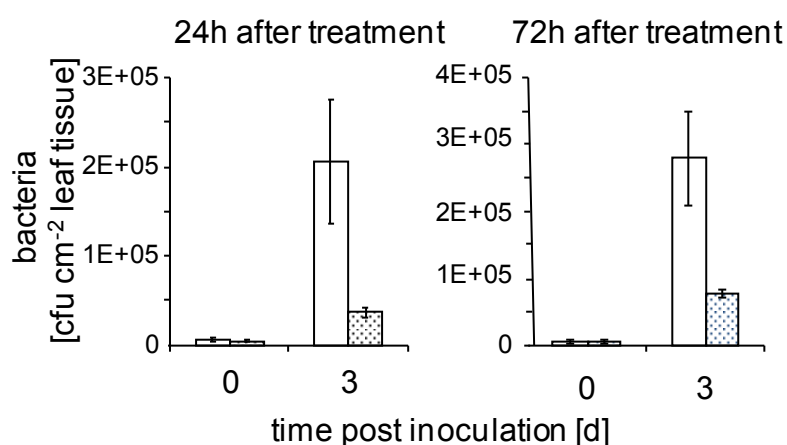


Figure 16. Effect of exogenously applied ILA on susceptibility towards avirulent *Pseudomonas syringae* infection.

Bacterial growth in *Arabidopsis* leaves of wild-type plants sprayed with water (blank) or 1 mM ILA (dotted) 24 h or 72 h before infection. Plants were inoculated with 5×10^5 cfu ml⁻¹ of *P. syringae* and bacteria (cfu cm⁻²) were quantified 0 and 3 d after inoculation. The graphs represent the means and standard deviations of three replicates.

2.4.2. Involvement of *UGT76B1* in ILA action on regulation of defense genes

In *ugt76b1-1*, the lack of glucosylation of ILA can lead to the enhancement of SA-dependent and independent signaling. In the case of *UGT76B1-OE-7* line, *UGT76B1* overexpression generates more ILA glucoside and reduces the SA marker gene *PR1* expression. Consistent with this, exogenous ILA application can partially revert the suppression of *PR1* expression in *UGT76B1-OE-7* (Figure 17). *PR1* expression was already high in *ugt76b1-1*, thus it could not be induced any further by exogenous ILA. The JA marker gene *VSP2* was not changed in both *ugt76b1-1* and *UGT76B1-OE-7*. Thus ILA, not ILA-glucoside, could be the active compound inducing *PR1* expression.

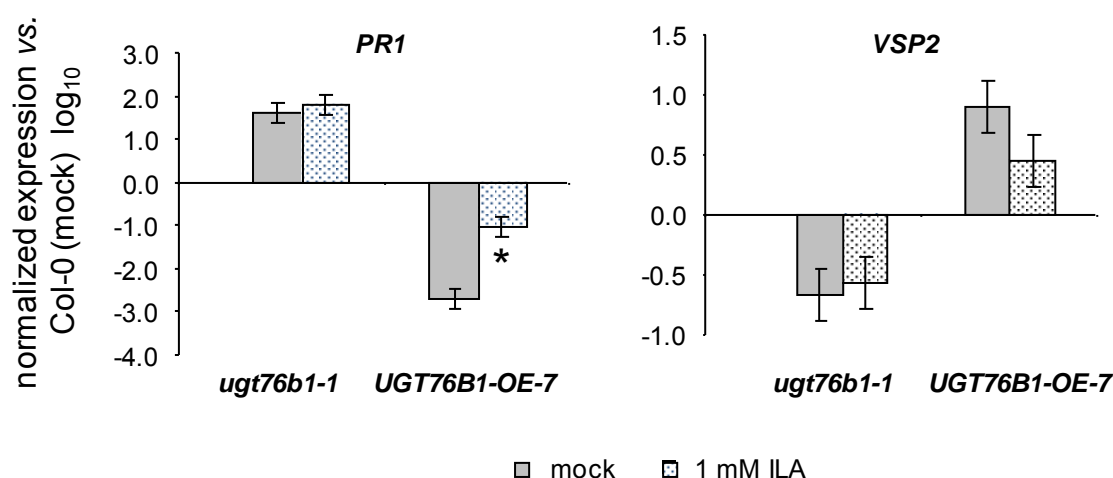


Figure 17. Isoleucic acid treatment in *ugt76b1-1* and *UGT76B1-OE-7*.

Gene expression of *PR1* and *VSP2* in five-week-old *ugt76b1-1* and *UGT76B1-OE-7* lines 24 h after ILA or mock (water) treatment measured by RT-qPCR. Expression levels are normalized to *UBIQUITIN5* and *S16* transcripts; levels relative to Col-0 mock treatment are displayed. Arithmetic means and standard errors, derived from log₁₀-transformed data of two experiments with each consisting of three independent replicates were calculated using ANOVA, * p-value < 0.05.

The recombinant protein UGT76B1 has *in vitro* glucosylation activity towards SA (von Saint Paul, 2010; Noutoshi et al., 2012). However, Noutoshi et al. (2012) reasoned that the increased defense by ILA was due to the inhibition of UGT76B1 to glucosylate SA (Noutoshi et al., 2012). This is in contradiction to our interpretation that ILA can directly impact on plant defense.

To test this, I analyzed defense marker genes after ILA application in the *ugt76b1 sid2* double mutant. Since SA accumulation and defense response indicated by enhanced *PR1* expression were already highly activated in the *ugt76b1* knockout line, probably there was not much room for further defense activation. However, the removal of *SID2* in *ugt76b1* can bring the

high expression of *PR1* to a lower level, thus enabling to test for a potential, *SID2*-independent induction of *PR1*. Indeed, *PR1* expression can be still induced in the *ugt76b1 sid2* line after ILA application (Figure 18A). Other defense genes *PDF1.2*, *FMO1*, *AIG1*, *PAD3*, *SAG13*, *NUDT6* and *YSL9* were also significantly induced by ILA in *ugt76b1 sid2* (Figure 18A and B). Furthermore, in the *NahG* line, which completely hydrolyzes SA, ILA can still activate most defense genes (Figure 18B). This strongly argued against the notion that exogenous application of ILA activates defense genes through inhibiting the glucosylation activity of UGT76B1 towards SA.

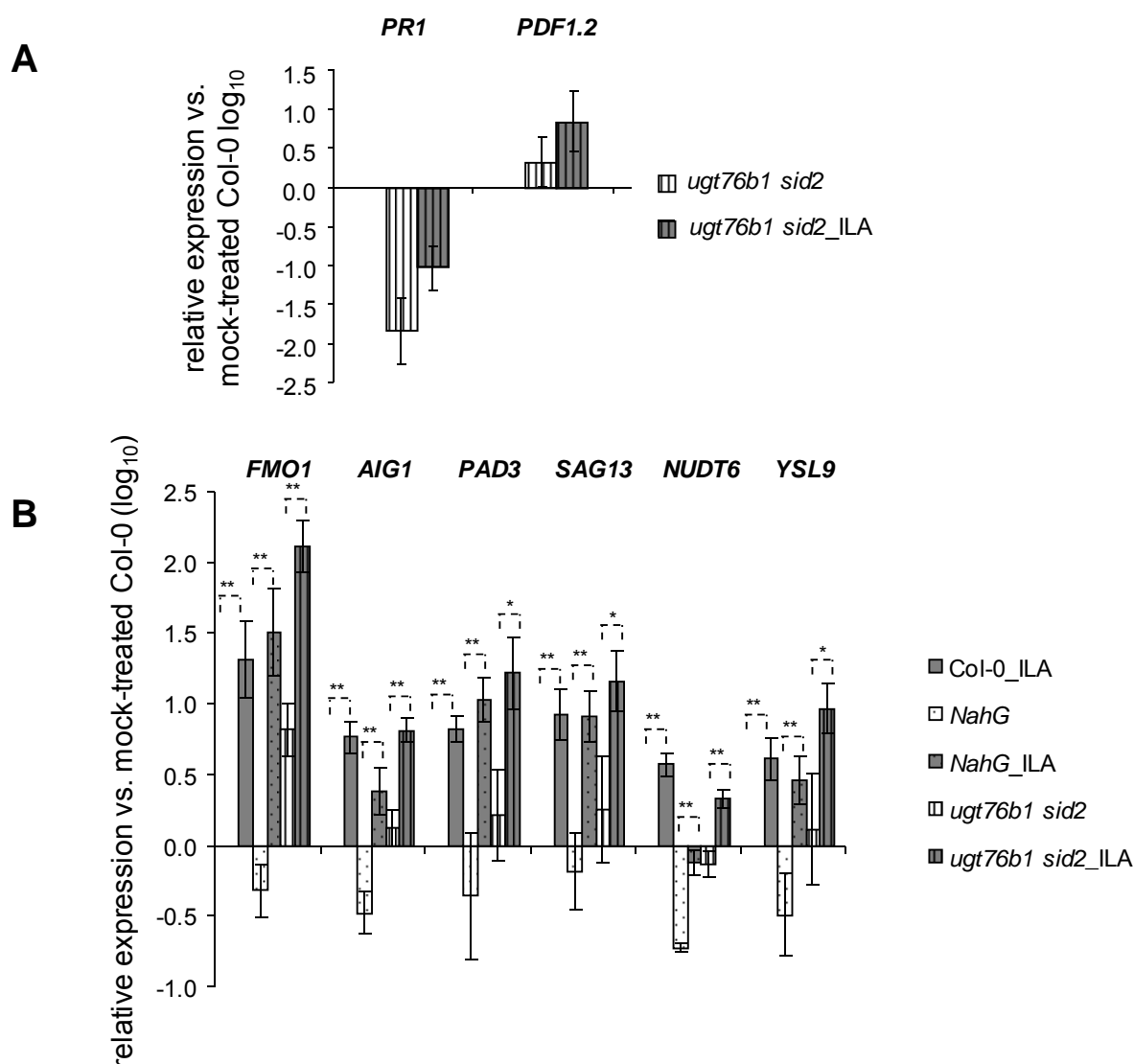


Figure 18. Effect of ILA in *ugt76b1 sid2* and *NahG* on activation of defense genes

(A) Transcript levels of *PR1*, *PDF1.2* and *UGT76B1* in leaves of four-week-old *ugt76b1 sid2*, 24 h after ILA or mock (water) treatment measured by RT-qPCR.

(B) Transcript levels of *FMO1*, *AIG1*, *PAD3*, *SAG13*, *NUDT6* and *YSL9* in leaves of four-week-old *ugt76b1 sid2* and *NahG* lines 24 h after 1 mM ILA treatment were measured by RT-qPCR. Expression

levels are normalized to *UBIQUITIN5* and *S16* transcripts; levels relative to Col-0 mock treatment are displayed. Means and standard errors were calculated from three independent biological replicates.

2.4.3. The requirement of SA and JA/ET pathways in ILA action on regulation of defense genes

From the above studies, it has been already known that ILA triggers defense responses very broadly including SA-mediated, JA/ET-mediated, senescence-related and camalexin-related responses.

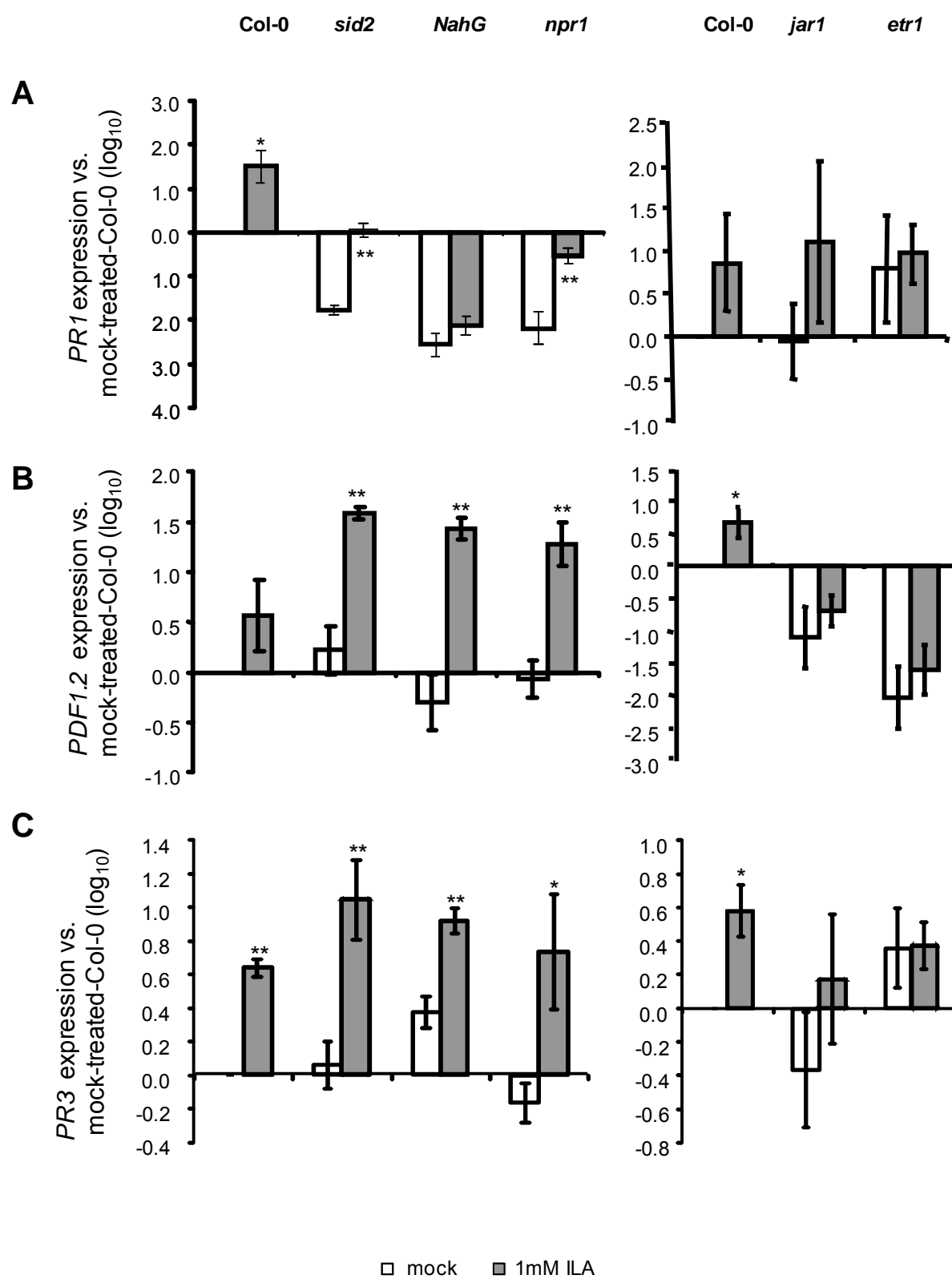
To assess the requirement of regulators and key steps in the SA and JA/ET pathways for the ILA action on defense, the expression of many defense genes was analyzed by RT-qPCR in the *sid2*, *NahG*, *npr1*, *jar1* and *etr1* mutants sprayed with ILA. These defense genes included the SA marker gene *PR1*, the JA/ET marker gene *PDF1.2*, the ET marker gene *PR3*, the senescence marker gene *SAG13*, the camalexin-biosynthetic gene *PAD3*, and the HR-related gene *AIG1*. The *sid2*, *NahG* and *npr1* lines are defective in SA response; the *jar1* mutant blocks JA response and the dominant mutant of ethylene receptor *etr1* causes an impaired response to ethylene.

Induction of *PR1* by ILA was completely lost in *NahG*, suggesting the dependence on SA total levels. However, *PR1* could be induced in *sid2* by ILA to a similar magnitude as in Col-0 though the expression level was still lower than the background of Col-0 (Figure 19A). Thus, basal SA levels in *sid2* were required and sufficient to induce *PR1* by ILA, whereas *SID2* was necessary for full expression of *PR1*. Similarly, *PR1* could be induced in *npr1* by ILA to a similar magnitude as in Col-0 (Figure 19A). Thus, *PR1* could be induced by ILA through a *SID2*- and *NPRI*-independent manner, but dependent on basal SA levels, however. *JAR1* was not required for *PR1* induction. *ETR1* seemed to be a negative regulator of SA pathway. This could explain high *PR1* expression in *etr1*, which could not be further enhanced by ILA (Figure 19B). Therefore the activation of SA response (induction of *PR1*) by ILA was dependent on SA basal levels but independent from *SID2* or *NPRI*.

The expression of the JA/ET marker genes *PDF1.2* and *PR3* was also assessed in ILA-treated mutants. *PDF1.2* was highly induced in *sid2*, *NahG* and *npr1* by ILA to a much higher expression level than in ILA-treated Col-0 (Figure 19B). Similarly, *PR3* expression induced by ILA showed a tendency to be higher in *sid2*, *NahG* and *npr1* (Figure 19C). The more pronounced *PDF1.2* and *PR3* induction in *sid2*, *NahG* and *npr1* was probably due to the elimination of antagonism from the SA pathway on the JA pathway. The expression of

PDF1.2 was abolished by *etr1* and *jar1* with no further enhancement after ILA application, suggesting requirement of both intact JA and ET pathways to induce *PDF1.2* (Figure 19B). In contrast, *JAR1*, but not *ETR1*, seemed to be required for *PR3* expression. The mutant *etr1* constitutively activated *PR3* expression, which could not be further induced by ILA (Figure 19C). Therefore the activation of JA/ET response by ILA was dependent on the intact JA and ET pathways. Additionally, the activation of JA/ET response by ILA was more pronounced in the lines compromised in SA response.

The role of the SA pathway and the JA/ET pathway in ILA action was further tested by measuring *SAG13*, *AIG1* and *PAD3* expressions. Expressions of *SAG13*, *PAD3* and *AIG1* were still induced by ILA in *NahG*, suggesting independence from SA accumulation (Figure 19D, E and F). The induction of *SAG13*, *PAD3* and *AIG1* as well as other defense genes *FMO1*, *NUDT6* and *YSL9* by ILA in *NahG* was confirmed by RT-qPCR (Figure 18B). Similarly, *SAG13*, *PAD3* and *AIG1* could be induced effectively by ILA in *npr1* and *sid2* (Figure 19D, E and F). Therefore, ILA could activate *SAG13*, *PAD3*, *AIG1* independent of the SA pathway. *SAG13*, *PAD3*, *AIG1* could be induced by ILA in *jar1* to an even higher expression than in Col-0 (Figure 19D, E and F), suggesting independence from *JAR1*. Interestingly the *etr1* mutant itself showed high expression of most defense genes such as *SAG13*, *PAD3* and *AIG1* (Figure 19D, E and F). This suggested that the ET pathway might negatively regulate these defense genes. Thus, ILA could activate defense response independent from SA or JA/ET pathways.



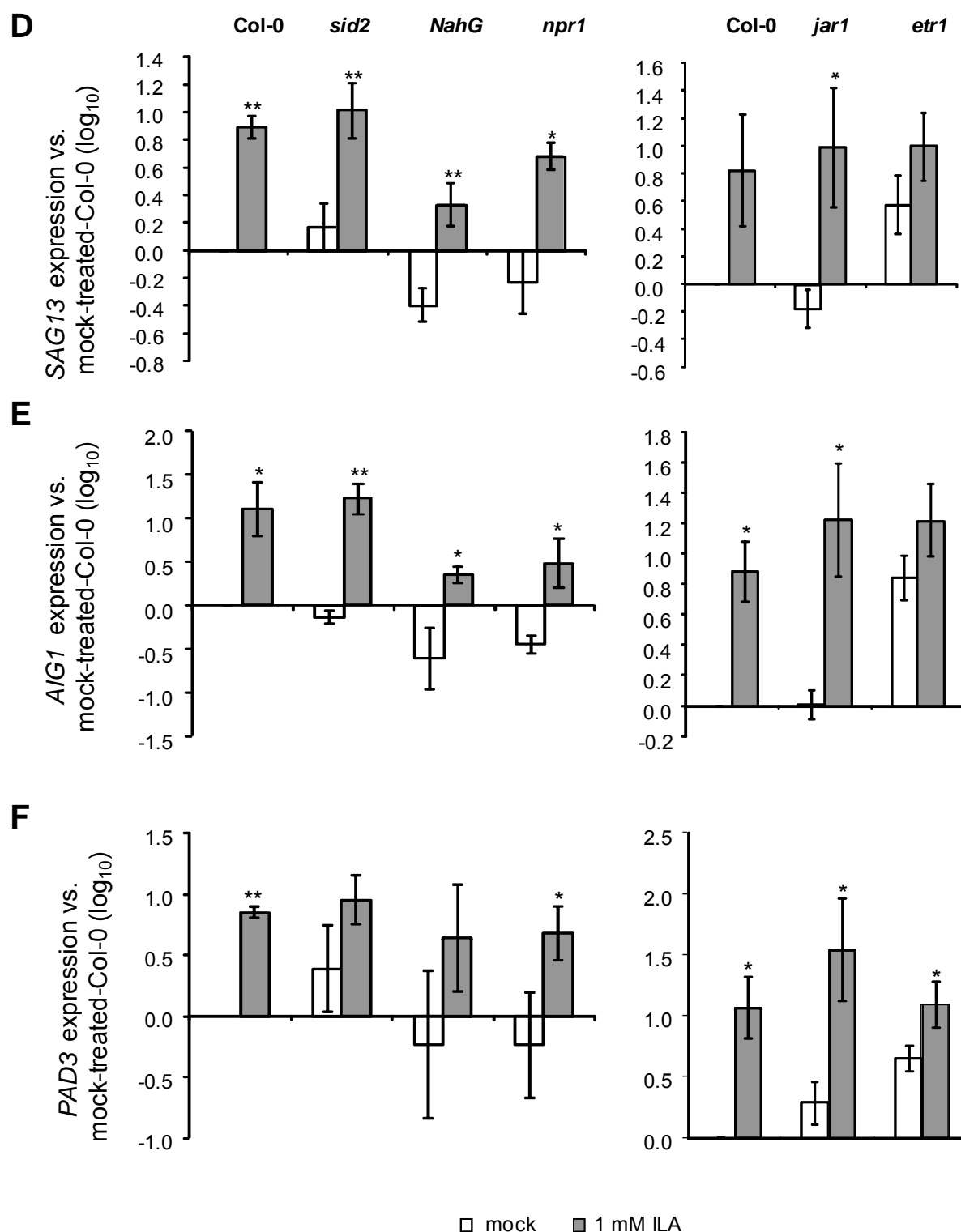


Figure 19. Defense marker genes expression by ILA treatment in lines deficient in SA (*sid2*, *NahG*, *npr1*), JA (*jar1*) and ET (*etr1*) pathways.

Gene expression of *PR1* (A), *PDF1.2* (B), *PR3* (C), *SAG13* (D), *AIG1* (E) and *PAD3* (F) in 4-week-old plants measured by RT-qPCR. All the lines were treated with 1 mM ILA (dissolved in sterile distilled water) or sterile distilled water (mock treatment). Expression levels are normalized to *UBIQUITIN5* and *S16* transcripts; levels relative to mock-treated Col-0 plants are displayed. Arithmetic means and standard errors were derived from \log_{10} -transformed data of three replicates.

Stars indicate significance of the difference compared to mock-treated Col-0, calculated by T-test (unpaired). ** p-value ≤ 0.01 , * p-value < 0.05 .

2.4.4 The kinetic activation of SA- and JA-mediated defense genes by exogenous ILA application

The above studies have shown that ILA can induce marker genes of both SA and JA pathways when assayed 24 h after application of the chemical compound. SA- and JA- responsive genes were measured 0 h, 1 h, 3 h, 5.5 h, 8 h and 24 h after ILA application by RT-qPCR in order to analyze the kinetics of the activation of the pathways. *EDS1* and *PAD4* are positive regulators of SA synthesis and can respond to stimuli at early time points. *SID2* contributes to mostly stress-related SA synthesis, while *PHENYLALANINE AMMONIA-LYASE 1* (*PAL1*) is involved in the synthesis of basal SA by catalyzing the first step of the phenylpropanoid pathway. They can also be induced at early time points. *JAZ10* and *OPR3* are early JA-responsive markers. *PR1* and *PDF1.2* are late SA- and JA-responsive marker genes, respectively.

Early SA-responsive marker genes *EDS1*, *SID2* and *PAD4* showed nearly no change with a slight induction less than twofold 1 h after ILA treatment, but reached the maximum induction, however, 24 h after ILA treatment. *PAL1* did not show any notable differences between ILA- and mock-treated plants (Figure 20A). In contrast, early JA-responsive marker genes *JAZ10* and *OPR3* were transiently induced more than fourfold 1 h after ILA application and declined back to background level very fast 3 h after ILA treatment (Figure 20A). This indicated that the JA response was transiently and rapidly activated, much earlier than the activation of the SA response.

To further analyze the kinetic expression patterns of late SA marker gene *PR1* and late JA marker gene *PDF1.2*, expression of *PR1* and *PDF1.2* was observed at different time points within 24 h. *PR1* started to be induced 8 h after ILA treatment, then reached the maximum expression 24 h after ILA treatment. *PDF1.2* started to increase 3 h after ILA treatment earlier than initiation of *PR1* induction by ILA, then reached the maximum expression 8 h after treatment and declined to a lower expression level 24 h after treatment. Nevertheless, the level of *PDF1.2* was still induced 24 h after ILA treatment relative to untreated Col-0. Interestingly the kinetic expression pattern of *UGT76B1* was similar to *PDF1.2* and showed induction earlier than *PR1* (Figure 20B).

To determine how long the activation of SA and JA responses by ILA would last, the kinetics of *PR1*, *PDF1.2* and *UGT76B1* expression were measured at 1 d, 3 d and 5 d after ILA application. The induction of *PR1*, *PDF1.2* and *UGT76B1* reached a peak 1 d after ILA application, but then declined very rapidly to basic levels 3 d after ILA treatment. No difference of *PR1*, *PDF1.2* and *UGT76B1* caused by ILA could be observed 3 d and 5 d after ILA treatment (Figure 20C). Therefore, the lasting period of SA and JA response as well as *UGT76B1* was evident only within the three days after ILA treatment.

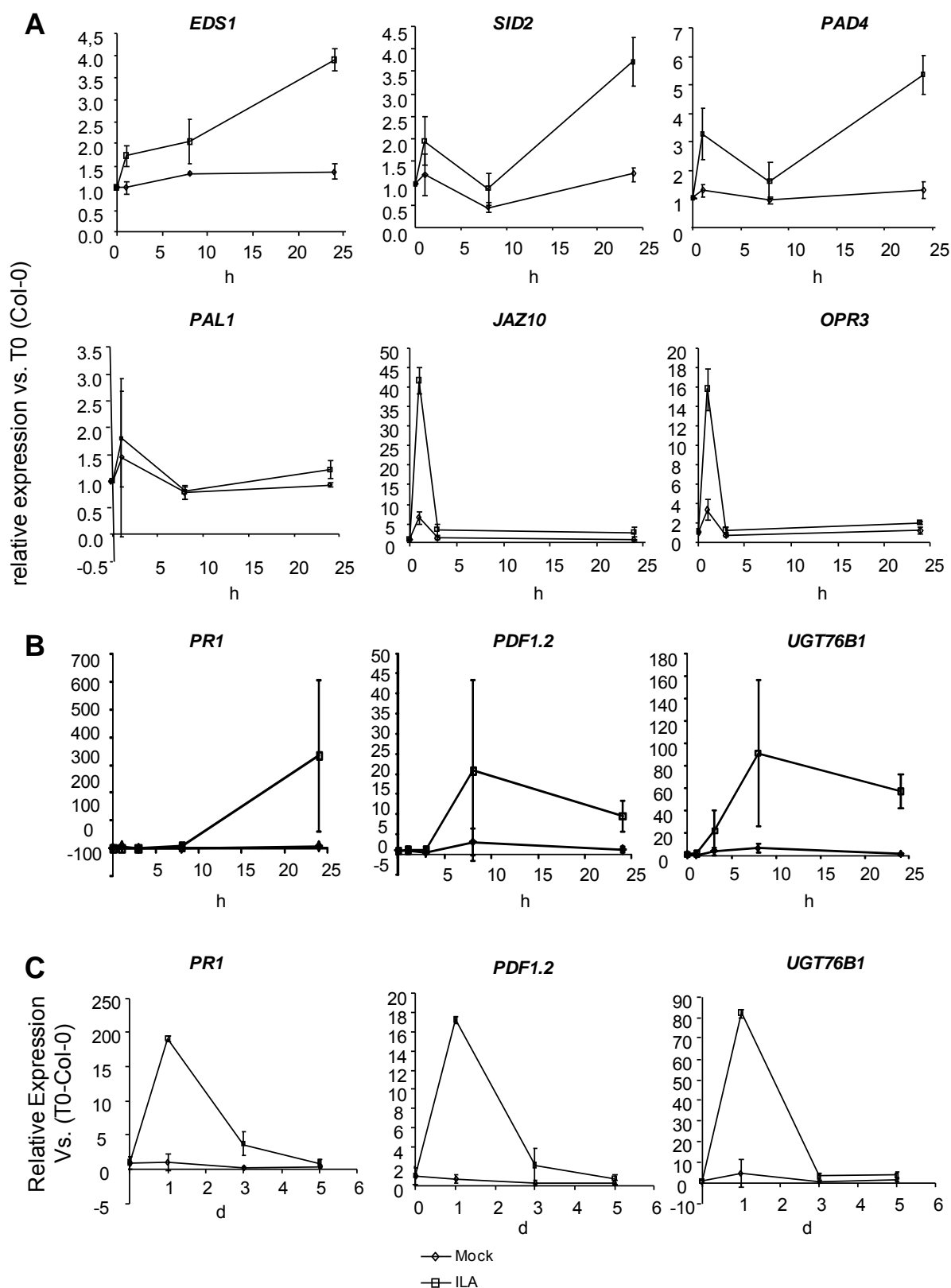


Figure 20. Time-course of expression of marker genes in SA and JA pathways and *UGT76B1* after ILA treatment.

ILA was applied to Col-0 at different time points including early time points before 24 h (0 h, 1 h, 3 h, 5.5 h, 8 h, 24 h) and late time points after 1 d (0 d, 1 d, 3 d, 5.d). (A) Transcript levels of JA early-responsive genes (*OPR3* and *JAZ10*) and SA early-responsive genes (*EDS1*, *PAD4*, *SID2* and *PAL1*)

were determined by RT-qPCR at 0 h, 1 h, 8 h and 24 h. (B) Transcript levels of *PR1*, *PDF1.2* and *UGT76B1* were determined at 0 h, 1 h, 3 h, 5.5 h, 8 h and 24 h. (C) Transcript levels of *PR1*, *PDF1.2* and *UGT76B1* were determined at 0 d, 1 d, 3 d and 5 d. Expression levels are normalized to *UBIQUITIN5* and *S16* transcripts; fold induction of all genes relative to Col-0 (T0) plants are displayed. Arithmetic means and standard errors were calculated from three replicates.

2.4.5 Measurement of SA- and JA-related metabolites after ILA treatment

Activation of both SA- and JA-responsive marker genes by ILA have demonstrated that ILA might directly impact on SA and JA synthesis. To test this, I measured SA- and JA-related metabolites after ILA treatment. Leucic acid (2-hydroxy-4-methyl pentanoic acid), an analogue of ILA, has a structure very similar to ILA. It may therefore have similar activities as ILA. Free SA, SA glucoside and SA ester were measured after application of ILA and its analogue leucic acid (2-hydroxy-4-methyl pentanoic acid).

Preliminary results showed free SA levels to be modestly increased after both ILA and its analogue leucic acid treatments. There was no difference observed with regard to the accumulation of SA glucose conjugates after application of ILA and leucic acid. SA ester levels were slightly induced by ILA, but not by leucic acid (Figure 21). Thus, ILA and leucic acid might slightly promote SA synthesis and the level of free SA.



Figure 21. Free SA and conjugated SA levels in 4-week-old seedlings of water-treated Col-0, ILA-treated Col-0 and leucic acid-treated Col-0.

Values represent the means and standard deviations from five replicates. FW, fresh weight.

JA-related metabolites Oxo-phytodienoic acid (OPDA), JA, JA-Ile and 12-OH-JA were measured 0 h, 3 h, 8 h, 24 h and 48 h after ILA treatment. At time point 0 h, the measurement of the *ugt76b1-1* knockout was taken for comparison. There were no obvious differences before and after ILA treatment with regard to the JA synthesis precursor OPDA, free JA and

the bioactive form JA-Ile. The degradation form 12-OH-JA can be significantly increased by ILA 8 h and 24 h after treatment (Figure 22). Thus, although the increase of 12-OH-JA suggests that ILA might slightly activate JA synthesis; there was no significant upregulation of OPDA, JA or JA-Ile.

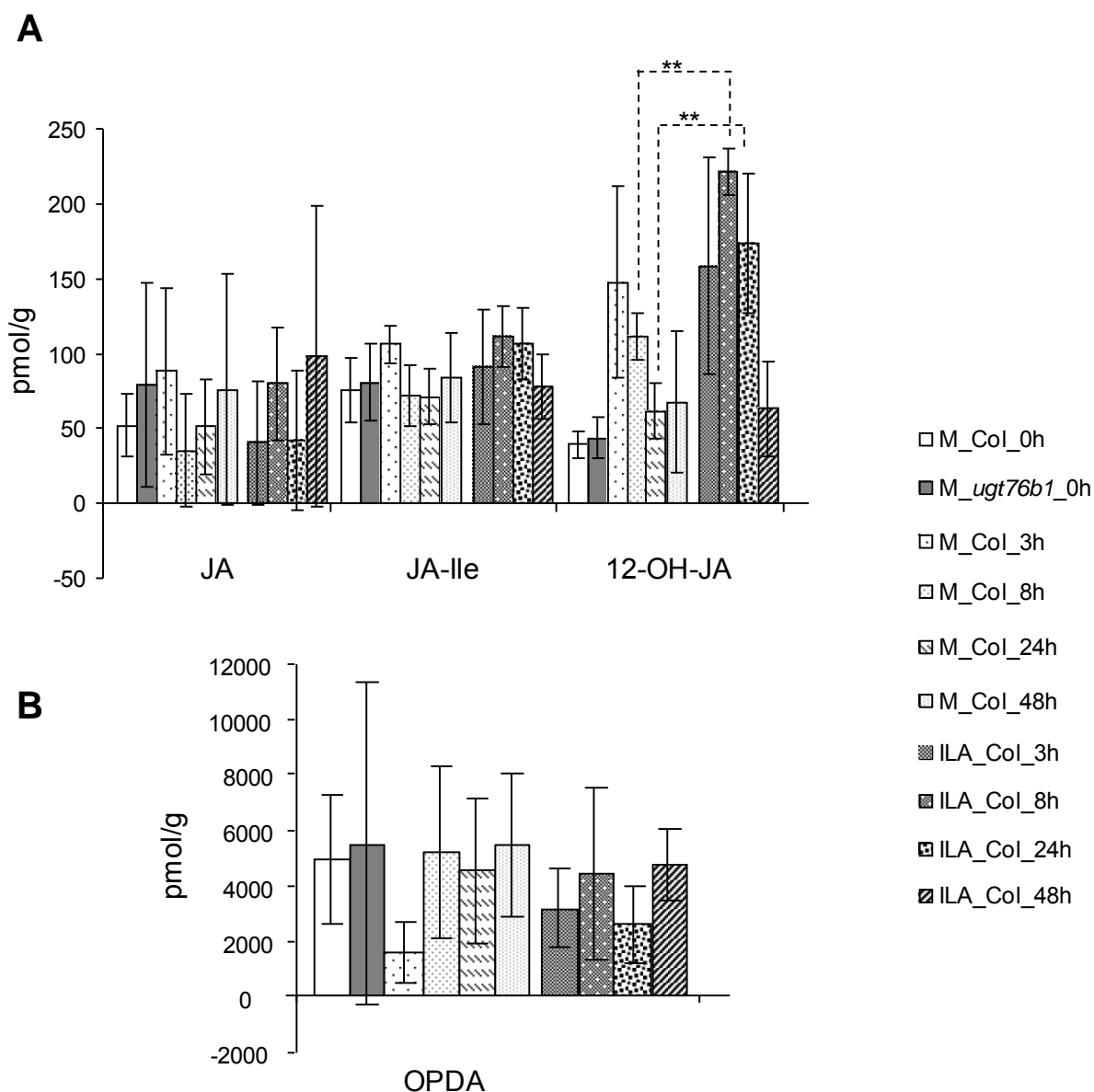


Figure 22. The measurement of JA-related metabolites.

(A) JA-related metabolites: JA, JA-Ile and 12-OH-JA were measured in ILA sprayed Col-0 or mock-treated (water) Col-0 at different time points after treatment (0 h, 3 h, 8 h, 24 h and 48 h). Mock-treated *ugt76b1-1* was as the control. (B) OPDA was measured at different time points. The measurement was repeated with similar results. Means and standard errors were calculated from five biological replicates. Stars indicate significance of the difference compared to mock-treated Col-0, calculated by the T-test (unpaired). ** p-value ≤ 0.01 .

2.4.6 The activity of ILA in inhibiting root growth

2.4.6.1 The activity of ILA in inhibiting root growth regulated by *UGT76B1* expression

The flagellin peptide flg22, which strongly interferes with the defense pathway of the leaves, also inhibits root growth of *Arabidopsis* seedlings (Gomez-Gomez and Boller, 2000; Zipfel et al., 2004). Furthermore, flg22 confers positive regulation on plant defense against pathogens in roots apart from the well-known regulation of defense responses against pathogens in leaves (Millet et al., 2010). Similarly the hormone SA, which is the crucial player in defense, and then non-protein amino acid BABA, which can confer resistance to pathogen infection were previously reported to inhibit root growth of *Arabidopsis* seedlings (Zimmerli et al., 2008; Wu et al., 2010).

To investigate whether ILA can inhibit seedling growth, the seedling growth was observed on plates containing ILA. Indeed, ILA clearly showed a root growth inhibition phenotype in a concentration dependent manner (Figure 23). Since *UGT76B1* is mainly expressed in the root tissue and ILA is the substrate of UGT76B1, the root growth inhibition by ILA was observed among lines with different *UGT76B1* expression. Consistent with being the substrate of UGT76B1, ILA caused a much stronger root growth inhibition phenotype of *ugt76b1-1*, but a less pronounced root growth inhibition of *UGT76B1-OE-7* as compared to Col-0 in a concentration dependent manner (Figure 23). This indicated that ILA, but not its conjugate ILA-glucoside, was active in inhibiting root growth.

Since *UGT76B1* is mainly expressed in the root of *Arabidopsis*, the susceptibility towards the root pathogen *Vertimicillum longisporum* was tested by our collaborator, the laboratory of Christiane Gatz (Universität Göttingen). However, there was no difference in susceptibility among the lines with different *UGT76B1* expression level and wild type (data not shown).

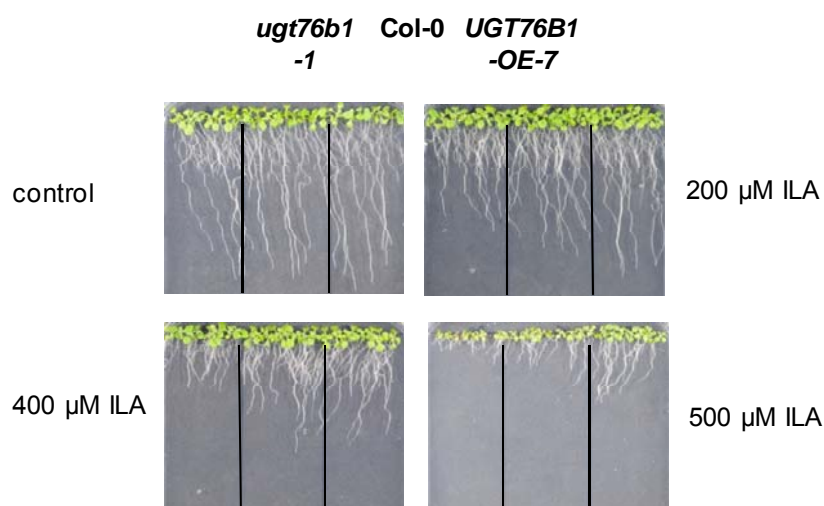


Figure 23. Direct effects of exogenously applied ILA.

Root growth inhibition phenotype of ILA inversely correlates with *UGT76B1* expression. Pictures were taken 10 d after sowing the seeds on plates containing 0, 200, 400 and 500 μM ILA.

2.4.6.2. Response to ILA in roots does not require SA, JA and ET pathways

Lines deficient in SA, JA or ET pathways were grown on plates containing ILA in order to explore whether or not the inhibition of root growth required SA, JA or ET pathways. The lines *NahG*, *npr1* and *sid2* are deficient in SA response; the *jar1* mutant is deficient in JA-mediated response and the *etr1* mutant is deficient in ET-mediated response. The mutation of CONSTITUTIVE EXPRESSION OF PR GENES 5 leads to the *cpr5* mutant with a constitutive activation of the SA pathway (Bowling et al., 1997). The root growth of seedlings of the *NahG*, *npr1* and *sid2* lines could still be inhibited by ILA indicating that ILA perception in the root was independent from the SA pathway. The root growth of seedlings of the *jar1* and *etr1* mutants could also be inhibited by ILA, suggesting independence of ILA perception of the JA/ ET pathways (Figure 24). The root inhibition in the *cpr5* line was effective, though SA levels were very high in the *cpr5* mutant (Figure 24).

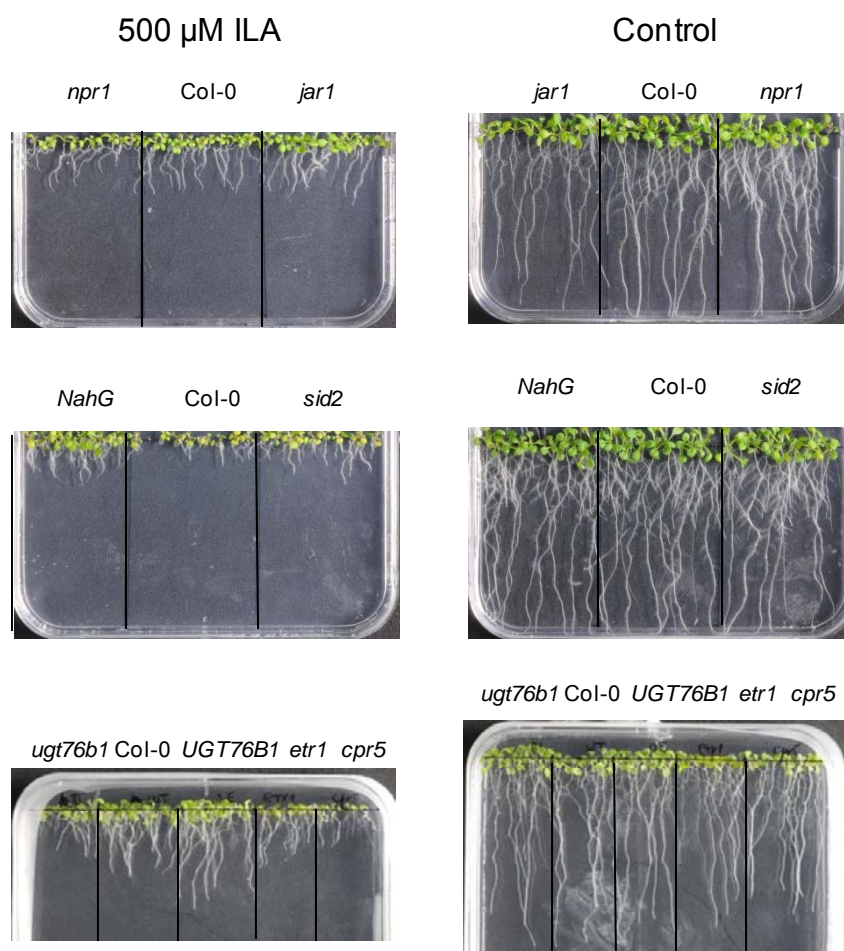


Figure 24. ILA perception by roots in lines deficient in SA, JA and ET pathways and the *cpr5*

Root growth inhibition phenotypes by 500 μM ILA were observed among lines deficient in SA pathway (*NahG*, *sid2*), JA pathway (*jar1*) and ET pathway (*etr1*) and the *cpr5* mutant. Col-0, *ugt76b1* and *UGT76B1* were taken as the control. The pictures were taken 10 d after sowing the seeds on plates containing 500 μM ILA.

2.4.6.3. The activity of ILA in inhibiting root growth regulated by *GOX3* expression

During the photo-respiratory process, glycolic acid, the simplest hydroxy acid, is produced by oxidation of RuBP and further exported to peroxisomes where it is then oxidized by glycolate oxidase (GOX) to glyoxylic acid, causing the parallel formation of H_2O_2 . Subsequently, glyoxylic acid is transferred to the amino acid glycine by glutamate: glyoxylate aminotransferase (Igarashi et al., 2003; Igarashi et al., 2006). Since ILA (2-hydroxy-3-methylpentanoic acid) has a very similar structure as the amino acid Ile, ILA may be converted to Ile via an intermediate precursor, 2-keto-3-methylpentanoic acid. This process would require a dehydrogenase. There are several candidates such as LDH and GOX. GOX3 has the function to oxidize the simple hydroxy acid to the keto form glyoxylic acid *in vivo*. To get a hint, the mutant *gox3* was placed on medium containing ILA to observe the root growth inhibition

phenotype. Shorter root length conferred by ILA in the *gox3* mutant suggested the potential of *GOX3* to catabolize ILA to the keto-form, the precursor of isoleucine (Figure 25). This could be linked to the amino acid precursor keto-acid forms and metabolism of ILA.

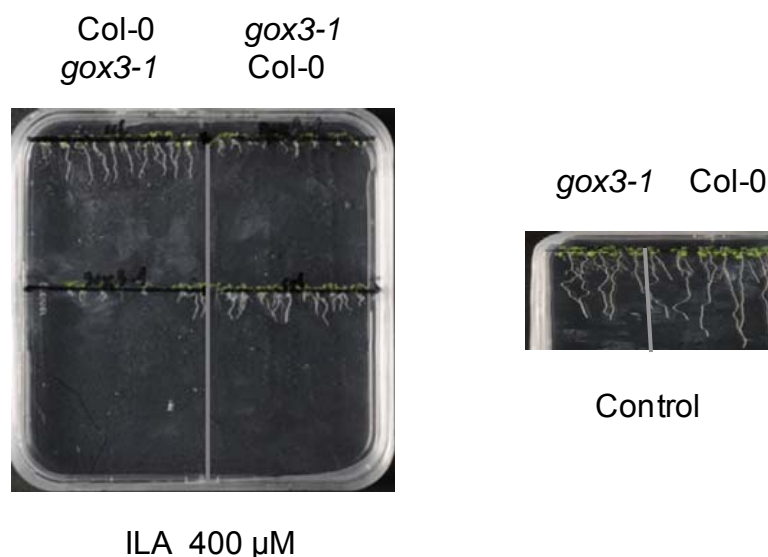


Figure 25. Root growth inhibition by ILA inversely correlates with *GOX3* expression.

The root growth of the *gox3-1* mutant was observed on media containing 400 μ M ILA relative to the wild type (Col-0).

2.5. Exogenous application of ILA leads to specific transformation to isoleucine

ILA differs from the branched-chain amino acid isoleucine only by replacing the 2-amino group with a 2-hydroxy group. The analogues of ILA, leucic acid and valic acid differ from leucine and valine, respectively, by replacing the 2-amino group with 2-hydroxy group just like in ILA. Since the respective 2-keto forms are the biosynthetic precursors and the primary degradation products of the amino acids, ILA and the corresponding 2-hydroxy acids could exist in plants and have similar properties.

Leucic acid and valic acid, the branched chain amino acids isoleucine, leucine and valine were measured by GC-MS along with more than 50 other metabolites in order to obtain information on the metabolism of ILA and the other two branched-chain amino acid-related analogues. Interestingly, among more than 50 metabolites, only isoleucine is significantly increased by exogenous ILA application with a fold change of 3.52 relative to the control (Table 8). Though the branched-chain amino acid share the same biosynthetic path in plants, the other two branched-chain amino acids leucine and valine were not increased. This

suggested that ILA was taken up into the leaves and ILA itself was converted to isoleucine. Similarly, leucic acid only caused the specific accumulation of structurally related leucine with a fold change of 5.53 (Table 8). However the application of valic acid did not lead to the significant accumulation of the corresponding amino acid, valine. The efficiency of take-up of ILA, leucic acid and valic acid was unknown, which might be the reason why only ILA and leucic acid caused accumulation of corresponding isoleucine and leucine, respectively.

Treatment Measurement	ILA treatment Fold change (Confidence interval) (P-value)	Leucic acid treatment Fold change (Confidence interval) (P-value)	Valic acid treatment Fold change (Confidence interval) (P-value)
Isoleucine	3.52 (2.64, 4.69) (0)	1.24 (0.91, 1.68) (0.1604)	1.19 (0.84, 1.69) (0.3044)
Leucine	1.93 (0.76, 4.91) (0.1508)	5.53 (2.45, 12.49) (0.0006)	1.24 (0.6, 2.57) (0.5349)
Valine	1.38 (1.13, 1.69) (0.0044)	1.2 (0.91, 1.57) (0.1744)	1.61 (1.2, 2.18) (0.00405)

Table 8. Measurement of branched-chain amino acids after treatment of ILA, leucic acid and valic acid in Col-0.

Branched-chain amino acids (isoleucine, leucine and valine) were measured by GC-MS after application of ILA, leucic acid and valic acid, respectively. Four-week-old *Arabidopsis* plants were sprayed with 1 mM ILA, leucic acid, valic acid (dissolved in ddH₂O) or mock (ddH₂O) as the control. Fold change indicates change relative to untreated Col-0. The confidence intervals above two indicates the reliability of fold change and are in “bold”. p-value indicates the significance of the change compared to control (untreated Col-0). Each measurement includes eight biological replicates. The significant changes more than twofold are marked in “blue”. The measurement has been performed by Dr. Edda von Roepenack-Lahaye from the Biozentrum of the LMU München.

2.6. A potential role of ILA in regulating defense response in crop plants

2.6.1. Mass peaks corresponding to ILA-glycoside and valic acid-glycoside accumulation in other crop species

Previously, based on a non-targeted metabolome analysis employing ultra-high-resolution FT-ICR MS, two peaks were identified in *Arabidopsis thaliana* positively correlated with *UGT76B1* expression as well. The first peak (mass-to-charge ratio m/z 293) was identified as the glucoside of ILA using recombinant protein UGT76B1 *in vitro* assay in combination with fragmentation profile of this peak showing a loss of a hexoside. Though no hexoside loss could be observed from the second peak (m/z 279), the putative aglycon of this peak after losing a hexoside was valic acid glycoside (von Saint Paul, 2010). The role of ILA-glycoside itself is not clear, however the *ugt76b1* knockout showed enhanced plant defense, in which less ILA-glycoside accumulated, suggesting a close association of ILA-glycoside/ILA and plant defense.

To explore whether these two metabolite peaks exist in other crops, FT-ICR MS was utilized to look for the peaks with m/z 293 and m/z 279 in the metabolite extraction of different crops including tomato, barley, maize, brassicas and *Arabidopsis lyrata*. Both mass peaks were observed in *Arabidopsis lyrata*, *Brassica*, tomato, tobacco, barley, maize and poplar (Figure 26), suggesting a common existence of these two peaks in plants. The intensity of both mass peaks in poplar is about 30 to 40 times higher than in *Arabidopsis lyrata*. First fragmentation of the mass peak with m/z 293 in extract of poplar leads to a partial fragmentation profile representing the standard ILA-glycoside, suggesting that ILA is the aglycon of this peak (data not shown, communication with Basem Kanawati from the institute of Ecological Chemistry of Helmholtz Zentrum München).

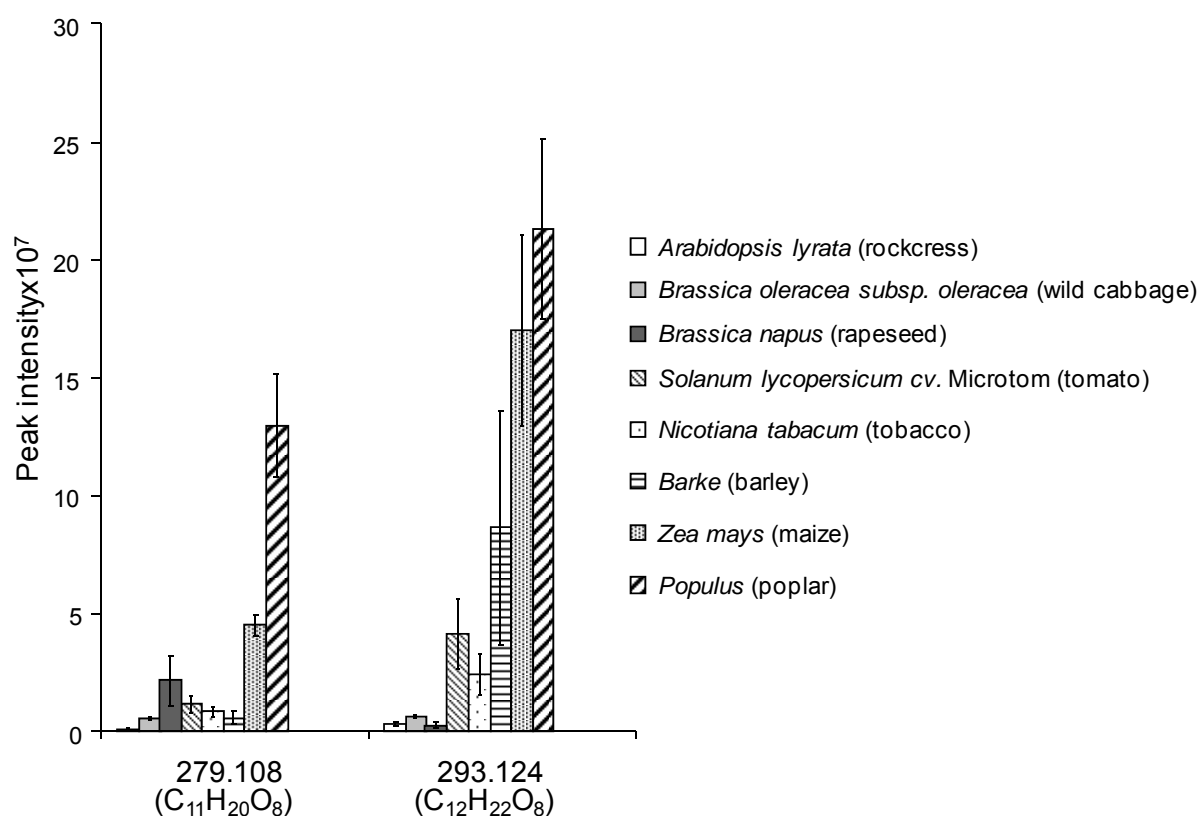


Figure 26. Intensity of mass peaks corresponding to ILA- and valic acid-glycoside in different plant species.

Mass peak with m/z 279.108 corresponding to valic acid-glucoside and mass peak with m/z 293.124 corresponding to ILA-glycoside were measured in the indicated plant species by FT-ICR mass spectrometry. Graph represents the mean and SD of at least five biological replicates.

2.6.2. ILA directly impacts plant defense in barley

To further investigate the effect of ILA regulating plant defense in the other plant species, barley (*Barke*) was first chosen to be treated by ILA to measure regulation of defense genes by semi-quantitative PCR. *HvPR1* and *HvPR10* were chosen as the defense marker genes (Jarosch et al., 2003; Chen et al., 2010b). The house keeping gene *EF1A_Hv* was chosen as the reference gene. Two-week-old *Barke* was sprayed with 1 mM ILA dissolved in 0.1 % Tween 20 or 0.1 % Tween as mock treatment. A positive control treated by BTH, which was known to activate *HvPR1* and *HvPR10* was included. The numbers of cycles for the semi-quantitative PCR were optimized such that clear bands of the house keeping gene *EF1A_Hv* should be observed in all the samples and clear bands of *HvPR1* and *HvPR10* should be observed in at least one sample. Eventually, two different numbers, 26 and 31 cycles were used. At both cycles, ILA treated *Barke* plants showed stronger intensity of both *HvPR1* and *HvPR10* bands than mock-treated plants similar as the positive control BTH in Figure 27). This suggested that ILA might activate SA-mediated defense response in barley, e.g. resistance to pathogen infection.

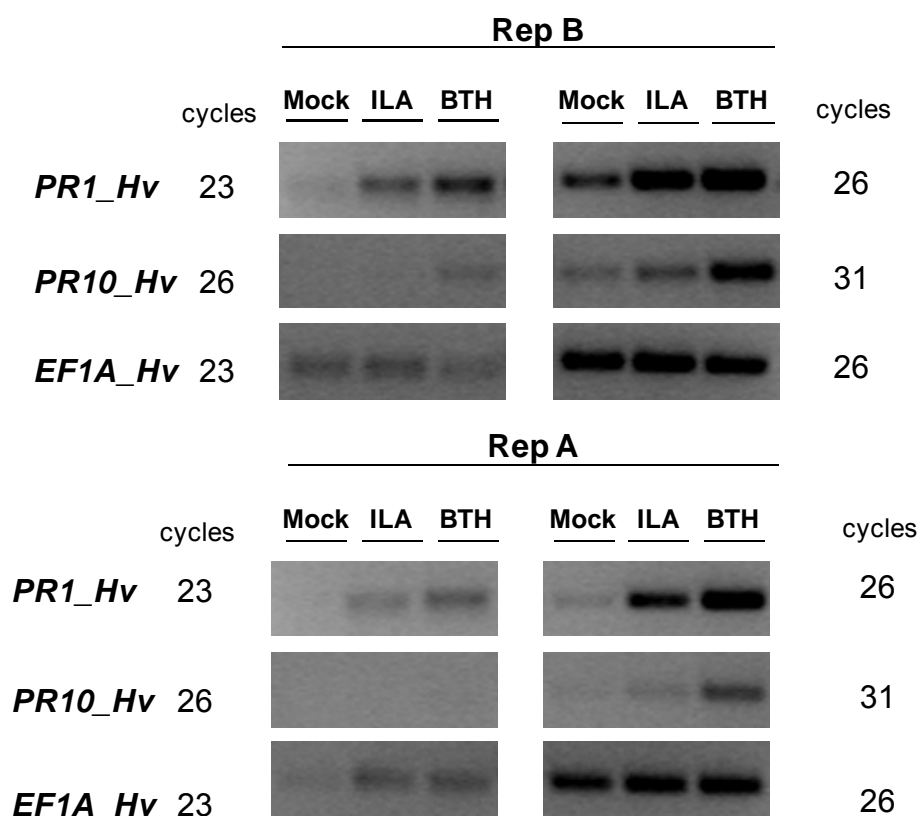


Figure 27. Direct impact of ILA on plant defense in barley.

Defense marker gene expression in barley (*barke*) after ILA treatment. Transcript levels of *PR1_Hv*, and *PR10_Hv* were determined in leaves of two-week-old plants 2 d after ILA, BTH or water treatment measured by semi-quantitative PCR. BTH is the positive control. *EF1A_Hv* is the reference gene.

2.7. UGT76B1 shows activity towards leucic acid and valic acid

2.7.1. The root inhibition by leucic acid and valic acid was dependent on *UGT76B1* expression

The extent of the inhibition of root growth by ILA in *Arabidopsis* was dependent on the *UGT76B1* expression level (Figure 23). The inhibition of root growth by ILA was more pronounced in *ugt76b1* knockout, but less obvious, however, in the *UGT76B1* overexpression line (referred to 2.4.6.1).

To test the specificity of the role of *UGT76B1* in regulating the root inhibition by ILA, the root inhibition of lines with different *UGT76B1* expressions by other compounds (the 2-hydroxy acids: 2-hydroxy-hexanoic acid, 2-ethyl-2-hydroxy butyric acid and 2-hydroxy-octanoic acid as well as amino acids: leucine, valine and beta-amino-butyric acid (BABA)) was observed on ½ MS media plates containing these compounds. All of the 2-hydroxy acid showed much stronger inhibition of root growth than all the amino acids did. However, no different root growth inhibition was observed by all these compounds among the *ugt76b1* knock and *UGT76B1* overexpression lines (Figure 28).

To further test the specificity of this regulation, the root inhibition by the more similar analogues of ILA (leucic acid and valic acid) in lines with different *UGT76B1* expression was observed. Interestingly, both leucic acid and valic acid showed stronger root growth inhibition in *ugt76b1-1*, but weaker inhibition in *UGT76B1-OE-7* compared to Col-0 (Figure 29A). Leucic acid and valic acid have structures very similar to ILA (Figure 30A). Thus apart from ILA, the inhibition of root growth by the analogues of ILA (leucic acid and valic acid) can also be regulated by *UGT76B1* expression.

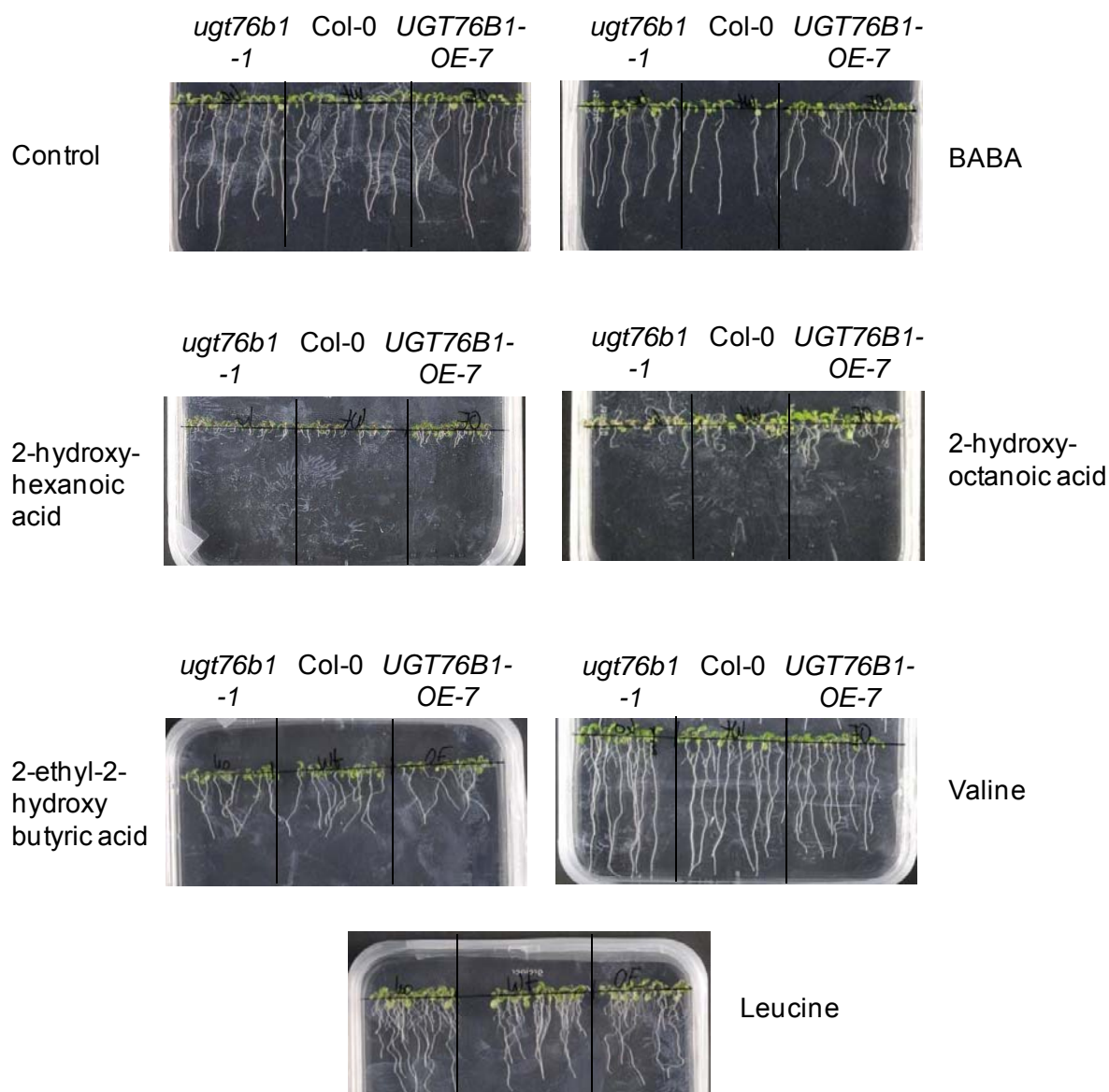


Figure 28. Direct effect of analogues of ILA on root growth.

Root growth inhibition phenotypes of analogues of ILA were observed among Col-0, *ugt76b1-1* and *UGT76B1-OE-7* on medium containing BABA, 2-hydroxy-octanoic acid, valine, leucine, 2-hydroxy-hexanoic acid and 2-ethyl-2-hydroxy butyric acid. Pictures were taken 10 d after sowing the seeds on plates containing 0, 200, 400 and 500 μ M ILA.

2.7.2. Recombinant protein UGT76B1 glycosylates leucic acid and valic acid *in vitro*

From the above observation that the inhibition of root growth by leucic acid and valic acid could be detoxified by UGT76B1, I speculated that UGT76B1 might glycosylate leucic acid and valic acid.

To test this speculation, an *invitro* recombinant protein UGT76B1 assay in combination with mass spectrometry was applied. Indeed, UGT76B1 glucosylated both leucic acid and valic acid to produce the corresponding glucosides with the supplementation of UDP-glucose as the

glucose source. Valic acid with m/z 117.0 could be converted to valic acid glucoside with m/z 279.1 by attaching a glucose moiety and losing a water moiety. Similarly, leucic acid with m/z 297.3 could correspondingly be converted to leucic acid glucoside with m/z 293.2 by recombinant protein UGT76B1 (Figure 29 B, C and D).

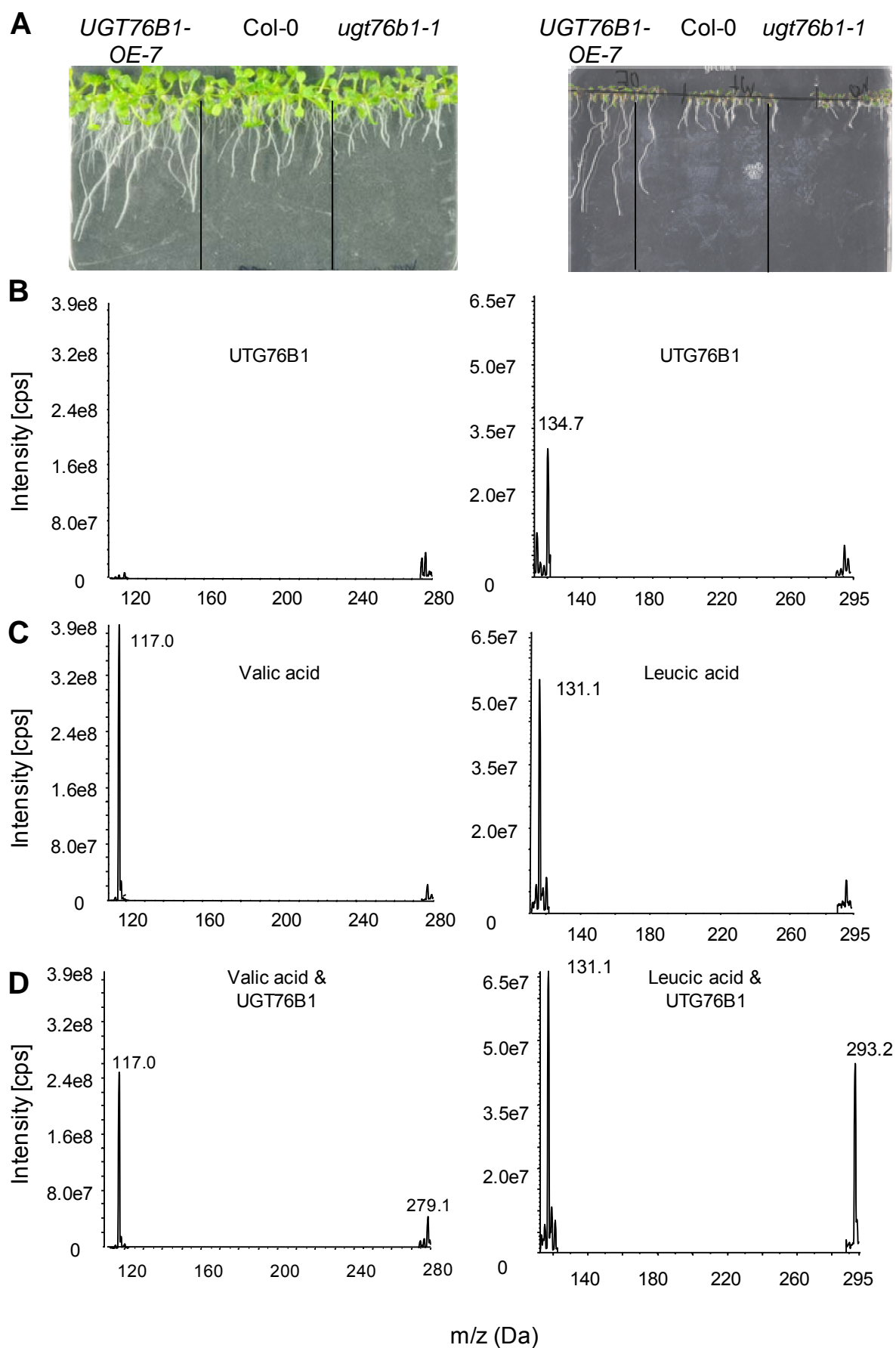


Figure 29. Valic acid and leucic acid, putative additional substrates of UGT76B1.

(A) Differential root growth of *ugt76b1-1* and *UGT76B1-OE-7* on medium containing valic acid and leucic acid relative to Col-0. Pictures were taken 10 d of growth on plates containing 800 μ M valic acid or 400 μ M leucic acid, respectively. (B, C, D) *In vitro* activity assay of recombinant UGT76B1 towards valic acid and leucic acid. The reactions were analyzed by mass spectrometry (Methods). The m/z values of the corresponding substrates and products of mass peak 279.1 (valic acid glucoside) and 293.2 (leucic acid glucoside) are indicated. (C) Mass spectrum of reaction without enzyme. (D) Mass spectrum of complete reaction.

2.8. Analogues of ILA can induce plant defense similar as ILA

The acceptance of leucic acid and valic acid by UGT76B1 raised the question whether other analogues of ILA could have an impact on defense.

To solve this, I measured the expression of the defense genes *PDF1.2*, *PR1*, *SAG13*, *FMO1*, *AIG1* and *PAD3* as well as *UGT76B1* after treatment with analogues of ILA including leucic acid (2-hydroxyisocaproic acid), valic acid ((S)-(+)-2-hydroxy-3-methylbutyric acid), 2-ethyl-2-hydroxybutyric acid, 2-hydroxyhexanoic acid, (\pm)-2-hydroxyoctanoic acid, 3-hydroxy-3-methylpentanoic acid, one carboxylic acid 3-methylpentanoic acid and isoleucine (Figure 30A). The induction of all measured genes similar to ILA by leucic acid, 2-hydroxy hexanoic acid, 2-ethyl-2-hydroxybutyric acid and 3-hydroxy-3-methylpentanoic acid suggested that different structures obtained by mere changing the position of the hydroxyl group or removing of methyl groups would not influence the impact on activation of defense genes (Figure 30B and C). Furthermore, 3-methylpentanoic acid without the hydroxyl group also induced defense genes similar to ILA, suggesting that the 2-hydroxyl group is not essential for ILA activity (Figure 30C). The induction of all measured genes by valic acid and 2-hydroxyoctanoic acid similar to ILA suggested that the length of carboxyl acid is not required for ILA activity either (Figure 30C). Isoleucine showed significant induction of *PR1*, *SAG13*, *FMO1* and *AIG1*, however showing much lower expression than ILA. In the case of *PR1*, *SAG13* and *PAD3*, for instance, isoleucine induced them around tenfold less than ILA did (Figure 30B). This suggested that isoleucine might regulate defense by a different mechanism from ILA or analogues of ILA (2-hydroxy acids).

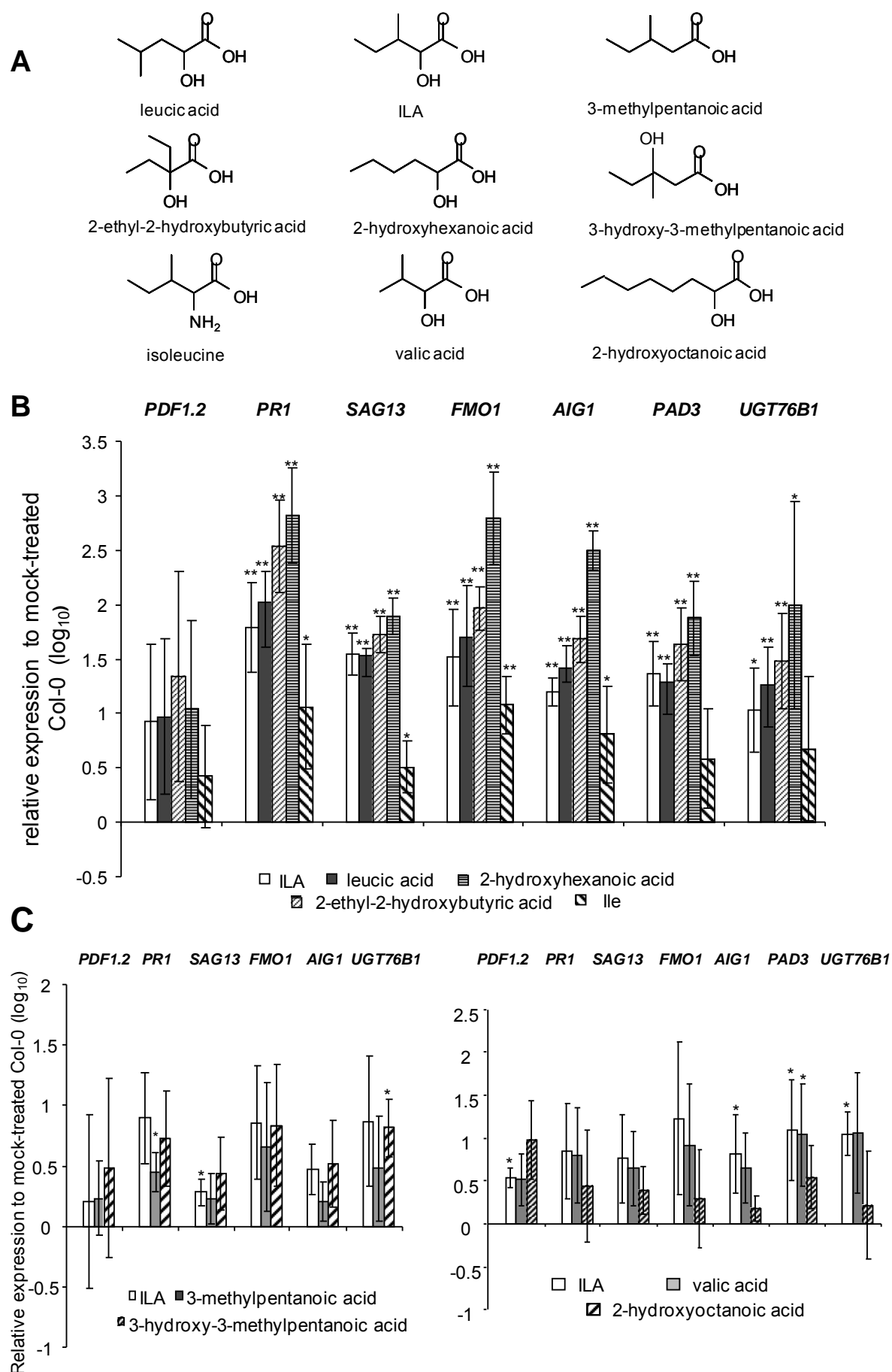


Figure 30. The expression of defense genes mediated by analogues of ILA.

(A) Molecular structures of ILA-related chemicals. (B) Transcript levels of *PDF1.2*, *PR1*, *SAG13*, *FMO1*, *AIG1*, *PAD3* and *UGT76B1* were measured by RT-qPCR in leaves of 4-week-old plants 24 h after ILA, Ile, leucic acid, 2-ethyl-2-hydroxybutyric acid and 2-hydroxyhexanoic acid or mock (water) treatment. (C) Transcript levels of *PDF1.2*, *PR1*, *SAG13*, *FMO1*, *AIG1*, *PAD3* and *UGT76B1* were measured by RT-qPCR in leaves of 4-week-old plants 24 h after ILA, valic acid, 3-methylpentanoic acid, 3-hydroxy-3-methyl-pentanoic acid and 2-hydroxyoctanoic acid or mock (water) treatment. Arithmetic means and standard errors of \log_{10} -transformed data were calculated from three replicates. Stars indicate significance of the difference compared to mock-treated Col-0, calculated by T-test (unpaired). ** p-value ≤ 0.01 , * p-value < 0.05 .

2.9. Induction of defense genes by acids

The result of 2.8 indicated that the carboxyl groups could be an important cause to trigger the activation of defense genes. The major effect of carboxyl groups leads to low pH. Low pH was reported to be active in triggering plant defense response characterized by activation of defense genes (Lager et al., 2010). Based on the structure ILA, it should have a somewhat higher, but similar pK_a like lactic acid with pK_a of 3.86. The pH of 1 mM ILA dissolved in distilled water was 3.63 and that of 1 mM lactic acid dissolved in distilled water was 3.35 indicating pK_a values of 4.26 and 3.70 respectively.

To compare the activity of ILA and lactic acid in activating defense response, expression of defense genes including *FMO1*, *AIG1*, *PR1*, *PR2*, *PDF1.2* and *PR3* was measured by RT-qPCR 24 h after treatment with 1 mM ILA or 1 mM lactic acid. All the measured defense genes showed similar inducibility by both lactic acid and ILA, respectively (Figure 31A). In contrast, when both ILA and lactic acid were adjusted to pH=5.7 by KOH before application to the leaves, the capability of activating defense genes was lost. This suggested that pH was apparently decisive for the activity of ILA and lactic acid in the upregulation of defense marker gene expression 24 h after application of the chemical (Figure 31A). To assess the role of *UGT76B1* expression and SA in the activity of lactic acid in activating defense genes, the expression of *FMO1*, *AIG1*, *PAD3*, *SAG13*, *NUDT6* and *YSL9* was measured after lactic acid application in *NahG*, which completely abolishes SA accumulation and the *ugt76b1 sid2* double mutant. The induction of all these genes showed independence from SA levels or *UGT76B1* expression (Figure 31B).

To further confirm the impact of low pH on defense marker genes, *PR1*, *PR2*, *PR3*, *PR4*, *PR5*, *SAG13*, *PDF1.2*, *SID2*, *FMO1*, *AIG1*, *PAD3* and *NUDT6* were analyzed after 1 mM acetic acid application in comparison to ILA treatment. Nearly all of the measured defense genes could be induced by both acetic acid and ILA treatment (Figure 32). However, expression of

PR1, *PR2*, *SAG13*, *FMO1*, *PR4*, *PR3*, *SAG13*, *PAD3* and *NUDT6* due to acetic acid was lower suggesting that there might be a specific impact of ILA on plant defense (Figure 32). Alternatively, this could still be tightly related to a pH effect, since acetic acid has a higher pK_a (4.76) than ILA, *i.e.* a 1 mM acetic acid solution is less acidic than 1 mM ILA.

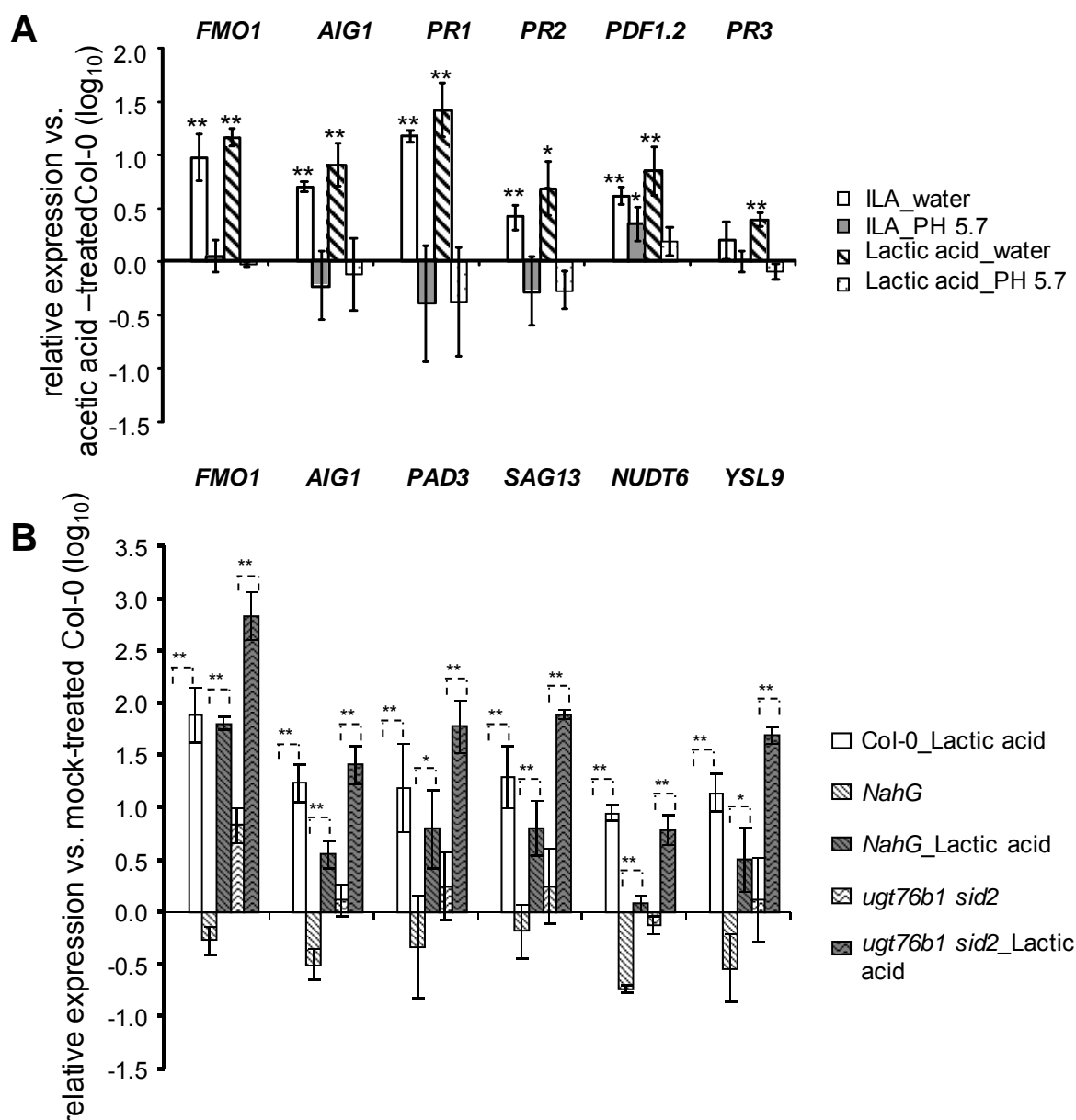


Figure 31. Defense marker gene expression after ILA, acetic acid and lactic acid application.

(A) Defense marker gene expression of *FMO1*, *AIG1*, *PR1*, *PR2*, *PDF1.2* and *PR3* was measured by RT-qPCR in leaves of 4-week-old plants, treated by 1 mM ILA, 1 mM lactic acid, 1 mM ILA (pH adjusted to pH=5.7, using KOH) or 1 mM lactic acid (pH adjusted to pH=5.7, using KOH). (B) Transcript levels of *FMO1*, *AIG1*, *PAD3*, *SAG13*, *NUDT6* and *YSL9* were measured in leaves of four-week-old *ugt76b1 sid2* and *NahG*, 24 h after 1 mM lactic acid treatment, measured by RT-qPCR. Expression levels are normalized to *UBIQUITIN5* and *S16* transcripts; levels relative to Col-0 mock treatment are displayed. Means and standard errors were calculated from three replicates. Arithmetic means and standard errors from \log_{10} -transformed data of three independent replicates from two

separate experiments were calculated using ANOVA. Stars indicate significance of the difference between the two bars connected by the dotted line: ** p-value < 0.01, * p-value < 0.05.

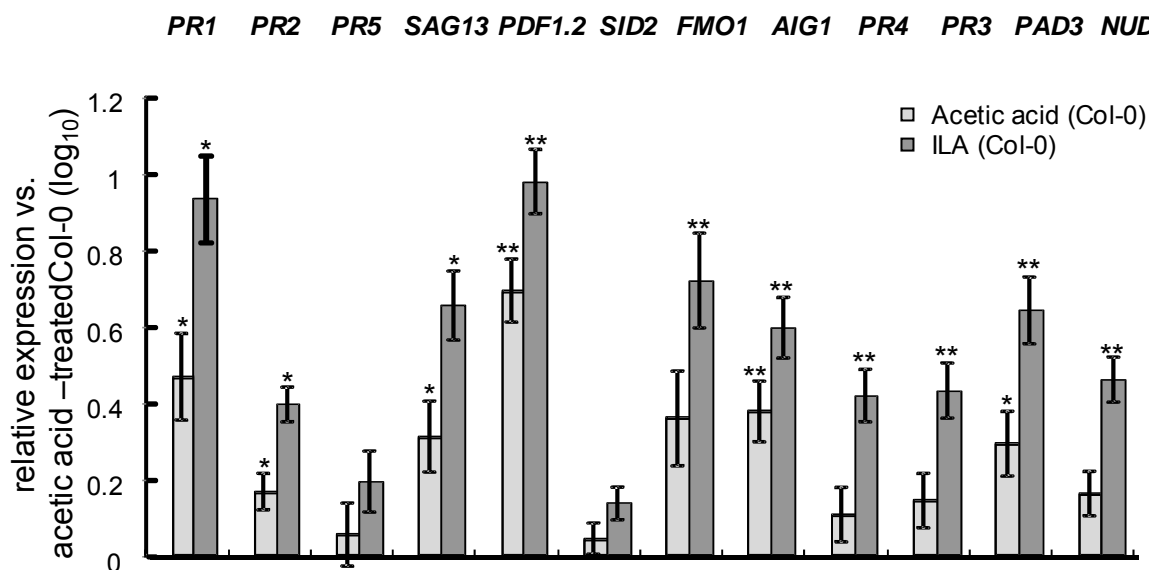


Figure 32. Defense marker gene expression induced by acetic acid application in comparison with ILA.

Col-0 was treated with 1 mM acetic acid, 1 mM ILA or sterile distilled water. Gene expression of *PR1*, *PR2*, *PR5*, *SAG13*, *PDF1.2*, *SID2*, *FMO1*, *AIG1*, *PR4*, *PR3*, *PAD3* and *NUDT6* in leaves of 4-week-old plants was measured by RT-qPCR.

Expression levels are normalized to *UBIQUITIN5* and *S16* transcripts; levels relative to water-treated Col-0 plants are displayed. Arithmetic means and standard errors from \log_{10} -transformed data of three independent replicates from two separate experiments were calculated using ANOVA. Stars indicate significance of the difference between the two bars connected by the dotted line: ** p-value < 0.01, * p-value < 0.05.

3. DISCUSSION

3.1. The integration of *UGT76B1* in SA-JA cross-talk

UGT76B1 has been shown to modify SA-JA cross-talk, suppressing the SA pathway, however, enhancing the JA pathway (von Saint Paul, 2010). The *ugt76b1* knockout and *UGT76B1* overexpression lines were crossed into the mutants compromised in either the SA or JA responses in order to further investigate how *UGT76B1* is integrated into SA-JA cross-talk. These genetic studies indicated that both the activation of the SA pathway and suppression of JA responses caused by the loss-of-function of *UGT76B1* were dependent on SA (Figure 7). *UGT76B1* may suppress SA responses *via* the known antagonism due to the activation of the JA pathway mediated by *MYC2* downstream of *JAR1* (Kazan and Manners, 2013). However, it is unlikely because the mutation of *JAR1*, a key positive player in the JA pathway, cannot reverse the suppression of SA responses by *UGT76B1* overexpression (Figure 7). Thus *UGT76B1* most probably regulated the SA pathway and thereby manipulating JA responses *via* SA-JA cross-talk (see below). The transcription factor *WRKY70* is a key player in orchestrating signals of the antagonistic SA and JA pathways. It acts as a positive regulator of SA-induced genes and resistance to *P. syringae* and as a negative regulator of JA-mediated genes (Li et al., 2004). The increased *WRKY70* expression in the *ugt76b1* knockout line was positively correlated to the induced SA responses. Therefore, *UGT76B1* might suppress *WRKY70* which might be involved in the suppression of the JA pathway (Figure 5).

Within the SA pathway the regulation of SA-induced genes (*PR1* and *SAG13*) by *UGT76B1* is independent from *SID2*. The mutation of *SID2* causes loss of most of the SA levels, basal SA levels remain, however, which are synthesized through PALs (Dempsey et al., 2011). The inability of *UGT76B1* to further repress SA response in *NahG*, which lacks SA, relative to the *ugt76b1 NahG* line, suggests that basal levels are required for the activity of *UGT76B1*. The activation of the SA response provoked by the loss of *UGT76B1* is also dependent on basal SA, but not on *SID2*, unless *NahG* has another unknown activity to influence the accumulation of other signaling compounds in *Arabidopsis* (Heck et al., 2003). The independence from *SID2* of the SA pathway suppression regulated by *UGT76B1* may indicate the requirement of an unknown component “X”. There are three possible scenarios for the factor “X” (Figure 33).

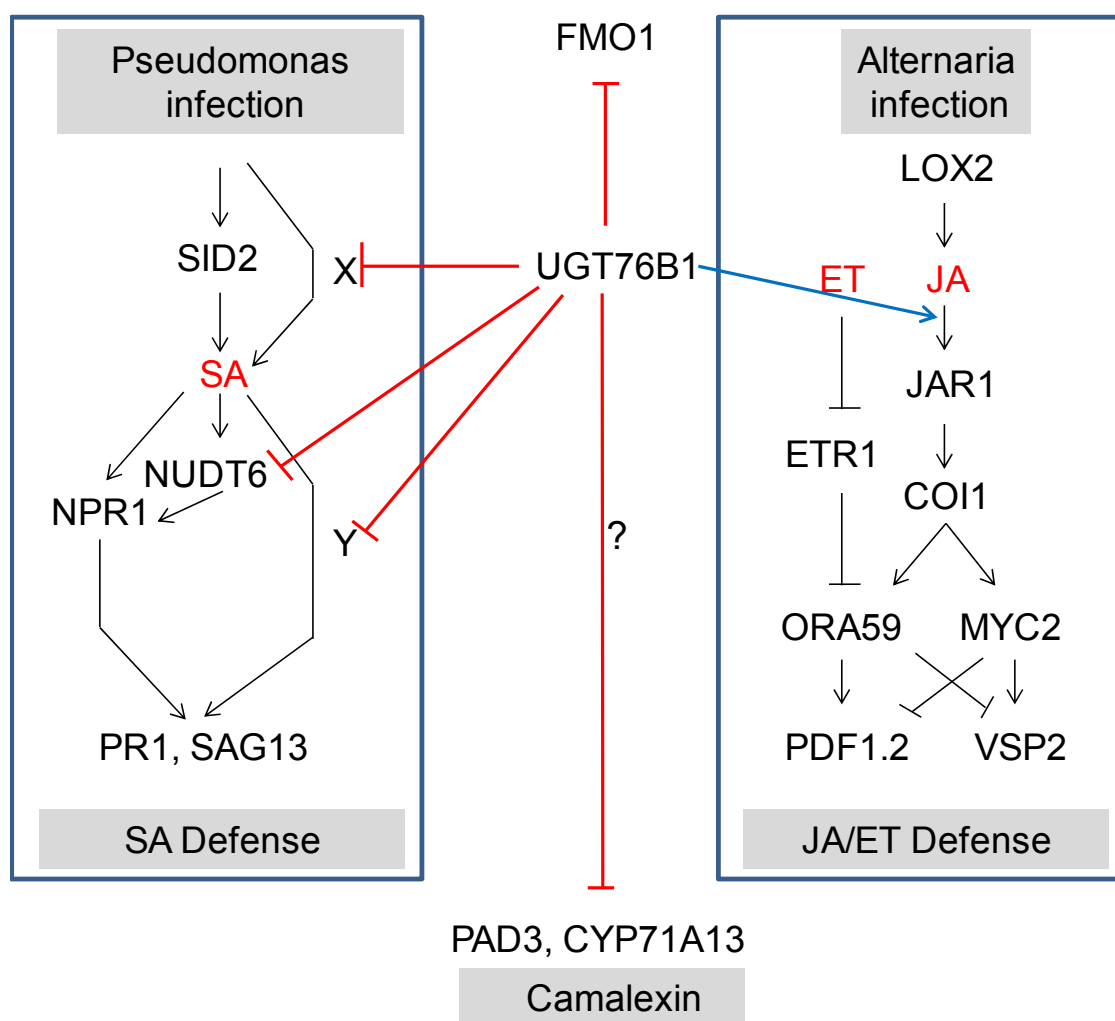


Figure 33. Model of the involvement of *UGT76B1* as a mediator in defense responses (SA mediated response, JA mediated response and other defense responses).

The model relates *UGT76B1* to SA and JA responses regulating defense against biotrophic and necrotrophic pathogens. *UGT76B1* induces JA response, however, suppresses the SA-dependent pathway, enhancing resistance against the necrotrophs and having a negative influence on the resistance to the biotrophs. Furthermore, *UGT76B1* negatively regulates camalexin synthesis genes *PAD3* and *CYP71A13* and the defense gene *FMO1*. Signaling molecules (SA, JA), activation (arrows), suppression (lines with vertical bar) and important genes are indicated. The black arrows are known regulations. Positive (blue) and negative (red) influences of *UGT76B1* are shown, respectively.

(1) Since both *SID2* and PALs can trigger SA synthesis, *UGT76B1* may regulate PALs independent from *SID2*. However, the transcript levels of the PALs (*PAL1*, *PAL2*, *PAL3* and *PAL4*) were not changed by *UGT76B1* expression based on microarray data. Therefore, this possibility is mostly unlikely to happen.

(2) *UGT76B1* is capable of glucosylating SA *in vitro* and it may therefore still be able to manipulate SA levels in *sid2*, thereby suppressing the SA pathway (von Saint Paul, 2010; Noutoshi et al., 2012). Many SA conjugation enzymes have been shown to convert SA to its

inactive derivatives such as SA O- β -glucoside (SAG), salicyloyl glucose ester (SGE), methyl salicylate (MeSA), methyl salicylate O- β -glucoside (MeSAG), and amino acid SA conjugates to inactivate SA (Vlot et al., 2009). So far it is still unclear whether UGT76B1 can glycosylate SA *in vivo* in *Arabidopsis*. SAG has been shown to be accumulated less caused by the loss-of-function of *UGT76B1* in the Wassilewskija background, suggesting that UGT76B1 takes a major role of glucosylating SA in Wassilewskija (Noutoshi et al., 2012). In contrast, the measurement of SAG in the accession Col-0 mainly used in this study has revealed that SAG is more in the *ugt76b1* knockout suggesting that UGT76B1 does not play a major role in conjugating SA. In addition, ILA-glucoside has been found to accumulate more in the *UGT76B1* overexpression line but less in the *ugt76b1* knockout. These results demonstrate that UGT76B1 mainly glucosylates ILA *in vivo* in Col-0 of *Arabidopsis*. Nevertheless UGT76B1 could also accept SA as a substrate. If this is the case, the introduction of a known *in vivo* SA glucosyltransferase such as UGT74F1 driven by the native UGT76B1 promoter into the *ugt76b1* knockout might reverse the phenotypes of the *ugt76b1* mutant.

(3) *UGT76B1* might directly act downstream of *SID2*, thus causing the independence from *SID2*. Once SA signaling is initiated even by the very small amount SA levels in *sid2*, the downstream regulation by *UGT76B1* will work. *NPR1* is the positive regulator of SA responses downstream of *SID2* in the canonical SA signaling. The genetic studies with double mutants to introgress the *ugt76b1* knockout and *UGT76B1* overexpression into *npr1* indicated that the *UGT76B1*-dependent regulation of SA-activated genes (*PR1*, *SAG13*, *EDS1* and *WRKY70*) is independent from *NPR1*. The pathway involving the component “Y” could be the same as the factor “X” (Figure 33).

The activation of the SA response regulated by the loss-of-function of *UGT76B1* was also independent from *sid2* (Figure 33). The scenarios for this involving the factor “X” are quite similar as *UGT76B1* overexpression. Since the transcript levels of *PAL1*, *PAL2*, *PAL3* and *PAL4* were not up-regulated in the *ugt76b1* knockout line, it is mostly unlikely that the loss-of-function of *UGT76B1* activated PALs independent from *sid2*. Secondly, the independence from *sid2* of inducing an SA response could be because the lack of the *UGT76B1* in *sid2* background to glucosylate SA led to the increased SA levels and thus activated an SA response independent from *SID2*. Though an SA response (expression of *PR1*) was induced in *sid2* background by the loss-of-function of *UGT76B1*, the expression level of *PR1* was still lower than in Col-0 (Figure 7A). It suggested that *SID2* might play a role amplifying the positive impact of loss-of-function of *UGT76B1* on SA response.

The expression of the SA marker gene *PR1* was effectively induced by *ugt76b1* knockout in an *npr1* background, however, the absolute expression level was lower than in Col-0 (Figure 7B). This suggests that the *ugt76b1* knockout does not activate signaling downstream of *NPR1* in the canonical SA-dependent pathway, however, it evokes a parallel path involving the factor “Y” to activate the SA responses (Figure 33). Many previous results have shown SA-dependent, but *NPR1*-independent pathways to mediate SA response (Clarke et al., 1998; Kachroo et al., 2000; Shah et al., 2001; Murray et al., 2002). In the case of the *ssi2* mutant, *PR1* was induced in an SA-dependent but *NPR1*-independent manner similar to the *ugt76b1* knockout (Shah et al., 2001). The independence of the *UGT76B1* impact from *NPR1* could be accomplished by either blocking an unknown activator or by enhancing an unknown inhibitor (Figure 33). The transcription factors WHIRLY (WHY) and MYB DOMAIN PROTEIN 30 (MYB30) were known as SA dependent but *NPR1*-independent activators (Desveaux et al., 2002; Desveaux et al., 2005; Raffaele et al., 2006). SUPPRESSOR OF NPR1-1 (SNI1) has been revealed to be the negative regulator, showing *NPR1*-independent regulation. So far the regulator, either being an activator or a repressor regulated by *UGT76B1* independent from *NPR1*, is still unknown and requires further research.

NUDT6, however, a gene encoding an ADP-ribose /NADH pyrophosphohydrolase, is a positive regulator of SA-mediated response which modulates *NPR1* activity (Ishikawa et al., 2010). *UGT76B1* and *NUDT6* were negatively correlated in both the *ugt76b1* knockout and *UGT76B1* overexpression lines, suggesting that *UGT76B1* repressed *NUDT6*. Therefore *NPR1*-dependent pathway might contribute to the regulation by *UGT76B1* in the SA pathway.

Collectively, the genetic studies indicate that *UGT76B1* could utilize an SA dependent but *NPR1*-independent pathway. Nevertheless, an additional *NPR1* contribution, *e. g.* involving *NUDT6*, cannot be ruled out.

From the side of the JA pathway, the suppression of *VSP2* by loss-of-function of *UGT76B1* was abolished by *NahG*, suggesting that the suppression of the JA pathway by loss-of-function of *UGT76B1* was dependent on SA accumulation (Figure 7A). The further enhancement of the JA pathway (*VSP2* expression) by *UGT76B1* overexpression in the *sid2* and *npr1* mutants suggested that the activation of JA pathway by *UGT76B1* did not rely on the suppression of *SID2* and *NPR1* (Figure 7A and B). The regulator of SA-JA cross-talk *WRKY70* could be further suppressed by *UGT76B1* overexpression in *npr1*, suggesting that

the regulation of *WRKY70* by *UGT76B1* was independent from *NPR1*. With regard to the regulation of *WRKY70* independent from *NPR1* it has been reported that *WRKY70* is additively regulated by both *NPR1* and the transcription factor *MYB44* (Li et al., 2004; Shim et al., 2013). The transcription factors *WRKY50* and *WRKY51* positively regulating SA, but negatively regulating the JA pathway can also regulate the suppression of the JA pathway independent from *NPR1* (Gao et al., 2011). It is, however, unclear how *WRKY50* can be regulated independent from *NPR1*. *WRKY50* was significantly induced in *ugt76b1-1* but suppressed, however, in *UGT76B1-OE-7* (Table 3). Therefore, the enhancement of the JA pathway could be due to further suppression by *UGT76B1* overexpression of the regulators of SA-JA cross-talk such as *WRKY70* or *WRKY50*, thus leading to the alleviation of suppression of the JA pathway. Nevertheless, the possibility that *UGT76B1* may directly influence the JA pathway cannot be excluded. The suppression of JA response from SA pathway was reported to be downstream of *JAR1*, directly acting on the transcription factor *ORA59*, a positive regulator of the JA pathway (Van der Does et al., 2013). Since the activation of *VSP2* by *UGT76B1* overexpression is dependent on *JAR1*, the direct impact of *UGT76B1* on JA pathway could be regulated *via* increased ILA glucoside levels or another different function, yet both mechanisms require *JAR1* (Figure 33).

3.2. Integration of dynamic aspects of ILA on defense including SA and JA pathways

ILA has been identified as a substrate of *UGT76B1* and ILA glucoside levels were dependent on *UGT76B1* expression *in vivo*, yet the physiological function of ILA remained elusive (von Saint Paul, 2010). ILA simultaneously activated both SA marker genes (*PR1*, *PR2* and *PR5*) and JA/ET marker genes (*PDF1.2*, *PR3* and *PR4*) 24 h after treatment (Figure 32 and Figure 34). This strongly suggests that ILA positively impacts on both SA and JA/ET pathways. In agreement with this, many ILA-induced genes were responsive to treatment with SA, BTH and *Pseudomonas* infection (Table 5). ILA-induced genes were overrepresented in the JA response (Tables 6 and 7). Furthermore, the protection of the host plant by ILA against the *P. syringae* avirulent strain DC3000 AvrRpt2 was confirmed, which is fended off *via* the SA pathway (Figure 16). The protection by ILA against necrotrophic pathogens such as *Alternaria brassicicola* or *Botrytis cinerea*, which are fended off *via* the JA/ET pathway has not been confirmed so far and requires further study. Nevertheless, many cases have been reported in which a single elicitor can protect plants against both biotrophic and necrotrophic pathogens by activating SA and JA/ET pathways. Rhamnolipids (RLs) trigger defense against

the biotrophic pathogen *P. syringae* DC3000 and the necrotrophic pathogen *Botrytis cinerea* by activating both SA and JA pathways (Sanchez et al., 2012). The flagellin fragment flg22 confers resistance against *P. syringae* DC3000 and *Botrytis cinerea* (Zipfel et al., 2004; Ferrari et al., 2007). Interestingly, the simultaneous activation of SA and JA pathways can coordinately protect against the same pathogen infection. For instance, the activation of the JA response by RLs enhances the resistance against *Botrytis cinerea* in concert with the SA pathway (Sanchez et al., 2012). The enhancement of the JA response in systemic tissues upon local pathogen infection protects plants against *Pseudomonas* infection in collaboration with the SA pathway (Truman et al., 2007). Therefore, ILA is likely to protect plants against pathogens using different strategies, *i. e.* utilizing SA or JA/ET pathways separately to defend against corresponding pathogens or coordinately utilizing both pathways to defend against the same pathogens. Apart from activation of SA and JA responses, ILA activated defense genes (*SAG13*, *AIG1* and *PAD3*) completely independent from SA or JA/ET pathways (Figure 19 D, E, F). Similarly, the induction of *PAD3* by oligogalacturonides (OGs) and *Botrytis cinerea* independent from SA, JA/ET pathways has been reported (Sanchez et al., 2012). Furthermore, the protection against *Botrytis cinerea* by the elicitors oligogalacturonides (OGs) and flg22 has been shown to rely on *PAD3* but not, however, on SA or JA/ET pathways. Thus, *PAD3* may contribute to the activity of ILA to regulate defense coordinated with the complex SA and JA/ET network.

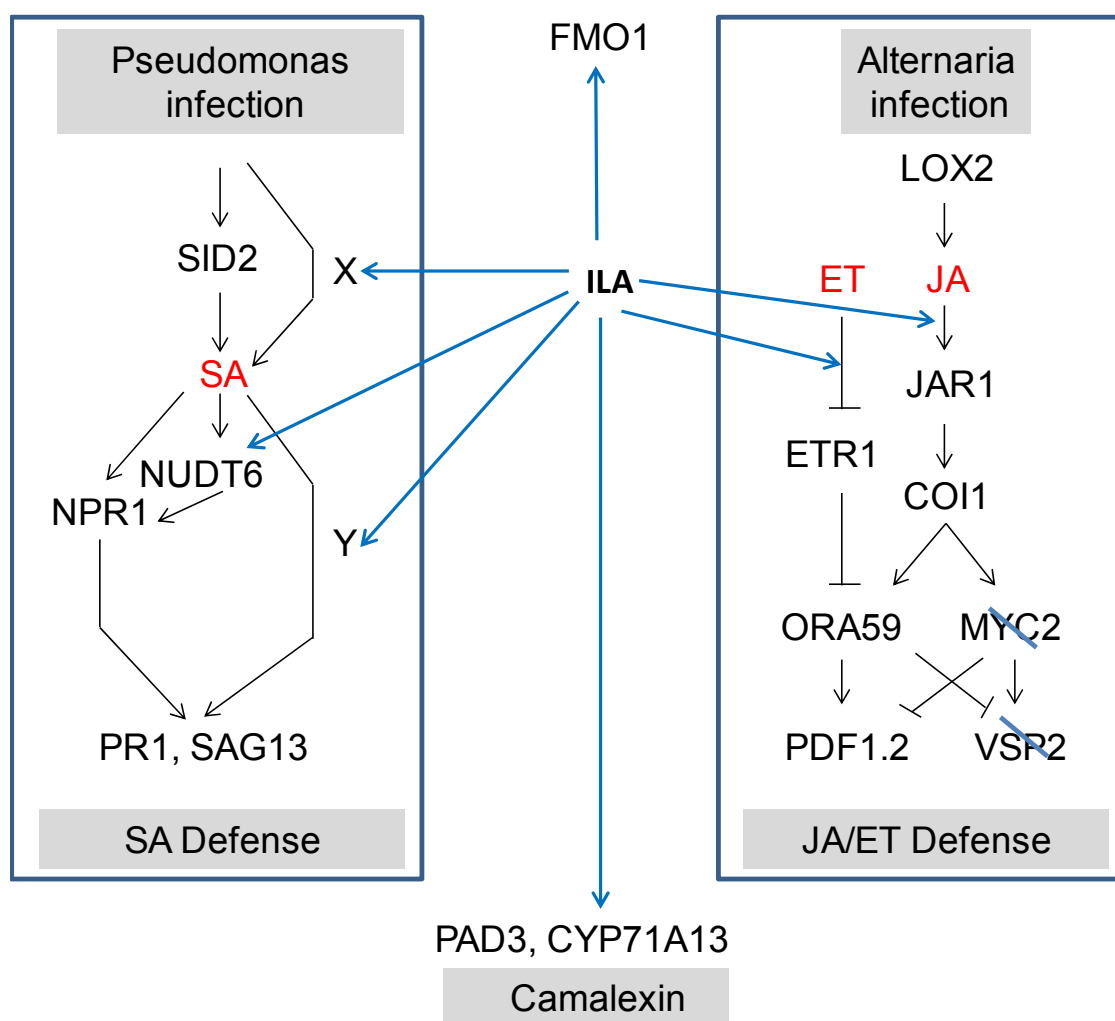


Figure 34. Model of the involvement of ILA as a mediator in defense responses (SA mediated response, JA mediated response and other defense responses).

ILA activated both SA and JA responses. ILA enhanced resistance against biotrophs. Furthermore, ILA activated camalexin synthesis genes *PAD3*, *CYP71A13* and the defense gene *FMO1*. Signaling molecules (SA, JA), activation (closed arrows), suppression (lines with vertical bar) and important genes are indicated. The black arrows are known regulations. Positive (blue) influences of ILA are shown.

SA and JA pathways have both synergistic and antagonistic interactions, dependent on e.g. the concentrations of SA and JA or the sequence of initiating both pathways (Schenk et al., 2000; Cipollini et al., 2004; Mewis et al., 2005; Mur et al., 2006; Spoel et al., 2007). Though SA and JA pathways can be simultaneously activated, they might not be necessarily synergistically induced. The more pronounced JA response (based on expression of *PDF1.2*) in lines deficient in the SA pathway (*NahG*, *sid2* and *npr1*) after ILA application demonstrated that the antagonism of the SA pathway on the JA pathway was part of the activity of ILA (Figure 19 B). SA was only slightly increased after ILA application (Figure 21), whereas JA and JA-Ile were not changed, although 12-OH-JA, a JA degradation

intermediate, could indicate some transient, yet undetected, minor rise in JA abundance (Figure 22). The exogenous application of SA and JA has shown that SA and JA responses can be simultaneously activated only when the chemicals are applied at low doses (Mur et al., 2006). Consistently, ILA was likely to marginally activate SA and JA synthesis to ensure the simultaneous activation of both SA and JA pathways. The effects of SA and JA pathways may transiently act in a synergistic manner and change to be antagonistic over a long term (Mur et al., 2006). Though ILA caused a short-term effect, the situation leading to the operation of internal SA and JA signals was very different from direct application of both SA and JA. ILA might have a period when SA and JA responses were synergistically activated. ILA might pass by this time frame much faster than the exogenous application of both SA and JA, which synergistically activated both pathways. Consistently, SA response (*SID2* and *PAD4*) and JA response (*JAZ10* and *OPR3*) seemed to be activated very early 1 h after ILA treatment (Figure 20A). At this time point the activation of SA response was very weak while the activation of JA response was much stronger and at its peak of induction; it is very unlikely that SA pathway would confer the suppression on the JA pathway at this time point. The activation of the SA response was amplified several hours later reaching the peak of induction 24 h after treatment. Nevertheless, the suppression on JA response was still effective even SA was applied 2 d and 3 d after JA application (Koornneef et al., 2008). Therefore it is reasonable that the suppression on JA response by the SA pathway was effective upon ILA treatment, when the activation of SA response was less than 24 hours later. Nevertheless, SA signaling was not strong enough to completely suppress JA activation due to ILA application.

There are intriguing similarities between my data and other results. Rhamnolipids (RLs) first transiently activated a JA response (activation of *PDF1.2*) and later induced an SA response (activation of *PR1*) similar to ILA (Figure 20B). An enhanced *PDF1.2* expression in SA-deficient lines (*NahG* and *sid2*) in response to RLs indicated suppression on JA signaling by the SA pathway (Sanchez et al., 2012). Interestingly, transcripts related to JA synthesis were upregulated within 4 h and JA increased transiently in systemic tissues in response to local infection with an avirulent strain of *Pseudomonas syringae*, followed by the activation of SA response (Truman et al., 2007). Similar action on SA and JA pathways in different situations, such as lipid RLs recognition, SAR and elicitation by the small molecule ILA, point out that there may be similar events to regulate these responses. This common mechanism may be one master regulator which can initiate a tandem of defense responses including the arrangement of sequential SA and JA responses. Since the chemical structures of ILA and of RLs are

different, it is unlikely they are recognized by the same “receptor”. For instance, the loss-of-function of FLS2 compromises most of defense response by flg22 including activation of SA and JA pathways (Zipfel et al., 2004; Tsuda et al., 2008). Alternately, a common chemical signal could be induced such as ROS and NO, both of which were known to positively impact on SA and JA synthesis (Referred to introduction). Accordingly, many genes related to balancing the redox state were enriched in ILA-induced genes (Figure 12A), though it is unclear whether the change of the redox state was the cause or the effect.

3.3. ILA activated defense responses which can be observed in systemic leaves upon local pathogen infection

Notably, ILA activity showed many defense aspects, which could be observed in the systemic leaves upon local pathogen infection. Firstly, SA-mediated response was induced by ILA, characterized by the induced marker genes (*PR1*, *PR2* and *PR5*) (Figure 32) and enrichment of SA responsive genes in ILA-induced genes (Table 5). The induction of SA responsive genes was also observed in the systemic leaves upon local pathogen infection. ILA only slightly increased SA accumulation, however it could still effectively protect against infection by *P. syringae*. Similarly, the increased SA levels could not always be detected in the systemic leaves upon local infection, but, however, effectively triggered the protection against pathogen infection in the systemic leaves. This phenomenon was defined as systemic acquired resistance to pathogen infection (SAR) (Zheng and Dong, 2013). Secondly, ILA can first activate the JA response and then induce the SA response (Figure 20A) in a similar way as known for the systemic leaves upon local pathogen infection. In the systemic tissues, without further pathogen infection, where SAR was induced, transcripts of JA-synthesis related genes were transiently activated within 4 h followed by activation of an SA response (Truman et al., 2007). Thirdly, many genes (*FMO1*, *PAD3* and *CYP71A13*) were induced by ILA application (Figure 15A) and in the systemic leaves without infection. The mutation of *FMO1*, an important regulator of SAR, led to compromised SAR induction in systemic tissues and triggering local protection by pipecolic acid against pathogens, a key signal of SAR (Navarova et al., 2012). The induction of *FMO1* and *PAD3* could be induced by exogenous ILA application completely not relying on SA abundance (Figure 18B and Figure 19F). Therefore, the induction of these genes by ILA should be regulated by another signal independent of the SA pathway. Nevertheless, this signal and SA could work additively to regulate the activity of ILA. Similarly, the mutation of a lipid transfer protein DEFECTIVE IN INDUCED RESISTANCE 1-1 (*dir1-1*) compromised SAR response, however showed no

change of SA levels, suggesting that another additional signal was required (Maldonado et al., 2002). The lipid transfer protein DIR1 was obviously responsible for allowing the activity of this additional signal. It remains unclear whether ILA can trigger the resistance to pathogen infection in systemic leaves.

Despite so many similar aspects regulated by both ILA and in systemic tissues upon local pathogen infection, ILA showed some different regulations as well. For instance, the induction of *FMO1* by ILA was completely independent from SA levels (Figure 18B). In contrast, SA was required for the induction of *FMO1* in the systemic leaves upon local pathogen infection (Mishina and Zeier, 2006). Nevertheless, ILA and systemic leaves upon local infection have shown such similar behaviors to activate defense genes expression, suggesting that local response of ILA may trigger a signal similar to the signal which regulates defense response in the systemic tissues.

The induction of three homologous lipid transfer proteins (At4g12480, At4g12490 and At4g12500) by ILA along with their tight co-expression pattern with other defense genes (*AZII* and *PDF1.2*) provided evidence for an involvement of lipid transfer proteins in regulating the activity of ILA in defense (Table 7 and Figure 14). The tobacco lipid transfer protein 1 (LTP1) binds the signaling molecule JA to form LTP1-JA and only LTP1-JA, but not LTP1 or JA alone can enhance resistance to *Phytophthora parasitica* in tobacco (Buhot et al., 2004). This indicated that the lipid transfer proteins induced by ILA might bind to a signaling molecule such as JA or ILA itself to conduct the signaling.

3.4. Does acidification contribute to ILA action?

Placing hydroxyl group and methyl group of the ILA molecule at different positions or removing either the methyl or the hydroxyl group did not influence the capability of activating defense genes (Figure 30). Furthermore, lactic acid with high structural similarity to ILA as the simplest 2-hydroxy carboxylic acid with an alkyl (methyl) rest showed the same activity to induce defense response (Figure 31A). This challenged the specificity of ILA and caused speculation that low pH caused by carboxyl groups was capable of inducing defense. The very simple carboxylic acid acetic acid showed the ability to activate defense genes (Figure 32), confirming the speculation. Lager et al. (2010) had already shown that a shift from pH 6.0 to 4.5 using the inorganic acid HCl rendered rapid activation of defense genes and hence excluded that only organic acid could activate defense genes. Fifty-two common genes which are obviously related to pathogen defense were identified when comparing 212

genes induced by ILA (Figure 13A) and 691 genes activated 1 h or 8 h after shifting pH of *Arabidopsis* seedlings (Lager et al., 2010). For instance, At4g39030 (*EDS5/SID1*) involved in SA biosynthesis, At2g04450 (*NUDT6*), a gene known to positively regulate *NPR1*-dependent SA response, At2g46400 (*WRKY46*) and At4g18170 (*WRKY28*), both of which are involved in regulating SA-mediated defense, At3g26830 (*PAD3*) and At2g35980 (*YSL9*) are all defense-related genes. Hence, one may speculate that a subset of the transcriptional response to ILA treatment is driven by acidification. While the difference may be due to the different experiments, differential genes induced by ILA and pH shifting may pinpoint unique functions of ILA different from the acidic pH effect as well.

The dicarboxylic acid azelaic acid provided specific protection against a virulent *Pseudomonas syringae* strain (*PmaDG3*), when dissolved in the buffer to keep neutral pH (Jung et al., 2009). Other dicarboxylic acids (suberic acid and sebacic acid) could not provide this protection (Jung et al., 2009). Thus, the resistance to pathogens provided by the carboxylic acid azelaic acid is dependent on the structure, but not due to low pH (Jung et al., 2009). Other carboxylic acids such as hexanoic acid and citric acid can also trigger activation of defense marker genes independent of low pH as well (Finkemeier et al., 2013). Exogenous application of the hormone SA, which is usually dissolved in water and sprayed onto plants similar to ILA as applied in this study, will even cause a stronger shift in the pH due to the lower pK_a 2.97 of SA. This suggests that the acidic pH might play an even stronger role in influencing activity of SA on plant defense, whereas other evidence undoubtedly support that SA is a specific internal signal regulating defense in plants (Vlot et al., 2009). Additionally, apart from short-term activation of defense genes, ILA can induce a long-term resistance against *Pseudomonas* infection (Figure 16). In contrast, no evidence has been shown that lower pH can trigger a long-term protection against infection. Therefore, though the low pH may contribute to activate expression of defense genes, ILA may still be a specific signal molecule involved in activating defense. Nevertheless, these findings strongly suggest the need to explore the effect of ILA and other acids side-by-side not only in affecting defense marker genes, but also in a sustainable testing of activation of defense against pathogen infection.

Adjusting the pH in solutions of ILA and lactic acid to almost neutral pH=5.7 clearly eliminated the enhanced expression of defense genes, suggesting the decisive role of low pH in regulating ILA activity in defense (Figure 31A). In addition to the direct contribution of low pH in activating defense genes, the second plausible explanation is that low pH is

facilitating the uptake of ILA into *Arabidopsis*. In animals, a proton-coupled monocarboxylic acid transporter can transport SA. It has been reported that studies using tobacco suspension cultures suggest a rapid and transient uptake of SA in a pH-dependent manner, with a linear decrease in uptake between pH 3.5 and pH 8.5 (Chen et al., 2001). In *Arabidopsis* suspension cultures, import of SA declined very sharply with a pH change from 5.7 to 6.1. The proton gradient over the plasma membrane plays a decisive role for SA transport at the cellular level (Clarke et al., 2005). The specific accumulation of Ile after treatment with ILA solution without adjusting pH suggested that ILA was taken up into *Arabidopsis* at low pH and converted to Ile (Table 8). Therefore, at acidic pH, ILA can be taken up by plants; hence it may act as a signal molecule in the cell. The neutral pH of 5.7 could abolish the transport of ILA into the cell, thus preventing a role of ILA in regulating defense.

3.5. The association of ILA activity with UGT76B1

UGT76B1 was highly induced in the systemic leaves upon local infection with *Pseudomonas syringae* pv. *maculicola* ES4326 (Psm) (Gruner et al., 2013). Thus, *UGT76B1* might be involved in regulating the defense response in the systemic tissues upon local pathogen infection as well. This could be in line with the observation that the exogenous application of its substrate ILA is generating a scenario, which was observed in the systemic tissues upon local pathogen infection (see above 3.3). *PAD3* and *CYP71A13* were activated in the systemic leaves. They were negatively regulated by *UGT76B1* and induced by ILA. *PAD3* and *CYP71A13* do not necessarily require SA to be induced (Gruner et al., 2013). Indeed, the induction of *PAD3* by ILA did not require SA (Figure 18B and Figure 19F). It is likely that *PAD3* and *CYP71A13* were regulated by *UGT76B1* independent from SA. *AIG1* is an expression marker gene after infection with *Pseudomonas syringae* pv *maculicola* strain ES4326 dependent on the avirulent effector avrRpt2 (Reuber and Ausubel, 1996). *AGII* was not responsive to BTH, a functional analogue of SA (Rate et al., 1999) and it was negatively regulated by *UGT76B1*, suggesting that an additional signal, possibly ILA, was involved in the regulation of *AIG1*. In agreement with this, *AIG1* could be induced by ILA (Figure 15A and Figure 32). *FMO1*, an important SAR regulator, is regulated by *EDS1* independent from SA accumulation in local tissue, but it requires, however, SA to be induced in systemic tissues (Brodersen et al., 2002; Bartsch et al., 2006; Mishina and Zeier, 2006). *FMO1* was not enhanced in the *cpr6-1* and *mpk4* mutants with constitutive SA accumulation (Olszak et al., 2006), suggesting that SA alone is not adequate to activate *FMO1*. In contrast, *FMO1* was induced by the loss-of-function of *UGT76B1* and by ILA. Thus, a signal in the loss-of-

function of *UGT76B1*, which could be ILA, is adequate to induce *FMOL*. Furthermore, many genes activated by the loss-of-function of *UGT76B1* and by ILA were SA non-responsive genes (Table 4), suggesting the involvement of additional signal(s). Collectively, *UGT76B1* was proposed to modulate defense response associated with the regulation of systemic defense response upon local pathogen infection *via* an additional signal apart from SA, which might be ILA itself.

The majority of genes regulated by ILA (70%) were reversely regulated by *UGT76B1* (Figure 13A and B). Though the acidic pH might have contributed to the activity of ILA, the broadly overlapping transcripts regulated by both ILA and loss-of-function of *UGT76B1* opposed the idea that ILA activated defense genes only by acidification, since the loss-of-function of *UGT76B1* was unlikely to change the (extra-) cellular pH. Even within the SA pathway, ILA and the loss-of-function of *UGT76B1* showed similar regulations. The activation of the SA marker gene *PR1* by both the loss-of-function of *UGT76B1* and ILA showed independence from *SID2* and *NPR1* (Figure 7A and B, Figure 19 A, Figure 33 and Figure 34). Furthermore, both ILA and the loss-of-function of *UGT76B1* could activate an SA response and protect plants against *Pseudomonas* infection. However, there is no evidence showing that acidification can trigger long-term protection against infection. Hence the link between ILA-regulated and *UGT76B1*-regulated defense is likely to be attributed to the regulation by and of the signaling molecules, *i. e.* ILA itself or SA, but not, however, by a low pH effect.

Genes only induced by ILA (30%), but not by the loss-of-function of *UGT76B1* were enriched in JA response, pointing to an effect opposite to the negative regulation of JA response by the loss-of-function of *UGT76B1*. However, this might be due to the different effect of short-term chemical treatment and constant change of *UGT76B1* expression. For instance, the interaction of SA and JA pathways caused by the loss-of-function of *UGT76B1* might be very different from the interaction of SA and JA pathways upon ILA treatment.

It has been shown that the recombinant enzyme UGT76B1 can glucosylate SA and ILA, and that ILA can inhibit UGT76B1 to accept SA *in vitro*. Therefore, another explanation why ILA can activate defense was brought up: ILA can inhibit the activity of UGT76B1 to glucosylate SA, hence regulate SA abundance and subsequent signaling (Noutoshi et al., 2012). However, there were contradictory measurements of SA-conjugates in two *ugt76b1* knockout alleles generated in different *Arabidopsis* accessions: *ugt76b1-1* (Col-0) and *ugt76b1-3* (Wassilewskija). The Col-0 allele *ugt76b1-1* contained even more SA-glucoside than wild

type, clearly arguing against the notion that UGT76B1 would have SA glucosyltransferase activity (von Saint Paul, 2010; Noutoshi et al., 2012). In contrast, *ugt76b1-3* was shown to harbor less SA glucosides which would be in accordance with an SA glucosyltransferase activity of UGT76B1 (von Saint Paul, 2010; Noutoshi et al., 2012). However, apart from this accession discrepancy, the genetic studies to measure defense genes after ILA treatment strongly argued against a major impact of an SA glucosyltransferase activity of UGT76B1 *in vivo*. Firstly, ILA was effective to induce defense marker genes *FMO1*, *AIG1*, *PAD3*, *SAG13*, *NUDT6* and *YSL9* in *ugt76b1 sid2*, when *UGT76B1* was absent and therefore could not be further inhibited. Secondly, these genes were also induced by exogenous ILA even in the absence of SA in a *NahG* line (Figure 18B). Additionally many genes activated by ILA and the loss-of-function of UGT76B1 were not responsive to SA (Table 4). Thus, the activity of ILA did not rely on SA, therefore was not related to the inhibition of UGT76B1 to glucosylate SA. Nevertheless, this observation could be independently proven by a direct infection experiment of lines with reduced or abolished SA levels after ILA application.

ILA has been reported to exist in humans as the reduced form 2-keto-3-methylvaleric acid, a degradation product of the branched-chain amino acid Ile (Mamer and Reimer, 1992). ILA and its glucoside have been newly found in *Arabidopsis* by von Saint Paul (2010). To extend the knowledge, the existence of ILA glucoside was explored in other plants including crops by FT-ICR MS. Surprisingly, the peak corresponding to the ILA glucoside accumulated much higher in *Brassica*, tomato, tobacco, barley, maize and poplar (Figure 26), suggesting the common existence of ILA/ ILA glucoside in other plant species. Another m/z peak putatively corresponding to valic acid glucoside, which at least can be produced by UGT76B1 *in vitro* (Figure 29D), also accumulated much higher in these plants (Figure 26). Although the function of ILA/ILA glucoside in these plants is not known yet, ILA application in barley activated expression of defense genes (Figure 27) suggesting that ILA might also play a role in regulating defense in agricultural crops. So far, a highly conserved single copy homolog of UGT76B1 has been found by analysis of related *Brassicaceae* genomes (M. Das and G. Haberer, personal communication), suggesting that it may assume the role of glucosylating ILA in the *Brassicaceae*. Therefore, further studies should focus on the role of ILA in crops and which enzyme could assume the function of glucosylating ILA in these plants and its relationship to plant defense in crops.

4. MATERIALS AND METHODS

4.1. MATERIALS

4.1.1. Chemicals

Compounds leucic acid (2-hydroxyisocaproic acid), 2-ethyl-2-hydroxybutyric acid, 2-hydroxyhexanoic acid, valic acid ((S)-(+)-2-hydroxy-3-methylbutyric acid), (±)-2-hydroxyoctanoic acid, 3-methylpentanoic acid, 3-hydroxy-3-methylpentanoic acid, L-isoleucine and BABA (3-aminobutanoic acid) were obtained from Sigma-Aldrich. ILA [(2S, 3S)-2-hydroxy-3-methylpentanoic acid] was from Interchim (France).

4.1.2. Media

KB (Kings B):

20 g/L Tryptone (Difco), 1.5 g/L K₂HPO₄, 1.5 g/L MgSO₄, 10 ml/L Glycerol

Adjusted with HCl to pH=7

15 g/L Agar for solid medium

½ MS

2.2 g/L Murashige & Skoog Medium including vitamins (Sigma, Germany)

1-1.5 % (w/v) sucrose, adjusted with KOH to pH=5.7-5.8

0.25-5 % (w/v) Gelrite (Duchefa, The Netherlands) for solid medium

Malt extract medium

15 g/L malt extract, 7.5 g/L agar

4.1.3. Bacterial strains

Escherichia coli (DH-5α, BL21 (DE3) pLys)

Pseudomonas syringae (pv tomato DC3000, Abbreviation: *Ps-vir*)

Pseudomonas syringae (pv tomato DC3000 (avrRpt2), Abbreviation: *Ps-avir*)

Alternaria brassicicola strain CBS 125088

4.1.4. Vectors

pENTR1A (Invitrogen, Germany)

pBGWFS7 (Gent University, Belgium) (Karimi et al., 2002)

pB2GW7 (Gent University, Belgium), (Karimi et al., 2002)

pAlligator2 (Francois Parcy, France), (Bensmihen et al., 2004)

pDEST15 (Invitrogen, Germany)

4.1.5. Antibiotics

Rifampicin was dissolved in methanol and other antibiotic stock solutions were dissolved in water. All were kept at -20 °C.

Antibiotics and sources	Stock solution (mg/mL)	Working concentration (µg/mL)
Ampicillin (Roche, Mannheim, Germany)	100	100
Kanamycin (Sigma, Deisenhofen ,Germany)	50	50
Rifampicin (Sigma, Deisenhofen ,Germany)	10	25 (<i>Pseudomonas</i>) or 100 (<i>Agrobacterium</i>)
Spectinomycin (Sigma, Deisenhofen ,Germany)	10	50-100
Gentamycin (Roche, Mannheim, Germany)	50	25

4.1.6. Primers

4.1.6.1. Primers used for screening homozygous lines

Lines	AGI code	Forward/Reverse	Sequence
<i>NahG</i>	—	forward	tcacctcccagaaggtatcg
		reverse	gagatgaaagccaccacgtt
<i>sid2-1</i>	At1g74710	forward	tgcttggttagcacagttaca
		reverse	agctgatctgatcccgact
<i>npr1</i>	At1g64280	forward	ggcacttgactcggatgatatt
		reverse	accttccaaagttgcttctgat
<i>ugt76b1-1</i>	At3g11340	forward	aagatccaagatcaggggataag ttcataaccaatctcgatacac (T-DNA insertion)
		reverse	gtctgattatgggaatgcagatta

4.1.6.2. Primers used for RT-qPCR

Gene	AGI code	Forward/Reverse	Sequence
<i>UGT76B1</i>	At3g11340	forward	tggaagatcggattgcatt
		reverse	ccttcattgggcataatcctc
<i>PR1</i>	At2g14610	forward	gtgccaaagtgaggtgtaacaa
		reverse	cgtgtgtatgatgatcacatc
<i>PR2</i>	At3g57260	forward	tggtgtcagattccggtaca
		reverse	catccctgaaccttccttga
<i>PR5</i>	At1g75040	forward	atcgggagattgcaaatacg
		reverse	gcgtagctataggcgtcagg
<i>PDF1.2</i>	At5g44420	forward	ccaagtgggacatggctcag
		reverse	acttgtgtgctgggaagaca
<i>VSP2</i>	At5g24770	forward	ttggcaatatcggagatcaat
		reverse	gggacaatgcgatgaagatag
<i>SAG13</i>	At2g29350	forward	ttgccacccattgttaaa
		reverse	gattcatggctcctttgggt
<i>LOX2</i>	At3g45140	forward	tgcacgccaaagtcttgta
		reverse	tcagccaaccccttttga
<i>WRKY70</i>	At3g56400	forward	ggaagaagacaatcctcatcgt
		reverse	cgttttccattgacgtaact
<i>EDS1</i>	At3g48090	forward	cgaagacacagggccgta
		reverse	aagcatgatccgcactcg
<i>PAD4</i>	At3g52430	forward	ggttctgttcgtctgatgtt
		reverse	gttctcgggtgtttgagtt
<i>UBQ5</i>	At3g62250	forward	ggtgctaagaagaggaagaat
		reverse	ctccttctctggtaaacgt
<i>S16</i>	At5g18380, At2g09990	forward	tttacgccatccgtcagagtat
		reverse	tctggtaacgagaacgagcac
<i>PAL1</i>	At2g37040	forward	ttcgggatagccgatgtt
		reverse	tgcagtgacttcaatctcca
<i>SID2</i>	At1g74710	forward	tctcaattggcagggagact
		reverse	ctccttaataaaaagccttgct
<i>AOS</i>	At5g42650	forward	ccgattagcggaggagatta
		reverse	ggttcaaaccggagacattc
<i>OPR3</i>	At2g06050	forward	ttgaggatggcttataatggaa
		reverse	tgcgataaacagtctgccata
<i>JAZ10</i>	At5g13220	forward	gtcgtcgatggagacagatct
		reverse	gagaaaacgttcagtgcactt

<i>FMO1</i>	At1g19250	forward	atccctttatccgcttctctcaa
		reverse	ctcttctgcgtgccgtagtttc
AIG1	At1g33960	forward	tggccaacgatcagaagaata
		reverse	tccctgtacgcccaactaaaac
<i>PR4</i>	At3g04720	forward	gtgctgtagcccatccacctg
		reverse	atcagcgctgcaaagtccttc
<i>PR3</i>	At3g12500	forward	cagacttcccatgaaac
		reverse	ttggctcttctccgta
<i>CYP71A13</i>	At2g30770	forward	cgataccaatggcttcagttagat
		reverse	attcggatcagggagaaggata
<i>PAD3</i>	At3g26830	forward	tacttggtgagatggcattgttgaa
		reverse	cttctctctgcttcgccaat
<i>NUDT6</i>	At2g04450	forward	atcacgccaacctcctcaac
		reverse	cgagactggtgctttattgaaca
<i>YSL9</i>	At2g35980	forward	gggaaagcggttagtacca
		reverse	ctagactgtccggcgtaaaa

4.1.7. Plant materials

Arabidopsis thaliana ecotype Col-0 was the genetic background of wild-type plants and insertion lines. Insertion mutations for *UGT76B1* in this project were identified by Veronica von Saint Paul by screening the publicly accessible SIGnAL T-DNA Express database of the SALK Institute (<http://signal.salk.edu/cgi-bin/tdnaexpress>). Two *ugt76b1* mutant lines were identified by Veronica von Saint Paul, and two independent *UGT76B1* overexpression lines were also produced by her (von Saint Paul, 2010). In this project the mutant *ugt76b1-1* (SAIL_1171A11, Col-0 background) and the overexpression line *UGT76B1-OE-7* were used. Insertion mutations for *UGT76B1* and the mutant *npr1-1*, a point mutation of positive regulator of the SA pathway were obtained from the Nottingham Arabidopsis Stock Center (NASC) or from the Arabidopsis Biological Resource Center (ABRC, Ohio State University, USA, <http://www.biosci.ohio-state.edu/pcmb/Facilities/abrc/abrchome.htm>) (Scholl et al., 2000; Rhee et al., 2003). Seeds of other mutants or overexpression line (*sid2-1*, *npr1-1*, *jar1-1*, *etr1-1* and *NahG*) used in this work were kindly provided by Christian Lindermayr (Helmholtz Zentrum München) (Table 9). The *GOX3* related lines were nicely provided by Veronica Maurino (Düsseldorf University, Germany).

Table 9. *Arabidopsis* mutants and overexpression lines used in this project.

AGI code	Name	Ecotype	Screening method	Reference
At3g11340	<i>ugt76b1-1</i>	Col-0	PCR and Basta TM	Von Saint Paul <i>et al.</i> , 2011
At3g11340	<i>UGT76B1-OE-7</i>	Col-0	PCR and Basta TM	Von Saint Paul <i>et al.</i> , 2011
At1g74710	<i>sid2-1</i>	Col-0	CAPS marker	Nawrath and Metraux <i>et al.</i> , 1999
At1g64280	<i>npr1-1</i>	Col-0	CAPS marker	Huigao <i>et al.</i> , 1997
At2g46370	<i>jar1-1</i>	Col-0	MeJA insensitivity	Berger <i>et al.</i> , 2002
At1g66340	<i>etr1-1</i>	Col-0	Ethylene insensitivity	Bleecker AB <i>et al.</i> , 1988
—	<i>NahG</i>	Col-0	Kanamycin	Gaffney <i>et al.</i> , 1993
At4g18360	<i>gox3-1</i>	Col-0	-	Reumann <i>et al.</i> , 2004
At4g18360	<i>gox3-2</i>	Col-0	-	Reumann <i>et al.</i> , 2004

4.2. METHODS

4.2.1. Plant growth conditions

Arabidopsis thaliana plants (Col-0) were grown in soil under a light cycle of 14 h with the intensity of 45-60 $\mu\text{mol m}^{-2} \text{s}^{-1}$ at 20 °C in the light and at 18 °C in the dark with 75% relative humidity. To observe the root growth, seedlings of *Arabidopsis* were placed on square plates containing ½ MS medium and grown vertically under a light cycle of 16 h with the light intensity of 160 $\mu\text{mol m}^{-2} \text{s}^{-1}$ at 22-23 °C. To analyze metabolites by FT-ICR MS, *Arabidopsis lyrata* (rockcress), *Brassica oleracea subsp. oleracea* (wild cabbage), *Brassica napus* (rapeseed), *Solanum lycopersicum* cv. Microtom (tomato), *Nicotiana tabacum* (tobacco), *Hordeum vulgare* L. cv. Barke (barley), *Zea mays* (maize) and *Populus spp.* (poplar) were grown in the green house under a light cycle of 10 h at 24 °C in the light and at 18 °C in the dark with 60% relative humidity. To apply pathogen infection and measure defense marker genes, barley was grown under a light cycle of 14 h with a light intensity of 75 $\mu\text{mol m}^{-2} \text{s}^{-1}$; the temperature was set to 20 °C in the light and to 18 °C in the dark.

4.2.2. Seedling grown on solid medium

To sterilize seeds of *Arabidopsis*, seeds were dropped with 90 % ethanol on filter papers in sterile Petri dishes in the sterile hood. The procedure was repeated three times until seeds got completely dry on the filter papers. Then the sterile seeds were transferred to square Petri dishes (120 mm x 120 mm x 17 mm, Greiner bio-one, Germany) containing 50 mL ½ MS

medium (1.5 % sucrose, 0.5 % (w/v) Gelrite), using sterile toothpicks in the hood, which is followed by a two-day stratification at 4 °C in the darkness. After stratification, plates were taken into the growth chamber to grow in a vertical orientation under a 16 h light /8 h darkness cycle.

4.2.3. BASTA selection

Around two-week-old *Arabidopsis* seedlings grown on soil were sprayed with BASTA solution (Phosphinothricin, glufosinate ammonium), (Hoechst, Germany) until the plants got completely wet. The commercial formulation was diluted with water at a ratio of 1:800). The susceptible plants, which wilted four days after BASTA application, were pulled out from the soil or died; resistant plants were grown to maturity.

4.2.4. Wounding of *Arabidopsis* leaves

To study the response to wounding, four leaves (5th to 11th) from four-week-old *Arabidopsis* were mechanically wounded according to the instructions (Koo et al., 2009). The leaves were harvested 30 min after wounding to measure the abundance of JA-related metabolites and the expression of SA and JA marker genes. For the measurement of amino acids, the leaves from two-week-old *Arabidopsis* were harvested 1 h after wounding. All leaves were flash frozen in liquid nitrogen and stored at -80 °C.

4.2.5. Crossing

Plants at the stage of developing 5-6 inflorescences were used for crossing. All the immature anthers around stigmata of receptor flowers where the petals just started to appear were carefully removed to avoid self-fertilization. The pollen of open flowers of donor plants was transferred to the stigmata of the emasculated plants.

4.2.5.1. Generation of homozygous lines combining the lines with different *UGT76B1* expression and lines deficient in the SA pathway or the JA / ET pathway

To explore where and how *UGT76B1* is integrated in the SA and JA/ET pathways, lines with different *UGT76B1* expression were introgressed into lines deficient either in SA or JA/ET pathways. Homozygous lines were identified by those commercial PCR primes which can amplify the band when the T-DNA insertion is in the genome, the antibiotic markers or the Cleaved Amplified Polymorphic Sequences (CAPS) polymorphisms. The detail methods to

screen each line will be described in the following parts. The homozygous lines used in the project include *ugt76b1-1 sid2*, *UGT76B1-OE-7 sid2*, *ugt76b1-1 npr1*, *UGT76B1-OE-7 npr1*, *ugt76b1-1 NahG*, *ugt76b1-1 jar1* and *UGT76B1-OE-7 jar1*.

4.2.5.2. Genotyping for double mutants

To identify the homozygous mutation of the genes containing the T-DNA insertion sequence, two primer pairs were used for the subsequent PCR in a volume of 20 μ L, according to the protocol of Sigma (Extract-N-AmpTM plant PCR kit). One primer pair can recognize both the genomic DNA and the T-DNA insertion sequences and produce an amplicon with partial T-DNA sequences. The other primer pair can produce an amplicon containing only the genomic DNA sequences. The homozygous mutation was identified *via* observing the bands of the PCR products amplified from both primer pairs *via* DNA gel electrophoresis. Only the primer pair recognizing both genomic DNA and T-DNA insertion sequence can produce one band, whereas the other primer pair cannot produce any band, because of the huge T-DNA insertion. To identify mutants with point mutations causing a Cleaved Amplified Polymorphic Sequences (CAPS) polymorphisms (www.ncbi.nlm.nih.gov/projects/genome/probe/doc/TechDCAPS.shtml), 10 μ L of the PCR reactions were digested by the restriction enzyme which recognizes CAPS polymorphisms, whereas the remaining 10 μ L of the PCR reaction was used as the control. The homozygous mutation was identified by observing the pattern of the fragments depending on the particular marker analyzed (see below).

4.2.5.3. Production of the *ugt76b1-1 sid2* and *UGT76B1-OE-7 sid2* double mutants

The *sid2-1* mutant was introduced into *ugt76b1-1* and *UGT76B1-OE-7* to generate the double mutants. In *sid2-1*, the single nucleotide substitution of C to T in exon 9 results in the conversion Glu449STOP and diminishes the recognition site by the restriction enzyme *Mfe* I, thereby causing the CAPS polymorphisms. The primer pair was designed to amplify a fragment of 1112 bp in PCR with the substitution site included. In wild type, cleaving of the PCR products by *Mfe* I will generate two fragments of 392 bp and 720 bp, whereas the intact band of 1112 bp was observed in *sid2-1*. The homozygous *sid2* mutation was identified according to the criterion that only one band of 1112 bp after the digestion of PCR products by *Mfe* I could be observed on the DNA gel. A volume of 10 μ L of the 25 μ L of the PCR reaction was treated with 5 units of the restriction enzyme *Mfe* I.

The homozygous *ugt76b1* mutation was genotyped *via* PCR using the two pairs of primers from SALK (<http://signal.salk.edu/cgi-bin/tdnaexpress>) (Table in 4.1.6.1). In the F2 generation the homozygous *ugt76b1 sid2* line was obtained at a ratio of 1:16. The sequence of *UGT76B1* is linked together with a dominant BASTA-resistance marker in the *UGT76B1* overexpression lines. To identify the *UGT76B1-OE-7 sid2* double mutant, the *sid2* homozygous mutation was selected among the F2 generation progeny. The plants of the F2 generation including both homozygous and heterozygous sites for the insertion of *UGT76B1* were selected by the dominant BASTA resistance. The homozygous *UGT76B1-OE-7 sid2* double mutant was obtained by screening non-segregating BASTA resistance in the following F3 generation.

4.2.5.4. Production of the *ugt76b1-1 NahG* and *UGT76B1-OE-7 NahG* double mutants

The transgenic *NahG* line expressing an SA hydroxylase and degrading total SA levels (Gaffney et al., 1993) was introgressed into *ugt76b1-1* and *UGT76B1-OE-7*. The existence for the *NahG* sequence was genotyped by PCR using the primer pair designed based on *NahG* sequence (Table in 4.1.6.1). The homozygosity for *NahG* was identified without segregation in the next generation. The homozygosity for the *ugt76b1* knockout and *UGT76B1* overexpression were selected as above.

4.2.5.5. Production of the *ugt76b1-1 npr1* and *UGT76B1-OE-7 npr1* double mutants

The *npr1-1* mutant causes the substitution of the single nucleotide C to T, transforming a highly conserved histidine (residue 334) to tyrosine in the third ankyrin-repeat consensus sequence. The nucleotide substitution results in the loss of the recognition site by the restriction enzyme *Nla* III. The primer pair was designed to amplify a 272 bp fragment including the substitution site. The PCR products from wild type were cut by *Nla* III, yielding a 184 bp fragment and an 83 bp fragment whereas the PCR products from the mutant *npr1-1* could not be cut leading to an intact 272 bp fragment. The homozygous line of *ugt76b1-1 npr1* was selected from the F2 generation. The homozygous line of *UGT76B1-OE-7 npr1* was obtained in the F3 generation as above.

4.2.5.6. Production of the *ugt76b1-1 jar1* and *UGT76B1-OE-7 jar1* double mutant

The *jar1* mutant is resistant to the inhibition of root growth by MeJA, showing longer roots on a medium containing MeJA relative to wild type (Berger, 2002). The *jar1* mutant was crossed with *ugt76b1-1* and *UGT76B1-OE-7* to generate the *ugt76b1-1 jar1* and *UGT76B1-OE-7 jar1* double mutants in order to investigate the dependence of phenotypes caused by different *UGT76B1* expression on *JAR1*. The homozygous site for the *jar1* mutation was selected on ½ MS medium containing 10 µM MeJA. Then the lines with the homozygous *jar1* mutation were transferred to soil and further screened for homozygosities for the *ugt76b1* knockout or the *UGT76B1* overexpression.

4.2.6. Observation of root growth of *Arabidopsis* on plates containing chemicals

To observe the root growth in response to the treatment with different chemicals, *Arabidopsis* seedlings were grown on ½ MS medium supplemented with different chemical compounds. 100 mM stock solutions of the compounds were prepared in sterile ddH₂O sterilized by membrane filtration using the filters with 0.20 µm pore diameter (DIAFIL, Germany) and then stored at 4 °C. The stock solutions added to ½ MS medium were diluted to a final, required concentration before use.

4.2.7. ILA treatment

For ILA application, four-week-old *Arabidopsis* plants were sprayed with 0.5 or 1 mM ILA (diluted in sterile ddH₂O from 100 mM stock solution). Plants were covered with a Plexiglas lid for approximately 4 h to ensure that ILA entered the plants. Then the lid was half uncovered to let the liquid evaporate and the surface of leaves become dry. For ILA treatment of barley, two-week-old barley plants (cultivar *Barke*) were sprayed with 1 mM ILA (diluted in 0.01 % Tween to help ILA enter the leaves).

4.2.8. Pathogen infections

4.2.8.1. Biotrophic pathogen infection of *Arabidopsis*

The biotrophic pathogens *Pseudomonas syringae* pv *tomato* DC3000 (*Ps-vir*) and *P. syringae* pv *tomato* DC3000 (*avrRpm1*) (*Ps-avir*) were used in this project. Bacteria in -80 °C glycerol stock were streaked out onto fresh solid King's B medium and grown two days at 28 °C. An activated single colony was picked and suspended in liquid King's B medium to grow

overnight at 28 °C at a shaker speed of 170 rpm with appropriate antibiotics (100 µg/mL rifampicin for *Ps-avir* and *Ps-vir* and 50 µg/mL kanamycin for *Ps-avir*). When the bacterial growth reached to the late log phase of growth (OD₆₀₀ 0.6 to 1.0), bacteria were diluted to 5×10^5 cfu mL⁻¹ in 10 mM MgCl₂ for the inoculation of plants. An OD₆₀₀=0.2 is approximately 1×10^8 colony-forming unites/mL. Four leaves of five- to six-week-old *Arabidopsis* (6th to 11th) were marked by a blunted marker pen, followed by the infiltration using a 1 mL syringe. Control plants were infiltrated by 10 mM MgCl₂ as mock treatment. The leaf disc with an area of 0.20 cm² (a circle with the diameter of 0.25 cm) was cut using the lit of 0.5 mL eppendorf tube and harvested from the inoculated leaves. Two leaf discs from the individual infected plant were harvested. Six leaf discs from three individual plants were pooled to make one biological replicate. Three biological replicates were made. Bacterial growth was calculated according to the previous description (Katagiri et al., 2002).

4.2.8.2. Necrotrophic pathogen infection of *Arabidopsis*

The necrotrophic fungal pathogen *Alternaria brassicicola* strain CBS 125088 was used for the infection (Pogany et al., 2009). *A. brassicicola* was grown on malt extract agar medium under a 12 h light cycle at 22 °C for around two weeks until black spores were generated. Small pieces of solid medium with black spores were cut out and placed on the center of new plates with fresh medium to produce additional cultures. The spores were then washed away gently from the plates and suspended in sterile distilled water or the solution (8.5 g/L KH₂PO₄, 1g/L glucose in 0.01 % Tween 20, pH=6.0). One five µL droplet of the suspension with 1.5×10^6 conidia mL⁻¹ was directly dropped onto the adaxial surface of leaves (5th to 11th leaf). The concentration of the fungal was calculated by hemocytometer. The plants were covered by a plexiglas lid with the steam evaporating from a pot of warm water to keep the humidity inside high. The size of lesions on leaves was visualized by eye and recorded by camera 10 to 13 d after the inoculation.

4.2.9. Preparation of plant genomic DNA

An Extract-N-AmpTM plant PCR kit was used to isolate the plant genomic DNA according to the manufacturers protocol (Sigma) for genotyping the above mentioned homozygous lines.

4.2.10. RNA isolation

Plant leaf material was homogenized by a dismembrator in liquid nitrogen. Around 60 mg of leaf powders (the weight is adequate for the quantity of RNA and does not result in DNA contamination) were extracted for total RNA using RNeasy plant mini kit according to the protocols (Qiagen, Hilden, Germany). To ensure the avoidance of DNA contamination, DNase digestion was performed on the column as recommended. This method was used to isolate RNA to transcribe the first-strand cDNA for the subsequent RT-qPCR. For the purpose of a non-targeted transcriptome analysis, another method (recommendation from the colleague Malay Das) utilizing Trizol in combination with the RNeasy plant mini kit was used to isolate clean and salt free RNA. About 60 mg leaf powders were added to 1.0 mL of Trizol (Invitrogen) and mixed well by rapid vortexing to avoid thawing at room temperature (RT) prior to complete dispersion. Then the homogenized solution was incubated for 5 min at RT and vortexed frequently. Afterwards, 0.2 mL chloroform was added to the extraction solution followed by vortexing of the mixture for 15 s and incubating the suspension for 1 min at RT. Following vortexing the mixture again for 15 s, the top aqueous layer was separated by the centrifugation at 15,000 g for 10 min at 4 °C. Two hundred μ L of the aqueous phase were added to 700 μ L Qiagen RLT buffer in a new 2 mL Eppendorf tube. After mixing 500 μ L of 96-100% ethanol were added to the solution and mixed well by vortexing. Finally, the further purification of RNA was carried out using the RNeasy plant mini kit according to the manufacturer's protocol; DNase digestion was performed on the column as recommended. For the two methods mentioned above, total RNA was dissolved in 30 μ L of RNase/DNase free water and evaluated for both the quality and the concentration using the Nanodrop ND-1000 spectrophotometer (Kisker-Biotech, Germany).

4.2.11. Real-time PCR

4.2.11.1. Primer design

Primers for RT-qPCR were designed using the Primer Express 3.0 software (Applied Biosystems®) according to the reference mRNA sequences. The optimal primers would span the intron of the genomic DNA, because this could easily eliminate the disturbance of genomic DNA contamination, or would easily reveal any genomic contamination. The length of the primers was 20-22 bases. The annealing temperature for the primers was 55 °C and the amplicons generated had lengths of 120-130 bp. All the primer pairs were blasted to the genomic DNA for checking the specificity of binding to the gene of interest in SALK (<http://signal.salk.edu/cgi-bin/tdnaexpress>). The efficiency of primers was calculated based on

a serial cDNA dilution. Only primers with efficiency above 80 % were selected for the following procedure.

4.2.11.2. Synthesis of the first-strand cDNA without contamination by genomic DNA

The first-strand cDNA was transcribed from 1 µg total RNA using QuantiTect Rev. Transcription Kit (Qiagen, Germany). According to the Qiagen manual, the first strand cDNA was synthesized following the fast elimination of the genomic DNA as recommended in the protocol. To completely rule out any genomic DNA contamination, 1 µg total RNA from the same sample was subjected to the same procedure as transcription, but without the reverse transcriptase as the negative control. To ensure the success of transcription and avoidance of genomic DNA contamination, 1 µL solution from both the transcription reaction and reaction of the negative control were used to perform a normal PCR reaction. The primer pair for the PCR reaction was designed to amplify the fragment of the house keeping gene *TUBULIN 9* (At4g20890) (Forward: 5'-GTACCTTGAAGCTTGCTAATCCTA-3', Reverse: 5'-GTTCTGGACGTTTCATCATCTGTTC-3'). Since the primer pair spanned an intron, the genomic DNA contamination could be distinguished due to the bigger size of a *TUBULIN 9* fragment amplified from the genomic DNA than from the cDNA. The PCR reaction was done in a Multicycler PTC-200 (Biozym, Germany). The qualified reverse transcription was characterized by the band amplified from the transcription reaction, but, however, no band from the negative control.

Reactions for PCR mix

1 µL Template cDNA or the negative control
 2 µL 10x Reaction buffer
 2 µL 2 mM dNTPs
 1 µL 10 µM Forward primer
 1 µL 10 µM Reverse primer
 0.1 µL Taq polymerase (5 U/µL)
 12.9 µL double distilled water

4.2.11.3. Quantitative real time polymerase chain reaction (RT-qPCR)

The fluorescence dye SYBR Green (from Thermo Scientific or Bioline), binding to double-stranded DNA, was used to label the amplified double-stranded DNA. The concentration of the template negatively correlates with the number of cycles, which are required to reach the threshold of the fluorescence, *i. e.* when the signal exceeds background noise. The primers were designed by Primer Express 3.0 (Applied Biosystems®). The evaluation of the serial dilutions suggested an appropriate dilution ratio of 1:15 with the cycle numbers (Ct values) ranging from 18 to 30. The 7500 real-time PCR system (Applied Biosystems) was used to record the reactions. The master mixture containing of 4 µL cDNA, 10 µL of SYBR Green

Mastermix and 250 μ M of each primer in a 20 μ L reaction volume was loaded into 96 well plates. Each sample was repeated with two technical replicates. The reaction programs were as follows: (1) 95 °C for 15 min, followed by 40 cycles of 95 °C for 15 sec, 55 °C for 35 sec, and 72 °C for 45 sec and a final step of 95 °C for 15 sec, 60 °C for 1 min and 95 °C for 15 sec to collect the melting curve for the reaction run by SYBR from Thermo Scientific; and (2) 95 °C for 10 min, followed by 40 cycles of 95 °C for 15 sec, 55 °C for 15 sec, and 72 °C for 45 sec and a final step of 95 °C for 15 sec, 60 °C for 1 min and 95 °C for 15 sec to collect the melting curve for the reaction run by SYBR from Bioline.

4.2.11.4. Selection of reference genes and normalization of RT-qPCR

To select stable genes for normalization, putative housekeeping genes *TUB 9* (At4g20890), *UBQ5* (At3g62250) and *S16* (At5g18380, At2g09990) were evaluated by GeNorm. Among them, *UBQ5* and *S16* were chosen as the two reference genes to normalize the relative abundance of the genes of interest by GeNorm (Vandesompele et al., 2002).

4.2.12. Separation and analysis of the DNA fragments based on DNA gel electrophoresis

The amplified DNA fragments with the predicted length were separated by agarose (1%) gel electrophoresis containing 0.05 μ g/mL ethidium bromide in 1x TAE buffer. The PCR reaction was mixed with 6x loading dye buffer and then loaded in the gel. DNA fragments were visualized by UV light, 30 minutes after running of the gels at 5-10/cm.

4.2.12. SA determination

The rosette leaves (5th to 12th leaves) of four to six individual plants (snap-frozen in liquid nitrogen and stored at -80 °C) were pooled for one biological replicate to do the extraction of SA. Five biological replicates were made for each line from *UGT76B1-OE-7*, *ugt76b1-1* and Col-0. Then leaf materials were disrupted by a dismembrator in liquid nitrogen. Fine leaf powder ranging from 200 to 300 mg was extracted in 3.5 mL of the extraction buffer consisting of one part methanol and two parts 2% (v/v) formic acid with 25 μ L 500 μ g/mL *o*-anisic acid (Sigma-Aldrich, Germany; dissolved in methanol) added as an internal standard. The suspension was sonicated for 1 min at setting 50% (Branson Sonifier Cell Disruptor B15). Then the extract was centrifuged for 10 min at a high speed $\geq 10,000$ g at 4 °C and the supernatant was transferred to a new 15 mL falcon tube. The residual pellet was suspended in 1 mL fresh extraction buffer and sonicated for 1 min as above. The extraction solution was

centrifuged for 10 min at $\geq 10,000$ g and 4 °C. The supernatant was joined to the former one and adjusted to a final volume of 6 mL using methanol/ 2% (v/v) formic acid extraction buffer. Then the supernatant was split into three aliquots for the respective determination of free SA, SA glucosides and SA esters. For the determination of the SA conjugates, 1 mL of the supernatant was digested with β -glucosidase (Roth; Germany; see below) and 2 mL of supernatant were digested with esterase (Sigma-Aldrich, Germany; see below) overnight at 37 °C, followed by the termination of reaction by addition of 100 μ L 32 % HCl. For the determination of free SA, 3 mL of the solution was treated with 30 μ L 32 % HCl to block the activity of any residual SA metabolizing enzyme.

In all three cases, SA was purified under the acidic condition using the reversed-phase sorbent cartridges (Oasis HLB 1 cc; Waters) column. Before loading of the samples, 1mL 2 % formic acid was added to the column and driven out by N₂ or air blow with a speed of one drop/per sec to equilibrium the column. Then the sample was loaded onto the column and driven out via N₂ with the speed of one drop/per sec. The column was first washed with 500 μ L of 2 % formic acid followed by 200 μ L HPLC-degrade water. Finally SA was washed out in 500 μ L elution buffer (0.28 % NH₄OH in 20 % methanol) from the column. Then 25 μ L highly concentrated formic acid (98 %-100 %) was added to the eluate to maintain the stability of SA. The solution containing SA was transferred to a HPLC tube and run on the HPLC column Gemini 5 μ C6-Phenyl 110A (Phenomenex, Germany) to separate the metabolites. Twenty five μ L of both 10 μ g/mL authentic SA (Sigma-Aldrich) and 500 μ g/mL *o*-anisic acid SA (Sigma-Aldrich, dissolved in methanol) were added to 950 μ L buffer A as the standard. The standard was repeatedly run in the HPLC every five samples. Quantification of SA was based on the fluorescence (excitation 305 nm/emission 400 nm) of *o*-anisic acid and SA standards. The flow rate was 1 mL/min. Therefore, the content of free SA, Glc-conjugated SA and esterified SA in the sample could be calculated from the area of the SA peak.

HPLC buffer A for separating metabolites (2 L with pH=5.2)

Citric acid 30 mM

Sodium acetate 27 mM

Sodium hydroxide 4 g

2 L distilled water

Filtration and degassing for 8 min

HPLC buffer B for washing column

5 % buffer A in HPLC-grade methanol

degassing for 8 min

β -glucosidase treatment

Add 100 μ L 1M NH_4HCO_3 to 1 mL portion of extraction as the working buffer

Add 2 mL β -glucosidase enzyme solution (0.2 mg/mL dissolved in 0.1 M NaAC with pH=5.2)

Incubate the reaction at 37 °C overnight

esterase treatment

Add 500 μ L saturated NaHCO_3

Add 2 μ L esterase suspension (ready as bought)

Incubate the reaction at 37 °C overnight

HPLC program

Time (min)	Module	Function rely on	Value	Duration (min)
0.1	pump	% B	4	0.10
22	pump	% B	100	3
32	pump	% B	0.00	3
40	pump	% B	0.00	0

4.2.13. Non-targeted Metabolome Analysis by FT-ICR MS

The plant materials from *Arabidopsis lyrata* (rockcress), *Brassica oleracea subsp. oleracea* (wild cabbage), *Brassica napus* (rapeseed), *Solanum lycopersicum* cv. Microtom (tomato), *Nicotiana tabacum* (tabacco), *Hordeumvulgare* L. cv. Barke (barley), *Zea mays* (maize) and *Populus spp.* (poplar) were homogenized by a dismembrator in liquid nitrogen and subsequently extracted with 100 % methanol with 44 $\mu\text{g mL}^{-1}$ loganin as the internal control. Each plant species had at least five biological replicates. Metabolite extraction was made according to von Saint Paul (2010). The accurate 100 mg plant materials were extracted with 1 mL 100 % methanol which was rotated with the speed of 7 rpm (Heidolph Reax 2) at 4 °C for 1 h. Afterwards, the extraction buffer was centrifuged at the speed of $\geq 10,000$ g for 10 min at 4 °C. 750 μ L supernatant was added to 250 μ L HPLC water and mixed well, followed by 10 min centrifugation at $\geq 10,000$ g and 4 °C. 500 μ L of the upper supernatant phase were divided into 5 aliquots of 100 μ L each. For FT-ICR MS measurement, one aliquot was diluted 1:50 in 70 % methanol with 35 pmol mL^{-1} dialanin as the internal control. The measurements were done in the negative ionization mode in FT-ICR MS (12 Tesla instrument, Bruker) with assistance by Basem Kanawati and Philippe Schmitt-Kopplin.

4.2.14. Fragmentation Studies using FT-ICR MS

Further fragmentation of mass peaks by FT-ICR MS can indicate possible molecular formulas. Therefore, the targeted mass peaks were further fragmented in the machine. The ions were trapped in the first hexapole for 200 ms then selected inside a quadrupole mass filter. The isolated ions were accelerated to collide with argon atoms inside the second hexapole with a high pressure of 5×10^{-3} mbar. The time for ion accumulation inside the collision cell was 500 ms.

4.2.15. Measurement of JA-related metabolites by GC-MS

The measurement of JA-related metabolites by GC-MS was done by the collaborator Bettina Hause (from Halle, Germany) according to the previous protocol (Balcke et al., 2012).

4.2.16. Production of the recombinant protein UGT76B1

The sequence of the UGT76B1 open reading frame was amplified and inserted into the plasmid pDEST15 (Invitrogen). The translated protein of UGT76B1 was fused with a glutathione S-transferase tag (von Saint Paul, 2010), which allows for the purification through binding to glutathione-coupled sepharose beads using a binding affinity towards glutathione, according to the manufacturer's instructions (GE Healthcare, Germany). The protein UGT76B1 was concentrated by membrane filtration (Amicon Ultra-4; Millipore) and stored in 20 % glycerol at $-20\text{ }^{\circ}\text{C}$ (Messner et al., 2003).

4.2.17. *In vitro* analysis of the recombinant UGT76B1

UGT76B1 is a glucosyltransferase, which can transfer a sugar moiety from UDP-Glc to a small organic molecule. To analyze the activity of the recombinant enzyme UGT76B1, the UGT76B1 recombinant protein was incubated with the aglycons to be measured and supplied with UDP-Glc. The reaction mixture was made up to a final 50 μ L volume containing 0.1 M Tris-HCl buffer pH 7.5, 5 mM UDP-Glc, 0.5 mM aglycon, and \sim 1 μ g protein. The reaction was incubated for 1 h at 30 $^{\circ}$ C in a water bath and stopped by adding 200 μ L methanol. The mixture was cleared by centrifugation for 2 min at the speed of 15,000 g. Reactions were diluted to 1:50 in 70 % methanol to be analyzed. However, the reaction mixture with the aglycon valic acid was diluted 1:1 with 70 % methanol to increase the product concentration. The diluted reaction mixture was injected into the electrospray source on an API4000 mass spectrometer with a flow rate of 30 μ L/min. One hundred and fifty scans were applied to accumulate the intensity for each measurement in the negative ion monitoring mode. The signals of aglycon and product with the expected m/z ratios were monitored with a mass range of \pm 5 D.

4.2.18. Microarray Analyses

The *Arabidopsis* plants were grown under a long light cycle of 14 h under 45-60 μ mol $m^{-2} s^{-1}$ of light intensity. ILA is known to be the substrate of UGT76B1. To further understand the potential connection of ILA and *UGT76B1* in regulating defense in *Arabidopsis*, a transcriptome analysis at the genomic level was performed using an *Arabidopsis* Genechip from Agilent, consisting of over 8*60 K probes. The experiment was designed to compare the expression patterns of ILA-treated Col-0, mock-treated *ugt76b1-1* and mock-treated *UGT76B1-OE-7* compared with mock-treated Col-0. ILA was applied by spraying a 1 mM solution in water onto leaves; all non-treated plants were sprayed with water to allow a side by side comparison. Each line contained three biological replicates. Leaves from eight four-week-old *Arabidopsis* were harvested to be pooled for one replicate. The microarray analysis was done following the technique “One-color Microarray-Based Gene Expression Analysis-Low Input Quick Amp Labeling” from Agilent, according to the manual (Agilent G4140-90040). The Agilent 8-pack microarray format was applied in this project.

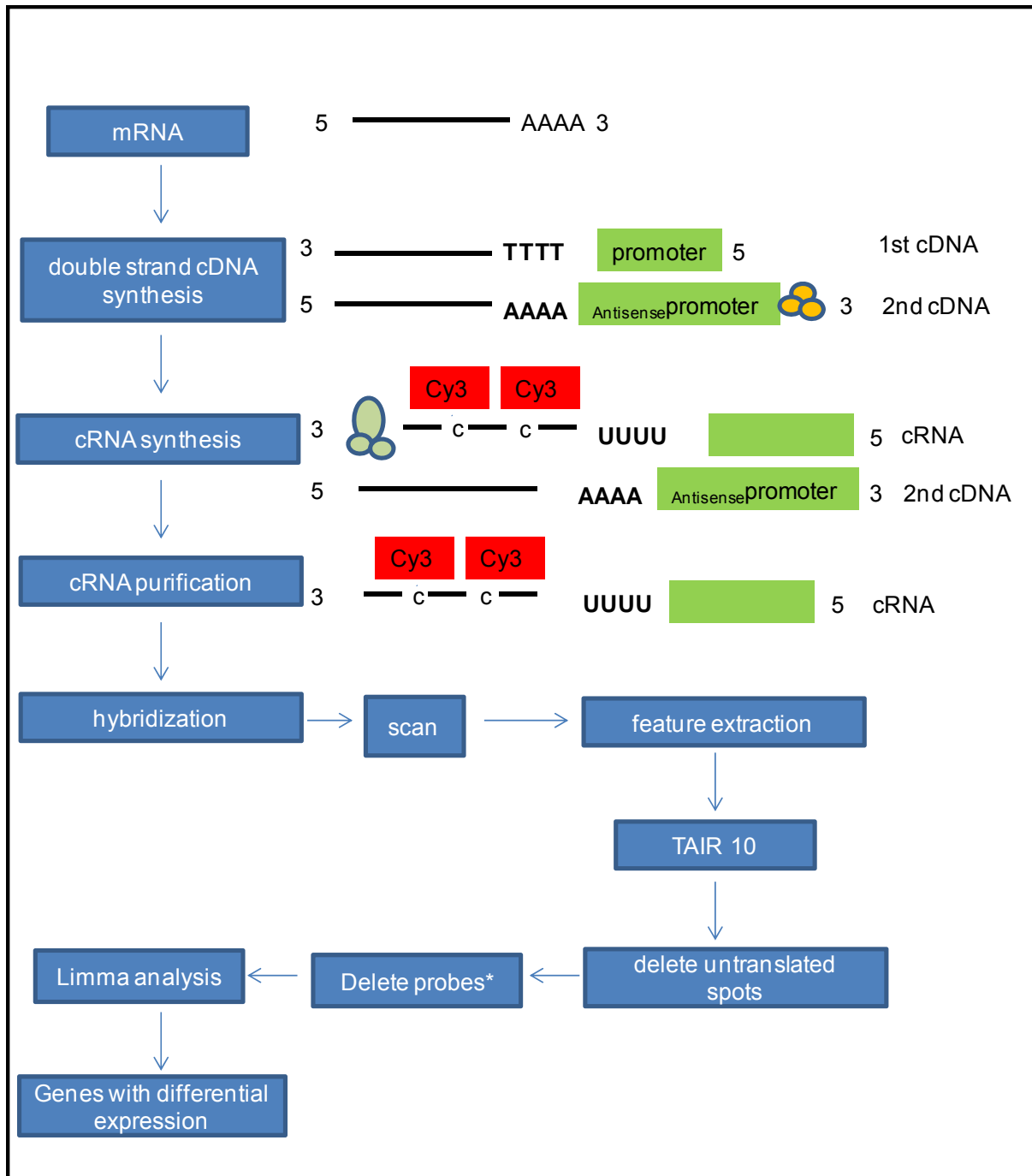


Figure 35. The workflow for microarray processing and data analysis

mRNA in total RNA was as template to synthesize cDNA with a promoter sequence, initiating the cRNA synthesis. CRNA was synthesized by T7 RNA polymerase, which can incorporate Cy3 labeled CTPs into newly synthesized cRNA. cRNA were purified and hybridized to Agilent microarray. After hybridization, the arrays were scanned and applied feature extraction using software v10.7 with the protocol GE1_107_Sep09. TAIR 10 was utilized for probes' annotation. The untranslated spots were deleted. Probes with \log_2 -transformed fluorescence value less than 4 in any sample were deleted (indicated as “*”). The software Limma was integrated to “R” to generate probes with differential expression.

4.2.19. Microarray data analysis

A pairs plot analysis was applied to monitor the correlation of the three biological replicates for each treatment separately (mock-treated Col-0, mock-treated *ugt76b1-1*, mock-treated *UGT76B1-OE-7*, ILA-treated Col-0). Each dot represented one signal and most of the signals from any two replicates scattered around the line with the slope of one. The closer all signals are to the line with slope of one, the better the co-correlation of the two replicates. Therefore it was indicated that all three biological replicates of any treatment were tightly correlated (Figure 36). The signals from the arrays were further analyzed by the GeneSpring 11.5 software (Agilent, USA). The fluorescent signals of all probes among all the samples were \log_2 -transformed. Probes with \log_2 -transformed fluorescence value less than four in any sample were deleted. The software Limma integrated into “R” was used to analyze the data for differential gene expression. Transcripts with more than twofold changes compared to the control (Col-0) and a significant change based on a corrected p-value smaller than 0.05 were extracted and further analyzed.

4.2.20. Bioinformatic analyses

BioMaps (www.virtualplant.org) version 1.3 was used to apply the annotation for the probes with AGI code. Hyper-geometric distribution was used to calculate the p-values of over-representation of gene classifications. A p-value smaller than 0.01 was considered to indicate a significant change. Mapman 3.5.1 was used to observe the pathogen defense enrichment pattern. Genevestigator (<https://www.genevestigator.com/gv/>) was used to compare the expression pattern of genes of interest with public data. The coexpression pattern for genes of interest was checked in ATTED-II (<http://atted.jp/>). Arithmetic means and standard errors from \log_{10} -transformed data of RT-qPCR data from more than three independent experiments were calculated by the software “R” using ANOVA.

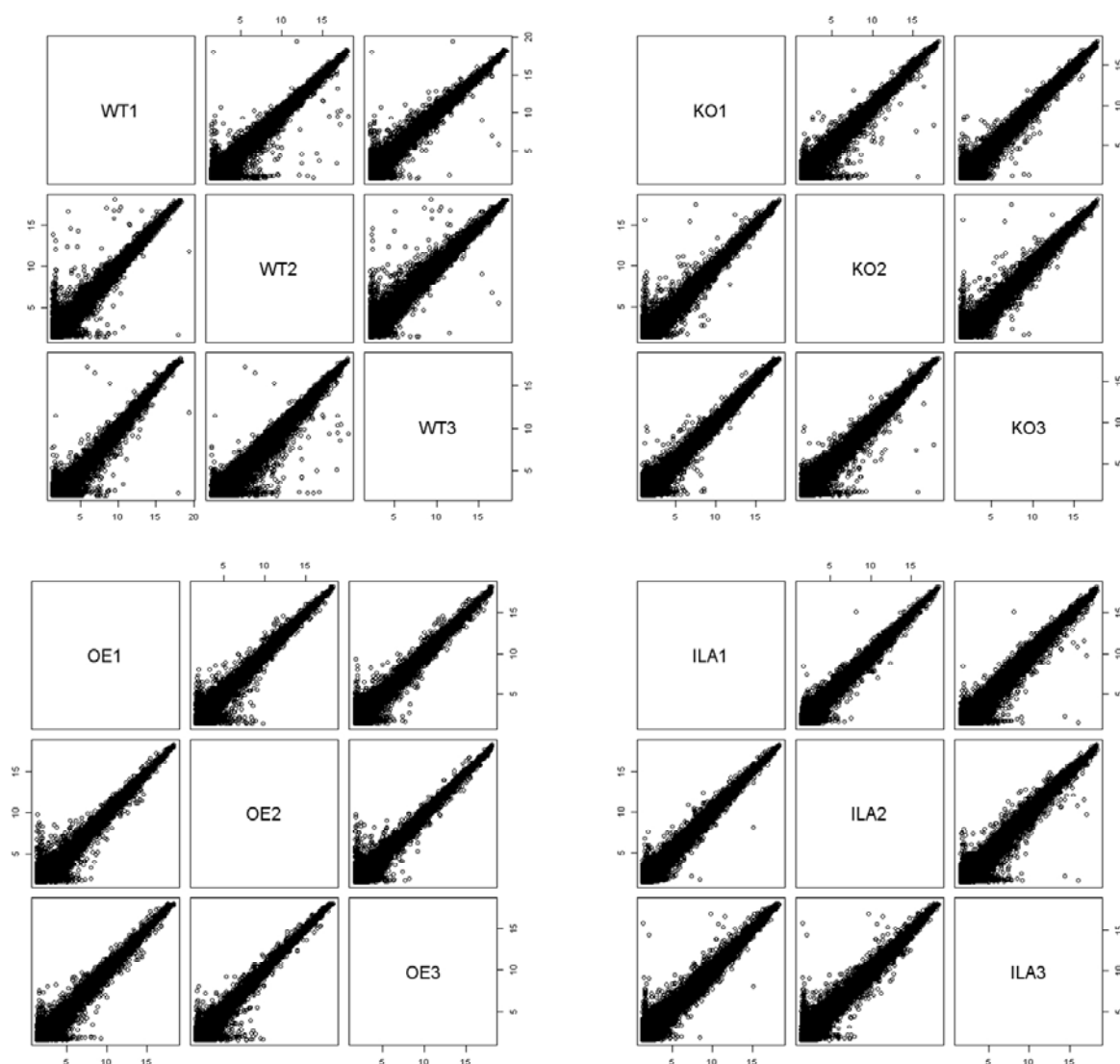


Figure 36. Pairs plots of microarray data for samples.

WT stands for mock-treated Col-0, KO stands for mock-treated *ugt76b1-1*, OE stands for mock-treated *UGT76B1-OE-7* and ILA stands for ILA-treated Col-0.

REFERENCES

- Asai, T., Tena, G., Plotnikova, J., Willmann, M.R., Chiu, W.L., Gomez-Gomez, L., Boller, T., Ausubel, F.M., and Sheen, J. (2002). MAP kinase signalling cascade in *Arabidopsis* innate immunity. *Nature* **415**: 977-983.
- Balague, C., Lin, B., Alcon, C., Flottes, G., Malmstrom, S., Kohler, C., Neuhaus, G., Pelletier, G., Gaymard, F., and Roby, D. (2003). HLM1, an essential signaling component in the hypersensitive response, is a member of the cyclic nucleotide-gated channel ion channel family. *Plant Cell* **15**: 365-379.
- Balcke, G.U., Handrick, V., Bergau, N., Fichtner, M., Henning, A., Stellmach, H., Tissier, A., Hause, B., and Frolov, A. (2012). An UPLC-MS/MS method for highly sensitive high-throughput analysis of phytohormones in plant tissues. *Plant Methods* **8**: 47.
- Bartsch, M., Gobbato, E., Bednarek, P., Debey, S., Schultze, J.L., Bautor, J., and Parker, J.E. (2006). Salicylic acid-independent ENHANCED DISEASE SUSCEPTIBILITY1 signaling in *Arabidopsis* immunity and cell death is regulated by the monooxygenase FMO1 and the Nudix hydrolase NUDT7. *Plant Cell* **18**: 1038-1051.
- Bensmihen, S., To, A., Lambert, G., Kroj, T., Giraudat, J., and Parcy, F. (2004). Analysis of an activated ABI5 allele using a new selection method for transgenic *Arabidopsis* seeds. *FEBS Letters* **561**: 127-131.
- Berger, S. (2002). Jasmonate-related mutants of *Arabidopsis* as tools for studying stress signaling. *Planta* **214**: 497-504.
- Birkenbihl, R.P., Diezel, C., and Somssich, I.E. (2012). *Arabidopsis* WRKY33 is a key transcriptional regulator of hormonal and metabolic responses toward *Botrytis cinerea* infection. *Plant Physiology* **159**: 266-285.
- Bowles, D., Isayenkova, J., Lim, E.K., and Poppenberger, B. (2005). Glycosyltransferases: managers of small molecules. *Current Opinion In Plant Biology* **8**: 254-263.
- Bowling, S.A., Clarke, J.D., Liu, Y., Klessig, D.F., and Dong, X. (1997). The *cpr5* mutant of *Arabidopsis* expresses both NPR1-dependent and NPR1-independent resistance. *Plant Cell* **9**: 1573-1584.
- Brodersen, P., Petersen, M., Pike, H.M., Olszak, B., Skov, S., Odum, N., Jorgensen, L.B., Brown, R.E., and Mundy, J. (2002). Knockout of *Arabidopsis* accelerated-cell-death 11 encoding a sphingosine transfer protein causes activation of programmed cell death and defense. *Genes & Development* **16**: 490-502.

- Bu, Q., Jiang, H., Li, C.B., Zhai, Q., Zhang, J., Wu, X., Sun, J., Xie, Q., and Li, C.** (2008). Role of the *Arabidopsis thaliana* NAC transcription factors ANAC019 and ANAC055 in regulating jasmonic acid-signaled defense responses. *Cell Research* **18**: 756-767.
- Buchanan-Wollaston, V., Page, T., Harrison, E., Breeze, E., Lim, P.O., Nam, H.G., Lin, J.F., Wu, S.H., Swidzinski, J., Ishizaki, K., and Leaver, C.J.** (2005). Comparative transcriptome analysis reveals significant differences in gene expression and signalling pathways between developmental and dark/starvation-induced senescence in *Arabidopsis*. *PlantJournal* **42**: 567-585.
- Buhot, N., Gomes, E., Milat, M.L., Ponchet, M., Marion, D., Lequeu, J., Delrot, S., Coutos-Thevenot, P., and Blein, J.P.** (2004). Modulation of the biological activity of a tobacco LTP1 by lipid complexation. *Molecular Biology Of The Cell* **15**: 5047-5052.
- Buxdorf, K., Rahat, I., Gafni, A., and Levy, M.** (2013). The Epiphytic Fungus *Pseudozyma aphidis* Induces Jasmonic Acid- and Salicylic Acid/Nonexpressor of PR1-Independent Local and Systemic Resistance. *Plant Physiology* **161**: 2014-2022.
- Cao, H., Glazebrook, J., Clarke, J.D., Volko, S., and Dong, X.** (1997). The *Arabidopsis NPR1* gene that controls systemic acquired resistance encodes a novel protein containing ankyrin repeats. *Cell* **88**: 57-63.
- Chen, H.J., Hou, W.C., Kuc, J., and Lin, Y.H.** (2001). Ca^{2+} -dependent and Ca^{2+} -independent excretion modes of salicylic acid in tobacco cell suspension culture. *Journal Of Experimental Botany* **52**: 1219-1226.
- Chen, L., Zhang, L., and Yu, D.** (2010a). Wounding-induced WRKY8 is involved in basal defense in *Arabidopsis*. *Molecular Plant-Microbe Interactions* **23**: 558-565.
- Chen, R., Jiang, H., Li, L., Zhai, Q., Qi, L., Zhou, W., Liu, X., Li, H., Zheng, W., Sun, J., and Li, C.** (2012). The *Arabidopsis* mediator subunit MED25 differentially regulates jasmonate and abscisic acid signaling through interacting with the MYC2 and ABI5 transcription factors. *Plant Cell* **24**: 2898-2916.
- Chen, Z.Y., Brown, R.L., Damann, K.E., and Cleveland, T.E.** (2010b). *PR10* expression in maize and its effect on host resistance against *Aspergillus flavus* infection and aflatoxin production. *Molecular Plant Pathology* **11**: 69-81.
- Chinchilla, D., Zipfel, C., Robatzek, S., Kemmerling, B., Nurnberger, T., Jones, J.D., Felix, G., and Boller, T.** (2007). A flagellin-induced complex of the receptor FLS2 and BAK1 initiates plant defence. *Nature* **448**: 497-500.

- Cipollini, D., Enright, S., Traw, M.B., and Bergelson, J.** (2004). Salicylic acid inhibits jasmonic acid-induced resistance of *Arabidopsis thaliana* to *Spodoptera exigua*. *Molecular Ecology* **13**: 1643-1653.
- Clarke, A., Mur, L.A., Darby, R.M., and Kenton, P.** (2005). Harpin modulates the accumulation of salicylic acid by *Arabidopsis* cells via apoplastic alkalization. *Journal Of Experimental Botany* **56**: 3129-3136.
- Clarke, J.D., Liu, Y., Klessig, D.F., and Dong, X.** (1998). Uncoupling *PR* gene expression from NPR1 and bacterial resistance: characterization of the dominant *Arabidopsis cpr6-1* mutant. *Plant Cell* **10**: 557-569.
- Consonni, C., Humphry, M.E., Hartmann, H.A., Livaja, M., Durner, J., Westphal, L., Vogel, J., Lipka, V., Kemmerling, B., Schulze-Lefert, P., Somerville, S.C., and Panstruga, R.** (2006). Conserved requirement for a plant host cell protein in powdery mildew pathogenesis. *Nature Genetics* **38**: 716-720.
- De Vos, M., Van Zaanen, W., Koornneef, A., Korzelius, J.P., Dicke, M., Van Loon, L.C., and Pieterse, C.M.** (2006). Herbivore-induced resistance against microbial pathogens in *Arabidopsis*. *Plant Physiology* **142**: 352-363.
- de Wit, M., Spoel, S.H., Sanchez-Perez, G.F., Gommers, C.M., Pieterse, C.M., Voosenek, L.A., and Pierik, R.** (2013). Perception of low Red:Far-red ratio compromises both salicylic acid- and jasmonic acid-dependent pathogen defences in *Arabidopsis*. *Plant Journal* **75**: 90-103.
- Dempsey, D.A., Vlot, A.C., Wildermuth, M.C., and Klessig, D.F.** (2011). Salicylic Acid biosynthesis and metabolism. *The Arabidopsis Book* **9**: e0156.
- Desveaux, D., Marechal, A., and Brisson, N.** (2005). Whirly transcription factors: defense gene regulation and beyond. *Trends In Plant Science* **10**: 95-102.
- Desveaux, D., Allard, J., Brisson, N., and Sygusch, J.** (2002). A new family of plant transcription factors displays a novel ssDNA-binding surface. *Nature Structural Biology* **9**: 512-517.
- Devadas, S.K., Enyedi, A., and Raina, R.** (2002). The *Arabidopsis hrr1* mutation reveals novel overlapping roles for salicylic acid, jasmonic acid and ethylene signalling in cell death and defence against pathogens. *Plant Journal* **30**: 467-480.
- Dewdney, J., Reuber, T.L., Wildermuth, M.C., Devoto, A., Cui, J., Stutius, L.M., Drummond, E.P., and Ausubel, F.M.** (2000). Three unique mutants of *Arabidopsis* identify eds loci required for limiting growth of a biotrophic fungal pathogen. *Plant Journal* **24**: 205-218.

- Dodds, P.N., and Rathjen, J.P.** (2010). Plant immunity: towards an integrated view of plant-pathogen interactions. *Nature Reviews Genetics* **11**: 539-548.
- Dong, X.** (2004). NPR1, all things considered. *Current opinion in plant biology* **7**: 547-552.
- Ellis, C., and Turner, J.G.** (2001). The *Arabidopsis* mutant *cev1* has constitutively active jasmonate and ethylene signal pathways and enhanced resistance to pathogens. *Plant Cell* **13**: 1025-1033.
- Fernandez-Calvo, P., Chini, A., Fernandez-Barbero, G., Chico, J.M., Gimenez-Ibanez, S., Geerinck, J., Eeckhout, D., Schweizer, F., Godoy, M., Franco-Zorrilla, J.M., Pauwels, L., Witters, E., Puga, M.I., Paz-Ares, J., Goossens, A., Reymond, P., De Jaeger, G., and Solano, R.** (2011). The *Arabidopsis* bHLH transcription factors MYC3 and MYC4 are targets of JAZ repressors and act additively with MYC2 in the activation of jasmonate responses. *Plant Cell* **23**: 701-715.
- Ferrari, S., Galletti, R., Denoux, C., De Lorenzo, G., Ausubel, F.M., and Dewdney, J.** (2007). Resistance to *Botrytis cinerea* induced in *Arabidopsis* by elicitors is independent of salicylic acid, ethylene, or jasmonate signaling but requires PHYTOALEXIN DEFICIENT3. *Plant Physiology* **144**: 367-379.
- Finkemeier, I., Konig, A.C., Heard, W., Nunes-Nesi, A., Pham, P.A., Leister, D., Fernie, A.R., and Sweetlove, L.J.** (2013). Transcriptomic analysis of the role of carboxylic acids in metabolite signaling in *Arabidopsis* leaves. *Plant Physiology* **162**, 239-253.
- Frye, C.A., Tang, D., and Innes, R.W.** (2001). Negative regulation of defense responses in plants by a conserved MAPKK kinase. *Proceedings Of The National Academy Of Sciences Of The United States Of America* **98**: 373-378.
- Gachon, C.M., Langlois-Meurinne, M., and Saindrenan, P.** (2005). Plant secondary metabolism glycosyltransferases: the emerging functional analysis. *Trends In Plant Science* **10**: 542-549.
- Gaffney, T., Friedrich, L., Vernooij, B., Negrotto, D., Nye, G., Uknes, S., Ward, E., Kessmann, H., and Ryals, J.** (1993). Requirement of salicylic Acid for the induction of systemic acquired resistance. *Science* **261**: 754-756.
- Gao, Q.M., Venugopal, S., Navarre, D., and Kachroo, A.** (2011). Low oleic acid-derived repression of jasmonic acid-inducible defense responses requires the WRKY50 and WRKY51 proteins. *Plant Physiology* **155**: 464-476.
- Glazebrook, J.** (2005). Contrasting mechanisms of defense against biotrophic and necrotrophic pathogens. *Annual Review Of Phytopathology* **43**: 205-227.

- Gomez-Gomez, L., and Boller, T.** (2000). FLS2: an LRR receptor-like kinase involved in the perception of the bacterial elicitor flagellin in *Arabidopsis*. *Molecular Cell* **5**: 1003-1011.
- Greenberg, J.T., Guo, A., Klessig, D.F., and Ausubel, F.M.** (1994). Programmed cell death in plants: a pathogen-triggered response activated coordinately with multiple defense functions. *Cell* **77**: 551-563.
- Gruner, K., Griebel, T., Navarova, H., Attaran, E., and Zeier, J.** (2013). Reprogramming of plants during systemic acquired resistance. *Frontiers In Plant Science* **4**: 252.
- Hebelstrup, K.H., van Zanten, M., Mandon, J., Voesenek, L.A., Harren, F.J., Cristescu, S.M., Moller, I.M., and Mur, L.A.** (2012). Haemoglobin modulates NO emission and hyponasty under hypoxia-related stress in *Arabidopsis thaliana*. *Journal Of Experimental Botany* **63**: 5581-5591.
- Heck, S., Grau, T., Buchala, A., Metraux, J.P., and Nawrath, C.** (2003). Genetic evidence that expression of *NahG* modifies defence pathways independent of salicylic acid biosynthesis in the *Arabidopsis-Pseudomonas syringae* pv. tomato interaction. *Plant Journal* **36**: 342-352.
- Hiraga, S., Sasaki, K., Ito, H., Ohashi, Y., and Matsui, H.** (2001). A large family of class III plant peroxidases. *Plant & Cell Physiology* **42**: 462-468.
- Igarashi, D., Tsuchida, H., Miyao, M., and Ohsumi, C.** (2006). Glutamate:glyoxylate aminotransferase modulates amino acid content during photorespiration. *Plant Physiology* **142**: 901-910.
- Igarashi, D., Miwa, T., Seki, M., Kobayashi, M., Kato, T., Tabata, S., Shinozaki, K., and Ohsumi, C.** (2003). Identification of photorespiratory glutamate:glyoxylate aminotransferase (*GGAT*) gene in *Arabidopsis*. *Plant Journal* **33**: 975-987.
- Ishikawa, K., Yoshimura, K., Harada, K., Fukusaki, E., Ogawa, T., Tamoi, M., and Shigeoka, S.** (2010). AtNUDX6, an ADP-ribose/NADH pyrophosphohydrolase in *Arabidopsis*, positively regulates NPR1-dependent salicylic acid signaling. *Plant Physiology* **152**: 2000-2012.
- Jarosch, B., Jansen, M., and Schaffrath, U.** (2003). Acquired resistance functions in mlo barley, which is hypersusceptible to *Magnaporthe grisea*. *Molecular Plant-Microbe Interactions* **16**: 107-114.
- Jones, J.D., and Dangl, J.L.** (2006). The plant immune system. *Nature* **444**: 323-329.
- Jones, P., and Vogt, T.** (2001). Glycosyltransferases in secondary plant metabolism: tranquilizers and stimulant controllers. *Planta* **213**: 164-174.

- Journot-Catalino, N., Somssich, I.E., Roby, D., and Kroj, T.** (2006). The transcription factors WRKY11 and WRKY17 act as negative regulators of basal resistance in *Arabidopsis thaliana*. *Plant Cell* **18**: 3289-3302.
- Jung, H.W., Tschaplinski, T.J., Wang, L., Glazebrook, J., and Greenberg, J.T.** (2009). Priming in systemic plant immunity. *Science* **324**: 89-91.
- Kachroo, A., Lapchyk, L., Fukushige, H., Hildebrand, D., Klessig, D., and Kachroo, P.** (2003). Plastidial fatty acid signaling modulates salicylic acid- and jasmonic acid-mediated defense pathways in the *Arabidopsis ssi2* mutant. *Plant Cell* **15**: 2952-2965.
- Kachroo, P., Yoshioka, K., Shah, J., Dooner, H.K., and Klessig, D.F.** (2000). Resistance to turnip crinkle virus in *Arabidopsis* is regulated by two host genes and is salicylic acid dependent but NPR1, ethylene, and jasmonate independent. *Plant Cell* **12**: 677-690.
- Karimi, M., Inze, D., and Depicker, A.** (2002). GATEWAY vectors for Agrobacterium-mediated plant transformation. *Trends In Plant Science* **7**: 193-195.
- Katagiri, F., Thilmony, R., and He, S.Y.** (2002). The *Arabidopsis thaliana*-*Pseudomonas syringae* interaction. *The Arabidopsis Book* **1**: e0039.
- Kazan, K., and Manners, J.M.** (2012). JAZ repressors and the orchestration of phytohormone crosstalk. *Trends In Plant Science* **17**: 22-31.
- Kazan, K., and Manners, J.M.** (2013). MYC2: the master in action. *Molecular Plant* **6**: 686-703.
- Knoth, C., Salus, M.S., Girke, T., and Eulgem, T.** (2009). The synthetic elicitor 3,5-dichloroanthranilic acid induces NPR1-dependent and NPR1-independent mechanisms of disease resistance in *Arabidopsis*. *Plant Physiology* **150**: 333-347.
- Koo, A.J., Gao, X., Jones, A.D., and Howe, G.A.** (2009). A rapid wound signal activates the systemic synthesis of bioactive jasmonates in *Arabidopsis*. *Plant Journal* **59**: 974-986.
- Koornneef, A., Leon-Reyes, A., Ritsema, T., Verhage, A., Den Otter, F.C., Van Loon, L.C., and Pieterse, C.M.** (2008). Kinetics of salicylate-mediated suppression of jasmonate signaling reveal a role for redox modulation. *Plant Physiology* **147**: 1358-1368.
- Lager, I., Andreasson, O., Dunbar, T.L., Andreasson, E., Escobar, M.A., and Rasmusson, A.G.** (2010). Changes in external pH rapidly alter plant gene expression and modulate auxin and elicitor responses. *Plant, Cell & Environment* **33**: 1513-1528.
- Langenbach, C., Campe, R., Schaffrath, U., Goellner, K., and Conrath, U.** (2013). UDP-glucosyltransferase UGT84A2/BRT1 is required for *Arabidopsis* nonhost resistance to

- the Asian soybean rust pathogen *Phakopsora pachyrhizi*. *New Phytologist* **198**: 536-545.
- Langlois-Meurinne, M., Gachon, C.M., and Saindrenan, P.** (2005). Pathogen-responsive expression of glycosyltransferase genes UGT73B3 and UGT73B5 is necessary for resistance to *Pseudomonas syringae* pv tomato in *Arabidopsis*. *Plant Physiology* **139**: 1890-1901.
- Laurie-Berry, N., Joardar, V., Street, I.H., and Kunkel, B.N.** (2006). The *Arabidopsis thaliana* *JASMONATE INSENSITIVE 1* gene is required for suppression of salicylic acid-dependent defenses during infection by *Pseudomonas syringae*. *Molecular Plant-Microbe Interactions* **19**: 789-800.
- Lawton, K.A., Friedrich, L., Hunt, M., Weymann, K., Delaney, T., Kessmann, H., Staub, T., and Ryals, J.** (1996). Benzothiadiazole induces disease resistance in *Arabidopsis* by activation of the systemic acquired resistance signal transduction pathway. *Plant Journal* **10**: 71-82.
- Leon-Reyes, A., Van der Does, D., De Lange, E.S., Delker, C., Wasternack, C., Van Wees, S.C., Ritsema, T., and Pieterse, C.M.** (2010). Salicylate-mediated suppression of jasmonate-responsive gene expression in *Arabidopsis* is targeted downstream of the jasmonate biosynthesis pathway. *Planta* **232**: 1423-1432.
- Leon-Reyes, A., Spoel, S.H., De Lange, E.S., Abe, H., Kobayashi, M., Tsuda, S., Millenaar, F.F., Welschen, R.A., Ritsema, T., and Pieterse, C.M.** (2009). Ethylene modulates the role of *NONEXPRESSOR OF PATHOGENESIS-RELATED GENES1* in cross talk between salicylate and jasmonate signaling. *Plant Physiology* **149**: 1797-1809.
- Li, J., Brader, G., and Palva, E.T.** (2004). The WRKY70 transcription factor: a node of convergence for jasmonate-mediated and salicylate-mediated signals in plant defense. *Plant Cell* **16**: 319-331.
- Li, J., Brader, G., Kariola, T., and Palva, E.T.** (2006). WRKY70 modulates the selection of signaling pathways in plant defense. *Plant Journal* **46**: 477-491.
- Li, X., Zhang, Y., Clarke, J.D., Li, Y., and Dong, X.** (1999). Identification and cloning of a negative regulator of systemic acquired resistance, SNI1, through a screen for suppressors of *npr1-1*. *Cell* **98**: 329-339.
- Lim, E.K., Doucet, C.J., Li, Y., Elias, L., Worrall, D., Spencer, S.P., Ross, J., and Bowles, D.J.** (2002). The activity of *Arabidopsis* glycosyltransferases toward salicylic acid, 4-

- hydroxybenzoic acid, and other benzoates. *Journal Of Biological Chemistry* **277**: 586-592.
- Lindermayr, C., Saalbach, G., and Durner, J.** (2005). Proteomic identification of S-nitrosylated proteins in *Arabidopsis*. *Plant Physiology* **137**: 921-930.
- Lorrain, S., Vaillau, F., Balague, C., and Roby, D.** (2003). Lesion mimic mutants: keys for deciphering cell death and defense pathways in plants? *Trends In Plant Science* **8**: 263-271.
- Maldonado, A.M., Doerner, P., Dixon, R.A., Lamb, C.J., and Cameron, R.K.** (2002). A putative lipid transfer protein involved in systemic resistance signalling in *Arabidopsis*. *Nature* **419**: 399-403.
- Mamer, O.A., and Reimer, M.L.** (1992). On the mechanisms of the formation of L-alloisoleucine and the 2-hydroxy-3-methylvaleric acid stereoisomers from L-isoleucine in maple syrup urine disease patients and in normal humans. *Journal Of Biological Chemistry* **267**: 22141-22147.
- Messner, B., Thulke, O., and Schäffner, A.R.** (2003). *Arabidopsis* glucosyltransferases with activities toward both endogenous and xenobiotic substrates. *Planta* **217**: 138-146.
- Mewis, I., Appel, H.M., Hom, A., Raina, R., and Schultz, J.C.** (2005). Major signaling pathways modulate *Arabidopsis* glucosinolate accumulation and response to both phloem-feeding and chewing insects. *Plant Physiology* **138**: 1149-1162.
- Miersch, O., Neumerkel, J., Dippe, M., Stenzel, I., and Wasternack, C.** (2008). Hydroxylated jasmonates are commonly occurring metabolites of jasmonic acid and contribute to a partial switch-off in jasmonate signaling. *New Phytologist* **177**: 114-127.
- Miller, J.D., Arteca, R.N., and Pell, E.J.** (1999). Senescence-associated gene expression during ozone-induced leaf senescence in *Arabidopsis*. *Plant Physiology* **120**: 1015-1024.
- Millet, Y.A., Danna, C.H., Clay, N.K., Songnuan, W., Simon, M.D., Werck-Reichhart, D., and Ausubel, F.M.** (2010). Innate immune responses activated in *Arabidopsis* roots by microbe-associated molecular patterns. *Plant Cell* **22**: 973-990.
- Mishina, T.E., and Zeier, J.** (2006). The *Arabidopsis* flavin-dependent monooxygenase FMO1 is an essential component of biologically induced systemic acquired resistance. *Plant Physiology* **141**: 1666-1675.
- Miya, A., Albert, P., Shinya, T., Desaki, Y., Ichimura, K., Shirasu, K., Narusaka, Y., Kawakami, N., Kaku, H., and Shibuya, N.** (2007). CERK1, a LysM receptor kinase,

- is essential for chitin elicitor signaling in *Arabidopsis*. Proceedings Of The National Academy of Sciences Of The United States Of America **104**: 19613-19618.
- Mosher, R.A., Durrant, W.E., Wang, D., Song, J., and Dong, X.** (2006). A comprehensive structure-function analysis of *Arabidopsis* SN1 defines essential regions and transcriptional repressor activity. Plant Cell **18**: 1750-1765.
- Moussatche, P., and Klee, H.J.** (2004). Autophosphorylation activity of the *Arabidopsis* ethylene receptor multigene family. Journal Of Biological Chemistry **279**: 48734-48741.
- Mur, L.A., Kenton, P., Atzorn, R., Miersch, O., and Wasternack, C.** (2006). The outcomes of concentration-specific interactions between salicylate and jasmonate signaling include synergy, antagonism, and oxidative stress leading to cell death. Plant Physiology **140**: 249-262.
- Mur, L.A., Sivakumaran, A., Mandon, J., Cristescu, S.M., Harren, F.J., and Hebelstrup, K.H.** (2012). Haemoglobin modulates salicylate and jasmonate/ethylene-mediated resistance mechanisms against pathogens. Journal Of Experimental Botany **63**: 4375-4387.
- Murray, S.L., Thomson, C., Chini, A., Read, N.D., and Loake, G.J.** (2002). Characterization of a novel, defense-related *Arabidopsis* mutant, *cir1*, isolated by luciferase imaging. Molecular Plant-Microbe Interactions **15**: 557-566.
- Navarova, H., Bernsdorff, F., Doring, A.C., and Zeier, J.** (2012). Pipecolic acid, an endogenous mediator of defense amplification and priming, is a critical regulator of inducible plant immunity. Plant Cell **24**: 5123-5141.
- Nawrath, C., and Metraux, J.P.** (1999). Salicylic acid induction-deficient mutants of *Arabidopsis* express *PR-2* and *PR-5* and accumulate high levels of camalexin after pathogen inoculation. Plant Cell **11**: 1393-1404.
- Ndamukong, I., Abdallat, A.A., Thurow, C., Fode, B., Zander, M., Weigel, R., and Gatz, C.** (2007). SA-inducible *Arabidopsis* glutaredoxin interacts with TGA factors and suppresses JA-responsive *PDF1.2* transcription. Plant Journal **50**: 128-139.
- Noutoshi, Y., Okazaki, M., Kida, T., Nishina, Y., Morishita, Y., Ogawa, T., Suzuki, H., Shibata, D., Jikumaru, Y., Hanada, A., Kamiya, Y., and Shirasu, K.** (2012). Novel plant immune-priming compounds identified via high-throughput chemical screening target salicylic acid glucosyltransferases in *Arabidopsis*. Plant Cell **24**: 3795-3804.

- Olszak, B., Malinovsky, F.G., Brodersen, P., Grell, M., Giese, H., Petersen, M., and Mundy, J. (2006). A putative flavin-containing mono-oxygenase as a marker for certain defense and cell death pathways. *Plant Science* **170**: 614-623.
- Pandey, S.P., Roccaro, M., Schon, M., Logemann, E., and Somssich, I.E. (2010). Transcriptional reprogramming regulated by WRKY18 and WRKY40 facilitates powdery mildew infection of *Arabidopsis*. *Plant Journal* **64**: 912-923.
- Park, S.W., Kaimoyo, E., Kumar, D., Mosher, S., and Klessig, D.F. (2007). Methyl salicylate is a critical mobile signal for plant systemic acquired resistance. *Science* **318**: 113-116.
- Petersen, M., Brodersen, P., Naested, H., Andreasson, E., Lindhart, U., Johansen, B., Nielsen, H.B., Lacy, M., Austin, M.J., Parker, J.E., Sharma, S.B., Klessig, D.F., Martienssen, R., Mattsson, O., Jensen, A.B., and Mundy, J. (2000). *Arabidopsis* map kinase 4 negatively regulates systemic acquired resistance. *Cell* **103**: 1111-1120.
- Pogany, M., von Rad, U., Grun, S., Dongo, A., Pintye, A., Simoneau, P., Bahnweg, G., Kiss, L., Barna, B., and Durner, J. (2009). Dual roles of reactive oxygen species and NADPH oxidase RBOHD in an *Arabidopsis*-*Alternaria* pathosystem. *Plant Physiology* **151**: 1459-1475.
- Qiu, J.L., Fiil, B.K., Petersen, K., Nielsen, H.B., Botanga, C.J., Thorgrimsen, S., Palma, K., Suarez-Rodriguez, M.C., Sandbech-Clausen, S., Lichota, J., Brodersen, P., Grasser, K.D., Mattsson, O., Glazebrook, J., Mundy, J., and Petersen, M. (2008). *Arabidopsis* MAP kinase 4 regulates gene expression through transcription factor release in the nucleus. *EMBO Journal* **27**: 2214-2221.
- Radomska-Pandya, A., Czernik, P.J., Little, J.M., Battaglia, E., and Mackenzie, P.I. (1999). Structural and functional studies of UDP-glucuronosyltransferases. *Drug Metabolism Reviews* **31**: 817-899.
- Raffaele, S., Rivas, S., and Roby, D. (2006). An essential role for salicylic acid in AtMYB30-mediated control of the hypersensitive cell death program in *Arabidopsis*. *FEBS Letters* **580**: 3498-3504.
- Rasmussen, M.W., Roux, M., Petersen, M., and Mundy, J. (2012). MAP Kinase Cascades in *Arabidopsis* Innate Immunity. *Frontiers In Plant Science* **3**: 169.
- Rate, D.N., Cuenca, J.V., Bowman, G.R., Guttman, D.S., and Greenberg, J.T. (1999). The gain-of-function *Arabidopsis acd6* mutant reveals novel regulation and function of the salicylic acid signaling pathway in controlling cell death, defenses, and cell growth. *Plant Cell* **11**: 1695-1708.

- Reuber, T.L., and Ausubel, F.M.** (1996). Isolation of *Arabidopsis* genes that differentiate between resistance responses mediated by the RPS2 and RPM1 disease resistance genes. *Plant Cell* **8**: 241-249.
- Rhee, S.Y., Beavis, W., Berardini, T.Z., Chen, G., Dixon, D., Doyle, A., Garcia-Hernandez, M., Huala, E., Lander, G., Montoya, M., Miller, N., Mueller, L.A., Mundodi, S., Reiser, L., Tacklind, J., Weems, D.C., Wu, Y., Xu, L., Yoo, D., Yoon, J., and Zhang, P.** (2003). The *Arabidopsis* Information Resource (TAIR): a model organism database providing a centralized, curated gateway to *Arabidopsis* biology, research materials and community. *Nucleic Acids Research* **31**: 224-228.
- Robert-Seilanianantz, A., Grant, M., and Jones, J.D.** (2011). Hormone crosstalk in plant disease and defense: more than just jasmonate-salicylate antagonism. *Annual Review Of Phytopathology* **49**: 317-343.
- Ryals, J.A., Neuenschwander, U.H., Willits, M.G., Molina, A., Steiner, H.Y., and Hunt, M.D.** (1996). Systemic Acquired Resistance. *Plant Cell* **8**: 1809-1819.
- Sanchez, L., Courteaux, B., Hubert, J., Kauffmann, S., Renault, J.H., Clement, C., Baillieul, F., and Dorey, S.** (2012). Rhamnolipids elicit defense responses and induce disease resistance against biotrophic, hemibiotrophic, and necrotrophic pathogens that require different signaling pathways in *Arabidopsis* and highlight a central role for salicylic acid. *Plant Physiology* **160**: 1630-1641.
- Santner, A., and Estelle, M.** (2009). Recent advances and emerging trends in plant hormone signalling. *Nature* **459**: 1071-1078.
- Schenk, P.M., Kazan, K., Wilson, I., Anderson, J.P., Richmond, T., Somerville, S.C., and Manners, J.M.** (2000). Coordinated plant defense responses in *Arabidopsis* revealed by microarray analysis. *Proceedings Of The National Academy Of Sciences Of The United States Of America* **97**: 11655-11660.
- Scholl, R.L., May, S.T., and Ware, D.H.** (2000). Seed and molecular resources for *Arabidopsis*. *Plant Physiology* **124**: 1477-1480.
- Shah, J., Kachroo, P., and Klessig, D.F.** (1999). The *Arabidopsis* *ssi1* mutation restores pathogenesis-related gene expression in *npr1* plants and renders defensin gene expression salicylic acid dependent. *Plant Cell* **11**: 191-206.
- Shah, J., Kachroo, P., Nandi, A., and Klessig, D.F.** (2001). A recessive mutation in the *Arabidopsis* *SSI2* gene confers SA- and NPR1-independent expression of *PR* genes and resistance against bacterial and oomycete pathogens. *Plant Journal* **25**: 563-574.

- Sheard, L.B., Tan, X., Mao, H., Withers, J., Ben-Nissan, G., Hinds, T.R., Kobayashi, Y., Hsu, F.F., Sharon, M., Browse, J., He, S.Y., Rizo, J., Howe, G.A., and Zheng, N.** (2010). Jasmonate perception by inositol-phosphate-potentiated COI1-JAZ co-receptor. *Nature* **468**: 400-405.
- Shim, J.S., Jung, C., Lee, S., Min, K., Lee, Y.W., Choi, Y., Lee, J.S., Song, J.T., Kim, J.K., and Choi, Y.D.** (2013). AtMYB44 regulates *WRKY70* expression and modulates antagonistic interaction between salicylic acid and jasmonic acid signaling. *Plant Journal* **73**: 483-495.
- Shiu, S.H., and Bleecker, A.B.** (2001). Receptor-like kinases from *Arabidopsis* form a monophyletic gene family related to animal receptor kinases. *Proceedings Of The National Academy Of Sciences Of The United States Of America* **98**: 10763-10768.
- Spoel, S.H., Johnson, J.S., and Dong, X.** (2007). Regulation of tradeoffs between plant defenses against pathogens with different lifestyles. *Proceedings Of The National Academy Of Sciences Of The United States Of America* **104**: 18842-18847.
- Spoel, S.H., Koornneef, A., Claessens, S.M., Korzelius, J.P., Van Pelt, J.A., Mueller, M.J., Buchala, A.J., Metraux, J.P., Brown, R., Kazan, K., Van Loon, L.C., Dong, X., and Pieterse, C.M.** (2003). NPR1 modulates cross-talk between salicylate- and jasmonate-dependent defense pathways through a novel function in the cytosol. *Plant Cell* **15**: 760-770.
- Tada, Y., Spoel, S.H., Pajerowska-Mukhtar, K., Mou, Z., Song, J., Wang, C., Zuo, J., and Dong, X.** (2008). Plant immunity requires conformational changes [corrected] of NPR1 via S-nitrosylation and thioredoxins. *Science* **321**: 952-956.
- Tang, D., Christiansen, K.M., and Innes, R.W.** (2005). Regulation of plant disease resistance, stress responses, cell death, and ethylene signaling in *Arabidopsis* by the EDR1 protein kinase. *Plant Physiology* **138**: 1018-1026.
- Thomma, B.P., Nelissen, I., Eggermont, K., and Broekaert, W.F.** (1999). Deficiency in phytoalexin production causes enhanced susceptibility of *Arabidopsis thaliana* to the fungus *Alternaria brassicicola*. *Plant Journal* **19**: 163-171.
- Truman, W., Bennett, M.H., Kubigsteltig, I., Turnbull, C., and Grant, M.** (2007). *Arabidopsis* systemic immunity uses conserved defense signaling pathways and is mediated by jasmonates. *Proceedings Of The National Academy Of Sciences Of The United States Of America* **104**: 1075-1080.

- Tsuda, K., Sato, M., Glazebrook, J., Cohen, J.D., and Katagiri, F.** (2008). Interplay between MAMP-triggered and SA-mediated defense responses. *Plant Journal* **53**: 763-775.
- Van der Does, D., Leon-Reyes, A., Koornneef, A., Van Verk, M.C., Rodenburg, N., Pauwels, L., Goossens, A., Korbes, A.P., Memelink, J., Ritsema, T., Van Wees, S.C., and Pieterse, C.M.** (2013). Salicylic Acid Suppresses Jasmonic Acid Signaling Downstream of SCFCOI1-JAZ by Targeting GCC Promoter Motifs via Transcription Factor ORA59. *Plant Cell* **25**: 744-761.
- van Loon, L.C., Rep, M., and Pieterse, C.M.** (2006). Significance of inducible defense-related proteins in infected plants. *Annual Review Of Phytopathology* **44**: 135-162.
- van Verk, M.C., Bol, J.F., and Linthorst, H.J.** (2011). WRKY transcription factors involved in activation of SA biosynthesis genes. *BMC Plant Biology* **11**: 89.
- van Wees, S.C., de Swart, E.A., van Pelt, J.A., van Loon, L.C., and Pieterse, C.M.** (2000). Enhancement of induced disease resistance by simultaneous activation of salicylate- and jasmonate-dependent defense pathways in *Arabidopsis thaliana*. *Proceedings Of The National Academy Of Sciences Of The United States Of America* **97**: 8711-8716.
- Vandesompele, J., De Preter, K., Pattyn, F., Poppe, B., Van Roy, N., De Paepe, A., and Speleman, F.** (2002). Accurate normalization of real-time quantitative RT-PCR data by geometric averaging of multiple internal control genes. *Genome Biology* **3**: RESEARCH0034.
- Verhage, A., Vlaardingerbroek, I., Raaymakers, C., Van Dam, N.M., Dicke, M., Van Wees, S.C., and Pieterse, C.M.** (2011). Rewiring of the Jasmonate Signaling Pathway in *Arabidopsis* during Insect Herbivory. *Frontiers In Plant Science* **2**: 47.
- Vlot, A.C., Dempsey, D.A., and Klessig, D.F.** (2009). Salicylic Acid, a multifaceted hormone to combat disease. *Annual Review Of Phytopathology* **47**: 177-206.
- Vogel, J.T., Zarka, D.G., Van Buskirk, H.A., Fowler, S.G., and Thomashow, M.F.** (2005). Roles of the CBF2 and ZAT12 transcription factors in configuring the low temperature transcriptome of *Arabidopsis*. *Plant Journal* **41**: 195-211.
- von Saint Paul, V.** (2010). Stress inducible glycosyltransferases in *Arabidopsis thaliana* and their impact on plant metabolism and defense mechanisms. Dissertation.
- von Saint Paul, V., Zhang, W., Kanawati, B., Geist, B., Faus-Kessler, T., Schmitt-Kopplin, P., and Schaffner, A.R.** (2011). The *Arabidopsis* glucosyltransferase UGT76B1 conjugates isoleucic acid and modulates plant defense and senescence. *Plant Cell* **23**: 4124-4145.

- Wan, J., Zhang, X.C., Neece, D., Ramonell, K.M., Clough, S., Kim, S.Y., Stacey, M.G., and Stacey, G.** (2008). A LysM receptor-like kinase plays a critical role in chitin signaling and fungal resistance in *Arabidopsis*. *Plant Cell* **20**: 471-481.
- Wang, D., Amornsiripanitch, N., and Dong, X.** (2006). A genomic approach to identify regulatory nodes in the transcriptional network of systemic acquired resistance in plants. *PLoS Pathogens* **2**: e123.
- Wang, K.L., Li, H., and Ecker, J.R.** (2002). Ethylene biosynthesis and signaling networks. *Plant Cell* **14 Suppl**: S131-151.
- Wawrzynska, A., Rodibaugh, N.L., and Innes, R.W.** (2010). Synergistic activation of defense responses in *Arabidopsis* by simultaneous loss of the GSL5 callose synthase and the EDR1 protein kinase. *Molecular Plant-Microbe Interactions* **23**: 578-584.
- Wu, C.C., Singh, P., Chen, M.C., and Zimmerli, L.** (2010). L-Glutamine inhibits beta-aminobutyric acid-induced stress resistance and priming in *Arabidopsis*. *Journal Of Experimental Botany* **61**: 995-1002.
- Yoshida, S., Ito, M., Nishida, I., and Watanabe, A.** (2001). Isolation and RNA gel blot analysis of genes that could serve as potential molecular markers for leaf senescence in *Arabidopsis thaliana*. *Plant & Cell Physiology* **42**: 170-178.
- Zhang, X., Wang, C., Zhang, Y., Sun, Y., and Mou, Z.** (2012). The *Arabidopsis* mediator complex subunit16 positively regulates salicylate-mediated systemic acquired resistance and jasmonate/ethylene-induced defense pathways. *Plant Cell* **24**: 4294-4309.
- Zheng, Q., and Dong, X.** (2013). Systemic Acquired Resistance: Turning Local Infection into Global Defense. *Annual Review Of Plant Biology*.
- Zheng, X.Y., Spivey, N.W., Zeng, W., Liu, P.P., Fu, Z.Q., Klessig, D.F., He, S.Y., and Dong, X.** (2012). Coronatine promotes *Pseudomonas syringae* virulence in plants by activating a signaling cascade that inhibits salicylic acid accumulation. *Cell Host & Microbe* **11**: 587-596.
- Zhu, Z., An, F., Feng, Y., Li, P., Xue, L., A, M., Jiang, Z., Kim, J.M., To, T.K., Li, W., Zhang, X., Yu, Q., Dong, Z., Chen, W.Q., Seki, M., Zhou, J.M., and Guo, H.** (2011). Derepression of ethylene-stabilized transcription factors (EIN3/EIL1) mediates jasmonate and ethylene signaling synergy in *Arabidopsis*. *Proceedings Of The National Academy Of Sciences Of The United States Of America* **108**: 12539-12544.

- Zimmerli, L., Hou, B.H., Tsai, C.H., Jakab, G., Mauch-Mani, B., and Somerville, S.** (2008). The xenobiotic beta-aminobutyric acid enhances *Arabidopsis* thermotolerance. *Plant Journal* **53**: 144-156.
- Zimmermann, P., Hennig, L., and Gruissem, W.** (2005). Gene-expression analysis and network discovery using Genevestigator. *Trends In Plant Science* **10**: 407-409.
- Zipfel, C., Robatzek, S., Navarro, L., Oakeley, E.J., Jones, J.D., Felix, G., and Boller, T.** (2004). Bacterial disease resistance in *Arabidopsis* through flagellin perception. *Nature* **428**: 764-767.
- Zipfel, C., Kunze, G., Chinchilla, D., Caniard, A., Jones, J.D., Boller, T., and Felix, G.** (2006). Perception of the bacterial PAMP EF-Tu by the receptor EFR restricts *Agrobacterium*-mediated transformation. *Cell* **125**: 749-760.

CURRICULUM VITAE

Name: Wei Zhang
Date/place of birth: 17th January 1984, Jiang Xi, China
Nationality: Chinese

EDUCATION

09/2009-today PhD in Biochemistry at the Ludwig-Maximilians Universität München (Germany)
Title: *Stress inducible glycosyltransferases in Arabidopsis thaliana and their impact on plant metabolism and defense mechanisms.*
Advisor: PD Dr. Anton R. Schäffner, Helmholtz Zentrum München, Institute for Biochemical Plant Pathology.

09/2006-07/2009 Master in Biochemistry in Colleague of Life Sciences
Sichuan University in Chengdu, China

09/2002-07/2006 Bachelor in Biotechnology in Colleague of Life Sciences
Sichuan University in Chengdu, China

FELLOWSHIP

Chinese Scholarship Council (CSC) from 09/2009-08/2013

PUBLICATIONS

von Saint Paul V, **Zhang W**, Kanawati B, Geist B, Faus-Kessler T, Schmitt-Kopplin P, Schäffner AR (2011). The *Arabidopsis* glucosyltransferase UGT76B1 conjugates isoleucic acid and modulates plant defense and senescence. *Plant Cell* 23: 4124–4145.

Patent application:

Von saint Paul V, **Zhang W**, Schäffner AR. Plant protective composition containing Alpha-hydroxy acids. International application No: PCT/EP2012/064723. 2013

CONTRIBUTIONS TO SCIENTIFIC CONFERENCES

Presentations:

Oral presentation of “*Arabidopsis* UGT76B1, a small-molecule glucosyltransferase, impacts SA- and JA-dependent plant defense” at the international conference “SEB 2012” in Salzburg, Austria

Oral presentation of “*Arabidopsis* UGT76B1, a small-molecule glucosyltransferase, impacts SA- and JA-dependent plant defense” at the international conference “Botanikertagung 2011” in Berlin, Germany

Meetings:

Attendance of conference of Tri-National Arabidopsis Meeting 2012 and poster presentation
Attendance of conference of SEB 2012 and oral presentation (see above)
Attendance of conference of Botanikertagung 2011 and oral presentation (see above)
Attendance of Tri-National Arabidopsis Meeting 2010 and poster presentation
Attendance of 1st International Metabolomics Symposium 2010 in Freising, Germany

Trainings:

Participation of Research Management Training Workshop 2012, 9th-10th October 2012

Participation of Training of Protection and Commercialization of Intellectual Property 10th of May, 2011

Participation of ZEISS confocal Microscope Software LSM&ZEN Training I, 1st of June, 2010

Participation of Training of Protection and Commercialization of Intellectual Property 17th of May, 2010

Participation of Plant Workshop 2010 in Munich, 14th-16th April 2010

Participation at 10th Spring School in Bioinformatics and Systems Biology for Molecular Biologists 14th-17th March 2010 in Helmholtz Center Munich

ACKNOWLEDGEMENTS

I would like to express my deep thanks to my supervisor PD Dr. Anton R. Schäffner for his excellent supervision, enthusiastic encouragement and patient guidance. His personal scientific enthusiasm, constructive thinking and criticism towards science inspire and encourage me and will influence me for a long time.

I would also like to especially thank Prof. Dr. Jörg Durner for his advices during the thesis committee reports and the willingness to review my thesis. The discussions with him have been helpful and valuable for me.

My grateful thanks are also extended to Prof. Dr. Klaus Forstemann and PD Dr. Dietmar E. Martin and the other members of examination committee for reviewing this project.

I am deeply thankful to my former colleague Dr. Veronica von Saint Paul, who once supervised my work. Her experience and instructions helped me a lot to get familiar with the project. I also appreciate her help in daily life. I miss her very much.

I wish to extend my sincere gratitude to various people for their support for this project. Special thanks will be given to Dr. Basem Kanawati and Prof. Dr. Philippe Schmitt-Kopplin for providing access to the FT-ICR MS instrument, Dr. Cornelia Prehn for providing the access to the API4000 mass spectrometer, Prof. Dr. Bettina Hause for measuring the JA metabolites, Dr. Mohammad-Reza Hajirezaei for amino acid measurements, Dr. Theresa Faus-Kessler for the help with microarray data analyses and Birgit Geist for her excellent assistance especially for real-time PCR. The help from Dr. Barbro Winkler from EUS for setting up the green house is also appreciated.

I am extremely happy that I have so many nice colleagues surrounding me. I am very grateful that Dr. Stephan Dräxl is always the first to help, trying to encourage me all the time. I would also like to thank Dr. Jin Zhao, Chen Liu, Ming Jin and Rafal Maksym for sharing the stories and having fun together. I appreciate that the former colleague Dr. Ruohe Yin helped me to understand the topics in the group meeting. I am also thankful to the former colleague Kerstin Schuster especially for designing the painting of my apartment. I enjoyed the picnic and barbecue in Olympia Park with all the colleagues from our group and Dr. Dey, Sanjukta. Thanks for their help for painting “the lovely cat family” on the wall of my apartment.

I would also like to thank the former colleagues Dr. Malay Das and Dr. Gitto Kuruthukulangarakoola, who always tell jokes inside the lab to make me enjoy working with them. I am also thankful to Felicitas Groß, who always offers me nice chocolate.

I am also grateful to other friends and colleagues in BIOP and EUS: thanks to Zhen Bi, Feng Zhao and her wife Xin Zhao, Finni Wittek, Christian Holzmeister, Antonie Sophie Bernhard, Karoline Stoll for making the studying abroad so pleasant for me.

I would also like to thank the ‘Chinese Scholarship Council’ (CSC) for their financial support.

Finally, I would like to give thanks to my parents for their love and endless care. Special thanks go to my boyfriend Liang Zhao for supporting me whenever I need him, understanding and encouraging me and waiting for me with patience and love.